Characteristics and signatures of dipole vortices in ferroelectric nanodots: First-principles-based simulations and analytical expressions

S. Prosandeev[1,2] and L. Bellaiche[1]
[1]*Physics Department, University of Arkansas, Fayetteville, Arkansas 72701, USA*
[2]*Institute of Physics, Rostov State University, Rostov on Don 344090, Russia*
(Received 31 October 2006; revised manuscript received 10 January 2007; published 7 March 2007)

Characteristics and signatures of dipole vortex in ferroelectric nanodots are determined via the use of first-principles-based simulations and by analytical developments. For instance, the dependency of such vortex on size, shape, material, and temperature is provided. Moreover, peculiar features associated with such vortex, such as unique behaviors of the inhomogeneous and homogeneous strains and of the induced electric fields, are revealed. Finally, energetics of interacting vortices is also discussed.

DOI: 10.1103/PhysRevB.75.094102 PACS number(s): 77.84.Dy, 77.80.Bh, 77.22.Ej

I. INTRODUCTION

Recently, first-principles-based simulations predicted the existence of an unusual phenomena in nanodots of ferroelectrics, that is, the formation of a vortex structure for their electrical dipoles below a critical temperature.[1–3] Similar to magnetic nanostructures that also possess a vortex structure for their magnetic dipoles (which is usually referred to as the curling state),[4–6] the possibility of switching the chirality of the vortex in ferroelectric nanostructures opens exciting opportunities for designing "wunderbar" nanomemory devices.[2,7] Interestingly, while *ab initio* studies[2,7] suggested original ways to allow a practical control of the vortex chirality (namely, by using an *inhomogeneous* static electric field[7] or a time-dependent magnetic field[2]), dipole vortex in nanoferroelectrics remains to be *experimentally* found—to the best of our knowledge. One plausible reason for this lack of finding may be (in addition to the inherent difficulty in growing nanoferroelectrics) the current paucity of knowledge about the possible "signatures" of a dipole vortex. For instance, one may wonder how an electric field produced by a vortex differs from the one generated by a polarized sample. Similarly, it may be worthwhile to know if the strain associated with the vortex structure is dramatically different than the one associated with a spontaneous polarization. Other important and related issues that are poorly known (if not completely unknown) are the dependency of the vortex structure on the shape of the dot as well as on the material forming the dot, the energy landscape associated with vortices, or the energetics of interacting vortices.

The aim of this paper is to provide characteristics and signatures of dipole vortices in ferroelectric nanodots by performing first-principles-based computations as well as by deriving analytical expressions for electric fields generated by a vortex structure. This paper is organized as follows. Section II describes the *ab initio* method we used. In Sec. III, important atomistic, elastic, and energetic characteristics of vortex are revealed. Sections IV and V focus on the electric field produced by a vortex structure inside and outside a ferroelectric nanodot, respectively. Section VI discusses the energetics of interacting dipole vortices, while a summary is provided in Sec. VII. An Appendix is also offered for better understanding the origins of some formula given in Secs. V and VI.

II. EFFECTIVE HAMILTONIAN APPROACH

Here, we mostly study nanodots made of disordered $PbZr_{0.4}Ti_{0.6}O_3$ (PZT60), being Pb-O terminated at all surfaces. We also investigate nanodots made of $BaTiO_3$ (BT), being Ba-O terminated at all surfaces, for the sake of comparison with PZT60 nanodots. The total energy of such systems is written as

$$\mathcal{E}_{tot}(\mathbf{u}_i, \mathbf{v}_i, \eta_H) = \mathcal{E}_{Heff}(\mathbf{u}_i, \mathbf{v}_i, \eta_H) + \beta \sum_i \langle \mathbf{E}_{dep} \rangle \cdot Z^* \mathbf{u}_i, \quad (1)$$

where $\mathbf{u}_i$ is the local soft mode in the unit cell i of the dot, whose product with the effective charge Z^* yields the local electrical dipole in this cell, while η_H and $\mathbf{v}_i$ are the homogeneous strain tensor and inhomogeneous strain-related variables in unit cell i, respectively.[8]

$\mathcal{E}_{Heff}$ represents the intrinsic (effective Hamiltonian) energy of ferroelectric nanodots. Its analytical expression is the one of Ref. 8 for BT bulk and of Ref. 9 for PZT60 bulk (while its first-principles-derived parameters are those of Ref. 10 for BT and of Ref. 9 for PZT60), except for two main modifications. The first modification consists in adding energetic terms associated with the direct interaction between the vacuum surrounding the dot and both the surface dipoles and inhomogeneous strain near the surface.[1,11] The second modification consists in replacing the (reciprocal-space-based) matrix associated with long-range dipole-dipole interactions in the bulk[8] by the corresponding (real-space-based) matrix characterizing dipole-dipole interactions in the dot, implying that no supercell periodic boundary conditions are needed to simulate the dot. Such matrix is given in Refs. 3 and 12 and corresponds to ideal open-circuit (OC) conditions. Such electrical boundary conditions naturally lead to the existence of a maximum depolarizing field (denoted by $\langle \mathbf{E}_{dep} \rangle$ and determined from the atomistic approach of Ref. 3) inside the dot. The second term of Eq. (1) mimics a screening of $\langle \mathbf{E}_{dep} \rangle$ via the β parameter. More precisely, the residual depolarizing field resulting from the combination of the first and second terms of Eq. (1) has a magnitude equal to $(1-\beta)|\langle \mathbf{E}_{dep} \rangle|$. $\beta=0$ thus corresponds to ideal OC conditions, while an increase in β lowers the magnitude of the

Relation between dielectric responses and polarization fluctuations in ferroelectric nanostructures

I. Ponomareva,[1,*] L. Bellaiche,[1] and R. Resta[2,3]
[1]*Department of Physics, University of Arkansas, Fayetteville, Arkansas 72701, USA*
[2]*Dipartimento di Fisica Teorica, Università di Trieste, Strada Costiera 11, 34014 Trieste, Italy*
[3]*CNR-INFM DEMOCRITOS National Simulation Center, via Beirut 2, 34014 Trieste, Italy*
(Received 26 February 2007; revised manuscript received 4 October 2007; published 4 December 2007)

Analytical derivations and first-principles-based computations are combined to establish the link between dielectric responses and thermal fluctuations of polarization in low-dimensional systems under any possible electrical boundary condition. It is proven that the analytical expression (in terms of polarization fluctuations) of the "external" dielectric susceptibility of a nanostructure, which is defined as the polarization's response to an *external* field, is identical to that of the dielectric susceptibility in the *bulk* material. On the other hand, such expression has to be modified for the "internal" dielectric susceptibility of a nanostructure that characterizes the response of the polarization to the total *internal* field. Such modification originates from the existence of the depolarizing field, and involves the depolarizing coefficients, as well as the degree of screening of the polarization-induced surface charges.

DOI: 10.1103/PhysRevB.76.235403 PACS number(s): 77.22.Ej, 77.55.+f, 77.84.−s

I. INTRODUCTION

Fluctuation formulas relate the dielectric susceptibility to the mean-square average of the fluctuating polarization.[1] They have been of much use in classical simulations for bulk systems, including some concerning ferroelectric materials.[2–5] For a *bulk* system, the diagonal components of the dielectric susceptibility χ obey[1]

$$\chi_{\gamma\gamma} = \frac{V}{k_B T}[\langle (P_\gamma)^2 \rangle - \langle P_\gamma \rangle^2], \tag{1}$$

where V is the volume of the simulation cell, k_B is Boltzmann's constant, T is the temperature, P_γ is the γ component of the polarization, and "$\langle\ \rangle$" denotes thermal averages. A crucial point is how the long-range Coulomb interaction is accounted for in the simulation: Eq. (1) assumes periodic boundary conditions (also called Ewald-Kornfeld by practitioners of classical simulations), while other schemes are in use as well, and lead to different fluctuation formulas.[1] Equation (1) has been put in use to, e.g., provide a real-space interpretation of dielectric responses in various materials[2] and to understand the reasons behind unusual dielectric features[3,4] (examples, among others, of such unusual features are a broad dielectric peak in the so-called relaxor systems,[6–11] or greater broadening of the dielectric response when inserting defects[12–14]). Fluctuation formulas also have an obvious computational advantage since their use avoids the need of performing additional calculations, in which an electric field is turned on, to compute the dielectric response.

Interestingly, it is currently unknown if Eq. (1) has to be modified when investigating ferroelectric *nanostructures* that are systems of high current fundamental and technological interest (see Refs. 15–18 and references therein). In particular, one may wonder if and how the depolarizing field existing in low-dimensional ferroelectric systems affects the relation between dielectric response and polarization fluctuations. Note that such field is sensitive to the shape and dimensionality of the nanostructure, and is already known to dominate the polarization quantum fluctuations at $T=0$ K,[19] as well as to be responsible for some interesting phenomena. (Examples of such phenomena are the existence of a critical thickness below which no ferroelectricity can appear[20] and the observation and prediction of laminar stripe nanodomains with exceptional small periodicity in ferroelectric thin films;[21–23] and the formation of a vortex structure for the electric dipoles in zero-dimensional ferroelectrics.[24,25])

The aim of this paper is to establish the link between dielectric response and polarization fluctuations in ferroelectric nanostructures, via analytical derivations and atomistic simulations. As we will see, two different kinds of dielectric response have to be distinguished, with one of them needing a modification of the bulk formula given in Eq. (1). This paper is organized as follows. Section II reports the analytical development, while computational details and results are given in Sec. III. Finally, a summary is provided in Sec. IV.

II. FLUCTUATION FORMULAS

We consider the case where a ferroelectric nanostructure of volume V is polarized by a given *external* macroscopic field $\mathbf{E}_0$, defined as the field far outside the sample. The system response induces a depolarizing field, such that the *internal* field $\mathbf{E}$ differs from $\mathbf{E}_0$. Depending on the size and shape of the nanostructure, the field $\mathbf{E}$ can be either homogeneous or inhomogeneous. In either case, we define $\langle \mathbf{E} \rangle$ as the sample average of the microscopic field.

The Hamiltonian of a nanostructure under the applied field $\mathbf{E}_0$ and under any possible electrical boundary conditions can be written as[26,27]

$$H = H^{(0)} - V\mathbf{P} \cdot [\mathbf{E}_0 - \beta \langle \mathbf{E}^{(MD)} \rangle], \tag{2}$$

where $V\mathbf{P}$ is the dipole of the finite sample and $\mathbf{E}^{(MD)}$ is the maximum depolarizing field. (Notice that, since a mean value of $\mathbf{E}^{(MD)}$ occurs in the definition of Eq. (2), H is a "self-consistent" Hamiltonian.) $H^{(0)}$ gathers all the energetic terms (including ones related to the maximum depolarizing field) that do not explicitly depend on $\mathbf{E}_0$ and that correspond to an ideal "open-circuit" boundary condition. The β param-

Effects of vacancies on the properties of disordered ferroelectrics: A first-principles study

L. Bellaiche,[1] Jorge Íñiguez,[2] Eric Cockayne,[3] and B. P. Burton[3]
[1]*Physics Department, University of Arkansas, Fayetteville, Arkansas 72701, USA*
[2]*Institut de Ciencia de Materials de Barcelona (ICMAB-CSIC), Campus de la UAB, 08193 Bellaterra (Barcelona), Spain*
[3]*Ceramics Division, Materials Science and Engineering Laboratory, National Institute of Standards and Technology, Gaithersburg, Maryland 20899-8520, USA*

(Received 8 September 2006; revised manuscript received 2 November 2006; published 22 January 2007)

A first-principles-based model is developed to investigate the influence of lead vacancies on the properties of the disordered $Pb(Sc_{1/2}Nb_{1/2})O_3$ (PSN) ferroelectric. Lead vacancies generate large, inhomogeneous, electric fields that reduce barriers between energy minima for different polarization directions. This naturally explains why disordered ferroelectrics with significant lead vacancy concentrations have broadened dielectric peaks at lower temperatures, and why lead vacancies smear properties in the neighborhood of the ferroelectric transition in PSN. We also reconsider the conventional wisdom that lead vacancies reduce the magnitude of dielectric response.

DOI: 10.1103/PhysRevB.75.014111 PACS number(s): 61.72.Bb, 61.43.−j, 61.72.Ji, 77.84.Dy

I. INTRODUCTION

Experimentally, the introduction of vacancies into disordered ferroelectrics induces greater broadening of the dielectric response.[1–3] Other Pb-vacancy-induced effects include shifting of the dielectric peak to lower temperature; a decrease in the magnitude of the dielectric response; and a more "diffuse" phase transition.[1–3]

Defects are always present in real samples, and they often have a significant impact on measured properties, but the mechanisms responsible for vacancy-induced effects are mostly unknown. Understanding such mechanisms would illuminate the fundamentals of the behavior of disordered ferroelectrics, including those exhibiting the so-called *relaxor* features. One reason for this paucity of knowledge is that first-principles studies of (point) defects in ferroelectrics are scarce.[4–7]

Ultimately, one would like to study, via *ab initio* techniques, the effect(s) of Pb vacancies on the properties of disordered ferroelectrics exhibiting relaxor behavior, such as the prototype relaxor $Pb(Mg_{1/3}Nb_{2/3})O_3$ (PMN). Unfortunately, because of the markedly different chemical character of Mg and Nb, PMN is a very challenging subject for *ab initio* modeling. Thus, in this manuscript we investigate instead the $Pb(Sc_{1/2}Nb_{1/2})O_3$ (PSN) disordered ferroelectric, for which finite-temperature first-principles-based models are available.[8,9] Note that, unlike PMN which retains relaxor character down to 0 K (i.e., it exhibits no ferroelectric phase transition), chemically disordered PSN exhibits relaxor behavior between ~400 K and ~368 K, then transforms to a rhombohedral ferroelectric phase.[1,2] Interestingly, Ref. 1 reports that the introduction of 1.7% Pb vacancies into disordered PSN results in a ≈2.6% reduction of the T_m temperature at which the dielectric response is maximized (at low frequency), while smearing out the relaxor-to-ferroelectric transition. Furthermore, Ref. 2 indicates that lead vacancies can lead to the appearance of ferroelectricity at a slightly higher temperature than T_m.

Here we focus on static properties, because studying the dynamics of disordered ferroelectrics from first principles is not currently feasible. Admittedly, this restriction, plus the close proximity of T_m to the ferroelectric transition temperature in PSN, makes it difficult to distinguish between effects of Pb vacancies that pertain specifically to relaxor characteristics, and those that pertain to disordered ferroelectrics in general. Therefore, we limit our conclusions to the effects of Pb vacancies on the properties of disordered ferroelectrics. Our study clarifies the origin(s) of the vacancy-induced effects mentioned above, and suggests that the common wisdom that Pb vacancies reduce the magnitude of dielectric response should be reconsidered.

This manuscript is organized as follows: Section II describes the method. Section III presents and discusses results. Section IV is a brief summary.

II. METHOD

Our method is a generalization of the first-principles-derived effective Hamiltonian of Refs. 9–11 to investigate perovskites with chemical disorder on their B sites and Pb vacancies on their A sites, by writing the total energy as a sum of two terms:

$$E_{\text{PSN-DV}}(\{\mathbf{u}_i\}, \eta_H, \{\eta_I\}, \{\sigma_j\}, \{s_k\}) = E_{\text{PSN-D}}(\{\mathbf{u}_i\}, \eta_H, \{\eta_I\}, \{\sigma_j\}) + E_{\text{vac}}(\{\mathbf{u}_i\}, \{s_k\}), \quad (1)$$

where $E_{\text{PSN-DV}}$ is the total energy of the $Pb_{1-x}\square_x(Sc_{1/2}Nb_{1/2})O_3$ alloy (PSN-DV), $\square$ representing a vacant A site; $E_{\text{PSN-D}}$ is the total energy of chemically disordered PSN solid solutions (PSN-D); E_{vac} gathers the explicit energetics associated with Pb vacancies; $\mathbf{u}_i$ is the (B centered) local polar distortion in unit cell i (proportional to the local dipole moment); η_H and $\{\eta_I\}$ are the *homogeneous* and *inhomogeneous* strain tensors,[12] respectively; $\sigma_j = -1$ or $+1$ if there is a Sc or Nb cation, respectively, at the B-lattice site j of the $Pb_{1-x}\square_x(Sc_{1/2}Nb_{1/2})O_3$ alloy. Finally, $\{s_k\}$ characterizes the amount and distribution of A-site vacancies, i.e., $s_k = 0$ or 1 if the k'th A site is occupied by a lead atom or vacant, respectively.

For $E_{\text{PSN-D}}$, we use the analytical expression proposed in Ref. 9, which includes a term of the form $-\Sigma_i Z^* \mathbf{u}_i \cdot \epsilon_i[\{\sigma_j\}]$,

Domain evolution of $BaTiO_3$ ultrathin films under an electric field: A first-principles study

Bo-Kuai Lai, Inna Ponomareva, Igor A. Kornev, L. Bellaiche, and G. J. Salamo
Physics Department, University of Arkansas, Fayetteville, Arkansas 72701, USA
(Received 3 October 2006; published 8 February 2007)

A first-principles-derived method is used to study the morphology and electric-field-induced evolution of stripe nanodomains in (001) $BaTiO_3$ (BTO) ultrathin films, and to compare them with those in (001) $Pb(Zr,Ti)O_3$ (PZT) ultrathin films. The $BaTiO_3$ systems exhibit 180° periodic stripe domains at null electric field, as in PZT ultrathin films. However, the stripes alternate along [1–10] in BTO systems versus [010] in PZT systems, and no in-plane surface dipoles occur in BTO ultrathin films (unlike in PZT materials). Moreover, the evolution of the 180° stripe domains in the $BaTiO_3$ systems, when applying and increasing an electric field along [001], involves four regions: region I for which the magnitude of the "down" dipoles (i.e., those that are antiparallel to the electric field) is reduced, while the domain walls do not move; region II in which some local down dipoles adjacent to domain walls switch their direction, resulting in zigzagged domain walls—with the overall stripe periodicity being unchanged; region III in which nanobubbles are created, then contract along [110] and finally collapse; and region IV which is associated with a single monodomain. Such evolution differs from that of PZT ultrathin films for which neither region I nor zigzagged domain walls exist, and for which the bubbles contract along [100]. Discussion about such differences is provided.

DOI: 10.1103/PhysRevB.75.085412 PACS number(s): 68.55.−a, 77.80.Bh, 77.84.Dy, 77.80.Dj

I. INTRODUCTION

Ferroelectric materials are the heart of many applications such as nonvolatile memories, communication devices, and microactuators.[1] The continuing miniaturization of these devices has stimulated considerable research attention on ferroelectric thin films (see, e.g., Refs. 2 and 3, and references therein). Such systems can exhibit striking phenomena because of some finite-size effect. For instance, they can adopt periodic stripe domains with exceptionally small periods (i.e., in the order of a few nanometers), when experiencing some specific mechanical and electrical boundary conditions.[2–12] Interestingly, the morphology of such nanostripe patterns seem to dramatically depend on the materials, as suggested by the facts that 180° nanostripes are known to alternate along the [010] direction in (001) $Pb(Zr,Ti)O_3$ (PZT) and $PbTiO_3$ thin films[5,6,9–11] while Ref. 4 predicts that such stripes alternate along another direction (namely, along [1–10]) in (001) $BaTiO_3$ (BTO) ultrathin films. The exact reason behind such difference, that is reminiscent of distinct behaviors found in Pb- vs Ba-based alloys,[13,14] remains to be addressed. One may also wonder if other differences exist for the morphology of the stripe domains in PZT and BTO films, and, if so, why. For instance, do dipoles at the *surfaces* of BTO films also lie in-plane (to close the flux as in PZT films[6,9] and in the Landau-Lifschitz model of domains[15]), or rather prefer to all lie along the growth direction (as in the Kittel model of domains[16]), or even adopt an intermediate case (e.g., form an angle of 45° between the in-plane and out-of-plane directions)? Another fundamental question to be addressed regarding stripe domains in BTO thin films is their precise atomistic evolution under the application of the factor that lies at the heart of many ferroelectric devices, namely an external electric field. More specifically, how do the differences between the initial stripe domains in BTO and PZT films affect the (very unusual) stripe→ferroelectric nanobubble→monodomain transition sequence that has been recently predicted and documented in detail for PZT ultrathin films under applied fields?[9] In particular, it would be worthwhile to have a deep microscopic insight about the mechanisms leading to the disappearance of the nanostripes in favor of ferroelectric nanobubbles (that bear resemblance with ferromagnetic bubbles in ferromagnetic films[17]), and about the evolution of the morphology of these ferroelectric nanobubbles, under an electric field in BTO films—especially, when realizing that $BaTiO_3$ bulk is the most extensively studied system among all ferroelectrics[18] while little is still known about the domains[4] and their electric-field-induced domain evolution[9] in epitaxial $BaTiO_3$ ultrathin films.

The aims of this article are to use first-principles-based techniques to (i) provide atomistic details of domains in BTO ultrathin films, (ii) indicate how such domains evolve as a function of applied electric field, (iii) compare the properties of BTO ultrathin films with those of PZT ultrathin films, as well as to discuss and understand their similarities and differences.

The remainder of this paper is organized as follows. In Sec. II, the theoretical method is described. The stripe domains in 20-Å-thick BTO thin films, and their energetic origins, are presented in Sec. III A, with a special emphasis on explaining the difference in morphology between periodic nanostripes in BTO and PZT thin films. Section III B depicts the electric-field-induced domain evolution in the BTO ultrathin films, and compares it with the corresponding domain evolution in PZT ultrathin films. Finally, a conclusion is provided in Sec. IV.

II. THEORETICAL METHOD

The presently studied BTO and PZT ultrathin films are assumed to be grown along the [001] direction (z axis) and are Ba-O and Pb-O terminated, respectively, at all surfaces. The PZT films are disordered in nature, with a Ti overall

Finite-Temperature Properties of Multiferroic $BiFeO_3$

Igor A. Kornev,[1,2] S. Lisenkov,[1] R. Haumont,[3] B. Dkhil,[4] and L. Bellaiche[1]

[1]*Physics Department, University of Arkansas, Fayetteville, Arkansas 72701, USA*

[2]*Mads Clausen Institute for Product Innovation, University of Southern Denmark, Alsion 2, DK-6400 Sønderborg, Denmark*

[3]*Laboratoire de Physico-Chimie de l'Etat Solide (CNRS), ICMMO, Université Paris XI, 91405 Orsay, France*

[4]*Laboratoire Structures, Propriétés et Modélisation des Solides, Ecole Centrale Paris, CNRS-UMR8580, Grande Voie des Vignes, 92295 Châtenay-Malabry Cedex, France*

(Received 5 July 2007; published 30 November 2007)

An effective Hamiltonian scheme is developed to study finite-temperature properties of multiferroic $BiFeO_3$. This approach reproduces very well (i) the symmetry of the ground state, (ii) the Néel and Curie temperatures, and (iii) the intrinsic magnetoelectric coefficients (that are very weak). This scheme also predicts (a) an overlooked phase above $T_C \simeq 1100$ K that is associated with antiferrodistortive motions, as consistent with our additional x-ray diffractions, (b) improperlike dielectric features above T_C, and (c) that the ferroelectric transition is of first order with no group-subgroup relation between the paraelectric and polar phases.

DOI: 10.1103/PhysRevLett.99.227602 PACS numbers: 77.80.Bh, 75.50.Ee, 75.80.+q

Multiferroics form a class of materials that can simultaneously possess ferroelectricity and magnetic ordering [1]. They can therefore exhibit a magnetoelectric (ME) coupling that allows electrical properties to be tuned by a magnetic field or, conversely, magnetic properties to be varied by an electric field. These systems are experiencing a huge regain in interest (see, e.g., Ref. [2], and references therein). As a result, some controversial and/or puzzling effects have been recently reported in $BiFeO_3$ bulk—which is one of the most studied multiferroics, and has a T_N Néel temperature of $\simeq 625$–643 K [3,4] and another transition temperature around 1083–1103 K [4,5] at which the material transforms from a ferroelectric rhombohedral state to another phase. Examples of such effects are the symmetry of this latter high-temperature phase: is it paraelectric cubic [6], ferroelectric orthorhombic [7], or even something else that has been missed? Other intriguing features are the character of the phase transition around 1100 K (that is, said to be not soft-mode driven in Ref. [6]), and the magnetic-induced change of the dielectric constant that varies by several orders of magnitude for temperatures below versus above 175 K [8]—which raises questions about the value of the intrinsic ME coefficients or, equivalently, the importance of defects on the ME coupling in $BiFeO_3$ samples. First-principles techniques can lead to a better understanding of multiferroics (see, e.g., Refs. [9–11]), but not the point to address the aforementioned issues since these techniques are essentially restricted to the study of zero-temperature properties and cannot currently compute ME coefficients. Ideally, one desires an atomisticlike scheme with the capability of accurately predicting properties of multiferroics at finite temperature, including their ME couplings.

The purpose of this Letter is to demonstrate that it is possible to develop such an "ideal" approach and to apply it to $BiFeO_3$ bulk. The use of this scheme, and additional x-ray measurements we further conducted, provide answers to all the aforementioned issues and also yield overlooked phenomena.

Our numerical scheme is based on the generalization of the effective Hamiltonian of Ref. [12] to include magnetic degrees of freedom, in addition to ferroelectric (FE) and antiferrodistortive (AFD) motions. The total energy, E_{tot}, is written as a sum of two main terms, $E_{\text{FE-AFD}}(\{\mathbf{u}_i\}, \{\eta_H\}, \{\eta_I\}, \{\omega_i\})$ and $E_{\text{MAG-C}}(\{\mathbf{m}_i\}, \{\mathbf{u}_i\}, \{\eta_H\}, \{\eta_I\}, \{\omega_i\})$, where $E_{\text{FE-AFD}}$ is the energy provided in Ref. [12], while $E_{\text{MAG-C}}$ is an additional term gathering magnetic degrees of freedom and their couplings. $\mathbf{m}_i$ is the magnetic dipole moment centered on the Fe site i. $\mathbf{u}_i$ is the (Fe-centered) local soft mode in unit cell i, which is directly proportional to the electrical dipole centered on that site; $\{\eta_H\}$ and $\{\eta_I\}$ are the homogeneous and inhomogeneous strain tensors [13], respectively; $\{\omega_i\}$ is a (Fe-centered) vector characterizing the direction and magnitude of the AFD motions in unit cell i.

For $E_{\text{MAG-C}}$, we propose the following expression:

$$E_{\text{MAG-C}}(\{\mathbf{m}_i\}, \{\mathbf{u}_i\}, \{\eta_H\}, \{\eta_I\}, \{\omega_i\}) = \sum_i \sum_{j \neq i} D_{ij} \mathbf{m}_i \cdot \mathbf{m}_j + \sum_i u_i^2 \sum_{j \neq i} E_{ij} \mathbf{m}_i \cdot \mathbf{m}_j + \sum_i [\eta_1(i) + \eta_2(i) + \eta_3(i)] \sum_{j \neq i} F_{ij} \mathbf{m}_i \cdot \mathbf{m}_j + \sum_i \omega_i^2 \sum_{j \neq i} G_{ij} \mathbf{m}_i \cdot \mathbf{m}_j, \quad (1)$$

where the sums over i run over all the Fe sites while the sums over j run over the first, second, and third nearest neighbors of the Fe site i. $\eta_l(i)$ is the lth component, in Voigt notation, of the total strain at the site i, with the x, y, and z axes being along the pseudocubic [100], [010], and [001] directions, respectively. The first term of Eq. (1) represents the exchange

Influence of crystallographic steps on properties of ferroelectric ultrathin films: An *ab initio* study

S. Prosandeev[a)]
Physics Department, University of Arkansas, Fayetteville, Arkansas 72701 and Institute of Physics, Rostov State University, Rostov on Don 344090, Russia

L. Bellaiche
Physics Department, University of Arkansas, Fayetteville, Arkansas 72701

(Received 11 June 2007; accepted 20 July 2007; published online 13 August 2007)

A first-principles-based approach is used to investigate the effect of a crystallographic step on the existence and morphology of the recently discovered periodic nanostripe domains [S. K. Streiffer *et al.*, Phys. Rev. Lett. **89**, 067601 (2002)] in $Pb(Zr_{1-x}Ti_x)O_3$ ultrathin films. It is found that these domain structures do not vanish in the presence of such defect but rather evolve to form original stripe configurations to accommodate this step. The morphology and energetics of these original configurations are provided. Their dependencies on the film's thickness and the step's height is also discussed. © *2007 American Institute of Physics*. [DOI: 10.1063/1.2770764]

Ferroelectric materials are at the heart of many applications such as nonvolatile memories, communication devices, and microactuators.[1] The continuing miniaturization of these devices has generated considerable research attention on ferroelectric thin films (see, e.g., Refs. 2 and 3 and references therein). Such low-dimensional systems can exhibit unusual phenomena because of finite-size effects. Examples are the discovery of periodic stripe domains with nanometric periods[4–7] and their breaking up into ferroelectric nanobubbles under an applied electric field.[8] The dependency of the morphology of these unusually small periodic stripes on various factors has also been recently investigated and understood at a microscopic level. These factors are the ferroelectric material the film is made of,[9] the out-of-plane direction of the film,[10] and the asymmetric screening of the depolarizing field between the substrate/film interface and the top surface of the film.[11,12] On the other hand, very little is known on the effect of *defects* on properties of thin and especially ultrathin films, despite their potential importance (defects are known to dramatically affect properties of ferroelectric bulks, see, e.g., Refs. [13–18] and references therein). In particular, one may wonder how the presence of the defect that is unavoidably present in grown films, which is a crystallographic step, affects the recently discovered periodic stripe structure.[4] Does this step "wash out" this peculiar stripe structure (because their characteristic lengths can be both in the order of nanometers) or, rather, does the stripe structure "respond" to the existence of a step by adopting new morphologies? If so, what are these new morphologies and how can we understand them?

The aim of this letter is to determine the influence of crystallographic steps on the existence, morphology, and energetics of stripe domains in ferroelectric ultrathin films, via the use of a first-principles-derived technique.

Here, we consider (001) $PbZr_{1-x}Ti_xO_3$ (PZT) thin films with a Ti composition $x=0.6$. (Note that such composition generates a ferroelectric tetragonal ground state, in which the polarization points along a ⟨001⟩ direction, in the corresponding bulk.) These films are either defect-free or exhibit a crystallographic step, running along the x axis, at their top (001) surface—with the x, y, and z axes lying along the [100], [010], and [001] directions, respectively. Such systems are assumed to be grown on a nonconducting and nonferroelectric substrate, and to be surrounded by vacuum above their top surfaces. All their surfaces and interfaces are PbO terminated. These low-dimensional systems are mimicked by $l\times m\times n$ supercells (where l, m, and n are integers) that are periodic along the x and y directions but finite along the z axis. A region of $l\times(m/2)\times s$ dimensions (where $4s$ is the step's height in angstrom), located at the top of these supercells, is imposed to be made of vacuum, in the case of films exhibiting a step. The total energy of the studied systems is written as

$$E_{tot}(\{\mathbf{p_i}\},\{\mathbf{v_i}\},\{\sigma_i\},\hat{\eta}) = E_{mat}(\{\mathbf{p_i}\},\{\mathbf{v_i}\},\{\sigma_i\},\hat{\eta}) + E_{surf}(\{\mathbf{p_i}\},\{\mathbf{v_i}\}), \quad (1)$$

where $\mathbf{p_i}$ are the electric dipoles centered at the i sites of the supercell containing Zr or Ti atoms, and $\mathbf{v_i}$ are dimensionless vectors describing the inhomogeneous strain around these sites.[19] $\{\sigma_i\}$ characterizes the alloy configuration[20] that is presently randomly chosen, in order to mimic a disordered system. $\hat{\eta}$ is the homogeneous strain tensor. Here, we wish to mimic films that are compressively strained on a substrate with a misfit strain of 2.65%, since such mechanical boundary condition is known to generate periodic nanostripes in defect-free PZT films under open-circuit-like conditions.[5] Such mechanical boundary conditions are practically generated by freezing three components of $\hat{\eta}$ (namely, $\eta_6=0$, and $\eta_1=\eta_2=-2.65\%$), while the other three components (in Voigt notation) are allowed to relax. The expression and first-principles-derived parameters of E_{mat}, the intrinsic effective-Hamiltonian energy of the film, are those given in Ref. 20 for PZT *bulk* close to their morphotropic phase boundary, except for the dipole-dipole interactions for which we use the analytical expressions derived in Refs. 21 and 22 for our $l\times m\times n$ supercells under ideal open-circuit conditions. The second energetic term, E_{surf}, of Eq. (1) mimics how the existence of the top (001) free surfaces, and of the (010) free surface associated with the step, affects the dipoles

a)Electronic mail: sprossan@uark.edu

Asymmetric screening of the depolarizing field in a ferroelectric thin film

S. Prosandeev[1,2] and L. Bellaiche[1]
[1]*Physics Department, University of Arkansas, Fayetteville, Arkansas 72701, USA*
[2]*Institute of Physics, Rostov State University, Rostov on Don 344090, Russia*
(Received 13 April 2007; revised manuscript received 4 May 2007; published 31 May 2007)

A first-principles-based approach is developed to mimic the (asymmetric) screening of the depolarizing field at the top surface of ferroelectric ultrathin films. Varying the magnitude of this one-side screening (i) results in the formation of different kinds of periodic nanostripe domain patterns, including original ones that are highly asymmetric and that can be thought of as connecting (and generalizing) the traditional Landau-Lifshitz and Kittel models of dipolar domains, and (ii) leads to a change in the domain's period, suggesting that the asymmetric screening of the depolarizing field is responsible for the existence of two recently observed nanostripe phases.

DOI: 10.1103/PhysRevB.75.172109 PACS number(s): 68.55.−a, 77.22.Ej, 77.80.Bh, 77.80.Dj

Stripe domains in ferromagnetic and ferroelectric systems are of technological importance because the properties of such systems depend strongly on the dipole arrangement. They are also of great fundamental interest because, among other things, their morphology reveals the balance between competitive interactions. The first theory of stripe domain structures was developed by Landau and Lifshitz in 1935 for magnetic systems.[1] In this model, the dipoles at the surfaces lie in plane, while the dipoles inside the film are parallel or antiparrel to the film's orientation (to be referred to as the z axis). This results in a closure domain pattern (that does not produce any macroscopic field outside the film) with 90° domain walls. The stability of this kind of stripe domain is due to the anisotropy of the lattice, with the easiest axis being along the z axis, overcoming the energetic cost of having domain walls. Later on, Kittel[2] suggested another pattern for stripe domains in magnetic thin films, in which all dipoles (including the ones at the surface) point either along the $+z$ or $-z$ direction. Such pattern produces a (stray) magnetic field outside the film that results in a costly magnetostatic energy. Such a solution is thus only stable for "uniaxial" thin films, i.e., having a very large anisotropy that overcomes the magnetostatic energy. The traditional Landau-Lifshitz and Kittel models both lead to the annihilation of the so-called demagnetizing and/or depolarizing field inside the film, and both predict that the stripe pattern of a given film under a given mechanical boundary condition has a unique domain period (that solely depends on the thickness of the film). Recently, 180° periodic stripe domain structures, with remarkably small periods (of the order of nanometers), were observed in ultrathin ferroelectric films.[3] The morphology of such stripes were not determined because this represents a major experimental challenge. On the other hand, a rather surprising result was found; namely, that these stripes can have two different periods for the same film but for different temperatures. It was then suggested that the existence of these two periods (that roughly differ by a ratio of $\sqrt{2}$) is related to the asymmetry of the experimental setup; namely, that the top (free) surface and the bottom (substrate/film) interface do not provide the same quantitative screening (if any) of the depolarizing field and that this asymmetry is somehow temperature dependent.[3] One may want to know if this suggestion is indeed correct, and one may also wonder if other stripe patterns (that is, deviating from the traditional Landau-Lifshitz and Kittel pictures) can result from this asymmetric screening. (Note that Ref. 4 strongly hints that varying the magnitude of the asymmetric screening of the depolarizing field can indeed affect domain width. However, the authors of Ref. 4 assumed that the Kittel model always applies when describing the domain configuration, which may have prevented them from discovering other stripe patterns.) Obviously, first-principles-based methods constitute a powerful tool to answer such questions because of their accuracy and deep microscopic insight. However, such methods have "only" been developed and/or used so far (to the best of our knowledge) to tackle problems related to a *symmetric* screening of the depolarizing field,[5–9] that is, when both surfaces similarly contribute to the domain's morphology.

The aims of this study are twofold. First, we wish to develop a first-principles-based approach allowing an asymmetric screening of the depolarizing field. Secondly, we want to use such a method to provide answers to the aforementioned questions. As we will see, such asymmetric screening can result in other stripe domain patterns and can indeed explain the experimental observations of Ref. 3.

Here, we consider a (001) $PbZr_{1-x}Ti_xO_3$ (PZT) thin film sandwiched by a nongrounded metallic plate, from the top side, and by a nonconducting substrate, from the bottom side. The film is PbO terminated. The distance between the top BO layer (where B atoms are either Ti or Zr) of the thin film and the metallic plate is denoted as R_{met}, and is allowed to vary. A "dead layer" (separating the top PbO surface and the metallic plate) can thus exist in our simulation, with its thickness being denoted by D and being equal to $R_{met}-\frac{a}{2}$ (where a is the five-atom unit-cell parameter). Here, this dead layer is assumed to possess a dielectric permittivity equal to unity. Specifically, the Ti composition and the thickness of the film are chosen to be $x=0.6$ and 48 Å, respectively. Such film is mimicked by a $6\times48\times12$ supercell that is periodic along the x and y directions but finite along the z axis. (The x, y, and z axes lie along the [100], [010], and [001] directions, respectively.) Its total energy is written as

$$E_{tot}(\{\mathbf{p_i}\},\{\mathbf{v_i}\},\{\sigma_i\},\hat{\eta}) = E_{mat}(\{\mathbf{p_i}\},\{\mathbf{v_i}\},\{\sigma_i\},\hat{\eta}) + E_{surf}(\{\mathbf{p_i}\},\{\mathbf{v_i}\}) + E_{scr}(\{\mathbf{p_i}\}), \quad (1)$$

PHYSICAL REVIEW B 76, 020102(R) (2007)

Phase diagrams of $BaTiO_3/SrTiO_3$ superlattices from first principles

Sergey Lisenkov* and L. Bellaiche
Department of Physics, University of Arkansas, Fayetteville, Arkansas 72701, USA
(Received 20 June 2007; published 12 July 2007)

A first-principles-based technique is used to determine the temperature *versus* misfit strain phase diagram of epitaxially grown (001) $BaTiO_3/SrTiO_3$ superlattices of different periods. *Short* superlattices exhibit a phase diagram that resemble that of (001) $BaTiO_3$ thin films under short-circuit-like conditions. On the other hand, original domain patterns with unusual atomistic features occurred in the *longer* superlattices. The reason behind such a dramatic difference between short and longer superlattices is discussed.

DOI: 10.1103/PhysRevB.76.020102 PACS number(s): 77.80.Bh, 68.65.Cd, 81.05.Zx, 81.30.Bx

The fabrication of superlattices (SL) consisting of alternating layers of two or more ferroelectric oxides is currently possible, which has motivated a flurry of theoretical and experimental activities (see e.g., Refs. 1–14, and references therein). Such heterostructures can possess original and/or optimized properties due to their sensitivity to various factors. Some of such factors have been intensively studied in the past years, and are the ions and compositions of the constituent layers.[1–14] On the other hand, the epitaxial strain arising from the substrate on which the superlattice is grown is a parameter that has been much less investigated,[4,5] despite its promise in delivering novel features—as found in ferroelectric thin films (see, e.g., Refs. 15 and 16 and references therein). Determining the temperature versus misfit strain diagram of superlattices is thus of considerable importance. In particular, this determination, if accomplished by accurate atomistic approaches, can reveal if periodic nanostripe domains (rather than monodomains) can occur in SL, and, if so, what is their precise morphology (the existence and morphology of domains in SL are unsettled issues, to the best of our knowledge[2,14]). For instance, one may wonder if the atomistic features of domains in SL differ from those associated with the nanodomains recently found in two-dimensional (2D) ferroelectric thin films.[17–23] Determining from *ab initio* simulations the temperature versus misfit strain diagram for SL having different periods may also explain why observed properties (including dipole patterns) seem to adopt a different behavior between superlattices with short versus longer periods.[2,7,8,14]

Here, we use a first-principles-based approach to determine the temperature versus misfit strain diagram of $BaTiO_3$ (BT)/$SrTiO_3$ (ST) superlattices—which are the most widely investigated SL (see, e.g., Refs. 1–5, and references therein). As we will see, such superlattices exhibit a variety of dipole patterns, depending on the substrate-induced strain and SL period.

More precisely, we use the recently developed first-principles-based scheme of Ref. 24 to determine such phase diagrams. This atomistic method is an extension of the effective Hamiltonian approach of Ref. 25 for solid solutions, and has been successfully tested for disordered and ordered $Ba_{1-x}Sr_xTiO_3$ systems. Moreover, unlike direct first-principles calculations, this scheme can be easily applied to investigate *finite-temperature* properties of relatively *large* systems—which is of obvious advantage for determining complex dipole patterns—by using its total energy in Monte Carlo simulations (and thus obtain states that minimize the free energy). Epitaxially strained $[BaTiO_3]_n/[SrTiO_3]_n$ SL having n layers of $BaTiO_3$ alternating with n layers of $SrTiO_3$ along the [001] direction—which is chosen to be the z axis—are investigated here. We mostly focus on two different superlattice periods, corresponding to $n=2$ (ultrashort SL) and $n=10$ (longer SL). Note that the superlattice associated with $n=20$ was also considered, but we do not report or discuss its results since they are qualitatively similar to those corresponding to $n=10$. Moreover, the predictions to be shown below for $[BaTiO_3]_2/[SrTiO_3]_2$ and $[BaTiO_3]_{10}/[SrTiO_3]_{10}$ correspond to the use of $12\times12\times4$ (2880 atoms) and $12\times12\times20$ (14 400 atoms) supercells, respectively, that are periodic in all three directions—implying that our studied systems, as a whole, are under short-circuit electrical boundary conditions. Note that additional calculations were performed with different numbers of unit cells (namely, 16, 20, and 24) along the x and y directions (to be chosen along the [100] and [010] pseudocubic directions, respectively) with no major significant difference in properties being found. The epitaxial situations were mimicked by freezing some strain variables, in order to impose that *each* layer in the strained superlattice has the same in-plane lattice constant as the chosen substrate.[15,16,19,24,26]

Figure 1 shows our predicted temperature versus misfit

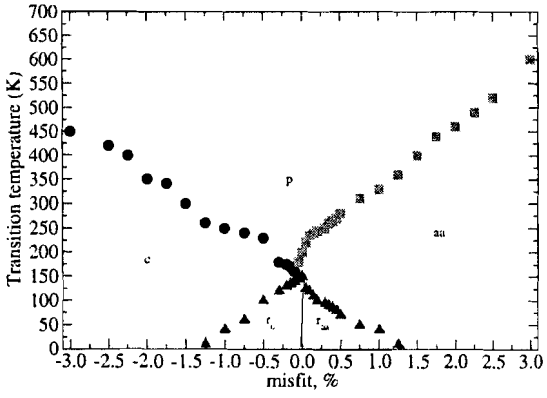

FIG. 1. (Color online) Temperature versus misfit strain phase diagram of the ultrashort ($n=2$) $[BaTiO_3]_2/[SrTiO_3]_2$ superlattice. The solid line displays the boundary between the r_c and r_{aa} states.

Dielectric Anomalies in Ferroelectric Nanostructures

I. Ponomareva,[1,*] L. Bellaiche,[1] and R. Resta[2,3]

[1]*Department of Physics, University of Arkansas, Fayetteville, Arkansas 72701, USA*
[2]*Dipartimento di Fisica Teorica, Università di Trieste, Strada Costiera 11, 34014 Trieste, Italy*
[3]*INFM DEMOCRITOS National Simulation Center, via Beirut 2, 34014 Trieste, Italy*

(Received 2 August 2007; published 29 November 2007)

First-principles-based methods are used to determine the external dielectric susceptibility (i.e., the polarization response to the *external* electric field) and the internal susceptibility (i.e., the polarization response to the average *internal* field) in ferroelectric dots, wires, and films, as a function of the electrical boundary conditions. While the external susceptibility is obviously positive, we find that the internal one is *negative* over a wide range of boundary conditions for all kinds of nanostructures. A Landau-type phenomenological model provides a rationale for all of our findings.

DOI: 10.1103/PhysRevLett.99.227601 PACS numbers: 77.22.Ej, 71.15.−m, 77.55.+f, 77.84.−s

Ferroelectric nanostructures (FEN) are of increasing technological interest because of their need in miniaturization of devices [1]. The low dimensionality is responsible for exotic phenomena, due to depolarizing fields' effects [2–7]. Recently, the occurrence of *negative* static dielectric susceptibilities has been predicted in *thin layers* [8,9]. Interestingly, a negative dielectric susceptibility is essential in the quest for systems exhibiting a negative index of refraction [10], but it is unclear how a static dielectric susceptibility can be negative without violating any stability requirement [11]. One may also wonder if this negative sign is only typical of thin films or rather if other FENs can also exhibit such anomaly. Similarly, it is worthwhile to know the influence of the magnitude of the residual depolarizing field and its related different dipole patterns [4,5,12,13] on this negative sign.

Here, we show that more than one dielectric susceptibility can be defined in FENs, in analogy with the magnetic case [14]. We define $\chi_{\gamma\gamma}^{(\mathrm{ext})}$ as the polarization response of the finite sample of volume V to the external field $\mathbf{E}_0$ and $\chi_{\gamma\gamma}^{(\mathrm{int})}$ as the response to the internal (screened) field $\langle\mathbf{E}\rangle$:

$$\chi_{\gamma\gamma}^{(\mathrm{ext})} = \frac{\partial\langle P_\gamma\rangle}{\partial E_{0,\gamma}}; \qquad \chi_{\gamma\gamma}^{(\mathrm{int})} = \frac{\partial\langle P_\gamma\rangle}{\partial\langle E_\gamma\rangle}, \tag{1}$$

where "$\langle\rangle$" denotes a double average: thermal average and average over the finite sample. γ refers to Cartesian coordinates and $V\langle\mathbf{P}\rangle$ is the dipole of the finite sample.

We then perform microscopic simulations via a model Hamiltonian, where the depolarizing field can be tuned by means of a screening parameter. We find that $\chi_{\gamma\gamma}^{(\mathrm{ext})}$, being proportional to the dipolar polarizability of a finite sample, is always positive in any studied FEN. At variance with this and for almost the whole screening parameter range, the internal susceptibility is *negative* in thin films but also in rods and dots. Finally, we establish a phenomenological model based on a Landau-type approach, which nicely reproduces (and helps understand) all of the main features emerging from the simulations, as well as leads to another result: there exists an intrinsic or "bulk" susceptibility (i.e., that is independent of boundary conditions and dimensionality) that neither coincides with $\chi_{\gamma\gamma}^{(\mathrm{ext})}$ nor with $\chi_{\gamma\gamma}^{(\mathrm{int})}$.

Here, we focus on ferroelectric nanostructures made of disordered $Pb(Zr_{0.4}Ti_{0.6})O_3$ (PZT60) solid solutions. We consider two-, one-, and zero-dimensional *stress-free* PZT60 nanostructures, represented by a thin film (periodic in two directions, x and y), a wire (periodic along one direction, z), and a cubic dot, respectively. The x, y, and z axes are chosen along the [100], [010], and [001] directions, respectively, and the lateral size of the structures along nonperiodic directions is 48 Å. The Hamiltonian of such nanostructures can be written as [4,12,13,15]:

$$H = H^{(0)} - V\mathbf{P}\cdot[\mathbf{E}_0 - \beta\langle\mathbf{E}^{(\mathrm{MD})}\rangle], \tag{2}$$

where $\mathbf{E}^{(\mathrm{MD})}$ is the maximum depolarizing field. [Notice that H is a "self-consistent" Hamiltonian since a mean value of $\mathbf{E}^{(\mathrm{MD})}$ occurs in the definition of Eq. (2).] $H^{(0)}$ gathers all the energetic terms that do not explicitly depend on $\mathbf{E}_0$ and that correspond to an ideal "open-circuit" (OC) boundary condition. More precisely, $H^{(0)}$ is an explicit function of the local dipoles, as well as of the atomic configuration of the alloy, macroscopic strain, and strain-related microscopic variables [16]. The expression and first-principles-derived parameters of $H^{(0)}$ are those given in Refs. [16] for PZT *bulk*, except for the dipole-dipole interactions for which we use the analytical expressions of Refs. [12,17] for nanostructures under ideal OC conditions. The β parameter allows to consider the effect of *any* electrical boundary condition [12,13]. The limiting value $\beta = 0$ corresponds to a free sample *in vacuo*, that is to OC boundary condition. The other limiting value $\beta = 1$, called "short circuit" (SC) boundary condition, corresponds to the sample embedded in a perfect metallic medium that fully screens the polarization-induced charges at the surfaces or interfaces. The β parameter thus controls the magnitude of the residual depolarizing field. As a result,

Tensors in ferroelectric nanoparticles: First-principles-based simulations

S. Prosandeev,[1,2] I. Kornev,[1] and L. Bellaiche[1]
[1]*Physics Department, University of Arkansas, Fayetteville, Arkansas 72701, USA*
[2]*Institute of Physics, Rostov State University, Rostov on Don, Russia 344090*
(Received 12 April 2007; revised manuscript received 30 April 2007; published 6 July 2007)

Material tensors are identified in ferroelectric nanostructures via the use of first-principles-based simulations and analytical developments. In particular, one of such tensors represents a form of electromechanical coupling occurring at the nanoscale, while another tensor can be considered as analogous of dielectric susceptibility when going from bulk to nanoparticles. The reasons behind the existence of such overlooked tensors are discussed.

DOI: 10.1103/PhysRevB.76.012101 PACS number(s): 77.80.Bh, 61.46.−w, 77.22.Ej

Tensors are mathematical objects associated with physical quantities, and are involved in many fields of science. To name a few, stress, strain, electrocaloric effect, elastic compliances, elastic stiffnesses, thermal and electrical conductivity, thermoelectricity, thermal expansion, electro-optical effect, electrostriction, permeability, dielectric susceptibility, and piezoelectric effects can all be fully characterized by tensors.[1] The existence of such tensors, as well as the magnitude and sign of their coefficients, is at the heart of the functionality of countless devices. Moreover, and in contrast to the concept of tensors that has been known for centuries, a new field of research has attracted interest in the last 15 years only. Such field is *nanoscience*, and has the potential to yield new phenomena that do not exist in the bulk materials. One may thus wonder if, e.g., new tensors remain to be discovered in nanoparticles.

If so, such discovery may open the way for designing novel devices operating at nanoscale and exhibiting new functionalities. Such discovery may also provide a solution for some roadblocks encountered during the quest of miniaturized and efficient devices. For instance, piezoelectricity (which is a fundamental process, transforming the mechanical energy into electricity and vice versa, that has been put in use in an extremely wide spectrum of applications,[2] ranging from injection of gas in cars and of ink in jet printers to sonar listening devices, via ultrasound machines and telephone speakers) was found to dramatically decrease in magnitude when going from bulk to nanoparticles made of the same material.[3] This, because these latter systems are predicted to exhibit a vortex structure for their dipoles rather than a spontaneous polarization—when they are under open-circuit-like electrical boundary conditions.[4] (Note that ferroelectric nanoparticles can still have a spontaneous polarization, but when they are under short-circuit-like electrical boundary conditions.[5])

One may thus ask if another tensor representative of a another kind of efficient electromechanical coupling (that is, different from piezoelectricity) can exist in nanoparticles.

The aim of this Brief Report is to demonstrate the existence of original tensors in nanodots made of ferroelectrics, via analytical derivations and *ab initio* calculations. In particular, we demonstrate the existence of a tensor representative of another kind of electromechanical coupling and that can be thought of as analogous of piezoelectricity when going from bulk to nanodot. The reasons for the existence of that original coupling are indicated and explained.

Let us first remind of the basic facts about piezoelectricity in a polar system. For that, it is useful to expand the thermodynamic potential Φ in linear order of external fields and stress as a sum of four terms, following Ref. 1. Such decomposition is shown in Table I. The first and second terms correspond to the coupling between the polarization $\mathbf{P}$ and $\mathbf{E}$ applied electric field and to the coupling between the $\boldsymbol{\sigma}$ applied stress and the $\boldsymbol{\eta}$ strain, respectively. The third energy involves the $\mathbf{d}$ piezoelectric tensor, while the last term Φ_0 gathers all the energies that are explicitly independent of both $\mathbf{E}$ and $\boldsymbol{\sigma}$. As indicated in Table I, minimizing the thermodynamic potential with respect to the field yields the mathematical equality associated with the so-called *direct* piezoelectric effect[1] (that characterizes the polarization's response to a stress). Similarly, the derivation of Φ with respect to $\boldsymbol{\sigma}$ leads to the *converse* piezoelectric effect—that represents the change of shape of a material when subject to an applied electric field.[1]

Interestingly, it was recently found[4] that ferroelectric nanoparticles adopt a vortex structure for their electric dipoles, when they are under open-circuit-like electrical boundary conditions. Such a vortex annihilates the spontaneous polarization in favor of a toroidal moment, to be denoted by $\mathbf{g}$ and which is proportional to a cross product of the $\mathbf{p}_i$ dipole moment at site i with the $\mathbf{r}_i$ position vector locating this site: $\mathbf{g}=\frac{1}{2V}\Sigma_i \mathbf{r}_i \times \mathbf{p}_i$ (note that, unlike in Ref. 4, the volume of the system, V, is introduced here in similarity to the

TABLE I. Analogy between the $\mathbf{d}$ piezoelectric tensor in polar systems and the $\mathbf{d}^g$ axial piezotoroidic tensor in materials exhibiting an electric dipole vortex. Φ, $\mathbf{P}$, $\mathbf{E}$, $\boldsymbol{\sigma}$, $\boldsymbol{\eta}$, $\mathbf{g}$, curl$\mathbf{E}$ represent the thermodynamic potential, polarization, electric field, stress, strain, toroidal moment, and the cross product $\nabla \times \mathbf{E}$, respectively. The tensor components are indicated in Voigt or matrix notation. The "eq" subscript is used to indicate the value of the properties at equilibrium, that is, before applying a field or a stress. Einstein conventions are used for indicating the summations over j and i in the second and third rows.

Polarization	Electric dipole vortex
$\Phi=-(\mathbf{P}-\mathbf{P}^{eq})\cdot\mathbf{E}-(\boldsymbol{\eta}-\boldsymbol{\eta}^{eq})\cdot\boldsymbol{\sigma}$ $+\mathbf{E}\cdot\mathbf{d}\cdot\boldsymbol{\sigma}+\Phi_0$	$\Phi=-(\mathbf{g}-\mathbf{g}^{eq})\cdot(\text{curl}\mathbf{E})-(\boldsymbol{\eta}-\boldsymbol{\eta}^{eq})\cdot\boldsymbol{\sigma}$ $+(\text{curl}\mathbf{E})\cdot\mathbf{d}^g\cdot\boldsymbol{\sigma}+\Phi_0$
$d\Phi/d\mathbf{E}=0\Rightarrow P_i=P_i^{eq}+d_{ij}\sigma_j$	$d\Phi/d\text{curl}\mathbf{E}=0\Rightarrow g_i=g_i^{eq}+d_{ij}^g\sigma_j$
$d\Phi/d\boldsymbol{\sigma}=0\Rightarrow \eta_j=\eta_j^{eq}+d_{ij}E_i$	$d\Phi/d\boldsymbol{\sigma}=0\Rightarrow \eta_j=\eta_j^{eq}+d_{ij}^g(\text{curl}\mathbf{E})_i$

Thickness dependency of 180° stripe domains in ferroelectric ultrathin films: A first-principles-based study

Bo-Kuai Lai,[a] Inna Ponomareva, Igor Kornev, L. Bellaiche, and Greg Salamo
Physics Department, University of Arkansas, Fayetteville, Arkansas 72701, USA

(Received 22 August 2007; accepted 25 September 2007; published online 12 October 2007)

A first-principles-based scheme is used to investigate the thickness dependency of domain width of 180° stripe domains in $Pb(Zr,Ti)O_3$ ultrathin films. Our study shows that (1) more metastable states with energy closer to the 180° stripe domain ground state occur in *thicker* films, (2) the Kittel law is valid for 180° stripe domains when the film thickness is above 1.6 nm, and (3) below 1.2 nm, the Kittel law cannot be applied anymore due to the disappearance of domains. The thickness dependency of the domain *morphology* is also discussed. © *2007 American Institute of Physics.* [DOI: 10.1063/1.2799252]

Over the past decade, ferroelectric thin films have attracted considerable research interest because of their various potential device applications.[1–3] Because of the devices' miniaturization, our fundamental understanding on nanoscale ferroelectric thin films is critical to push forward and advance beyond the existing technologies. It is now known that ferroelectric thin films usually behave differently than their bulk counterparts because their properties depend on the film thickness, mechanical and electrical boundary conditions, and surfaces and interfaces (see, e.g., Ref. 4 and references therein). Surprisingly, one law, that was developed originally for ferromagnetic[5,6] and then for ferroelectric *macroscopic* systems,[7] was recently found to still apply for ferroelectric *thin*, and even *ultrathin*, films—according to the two recent measurements of Refs. 8 and 9. This law is usually referred to as the Kittel law and states that the domain width is directly proportional to the square root of the sample's thickness.[5,6] Several features related to the Kittel law for ferroelectric ultrathin films are currently unknown, despite of their obvious importance. For instance, one may wondering if there is a *critical thickness* below which such law is violated, since Ref. 8 investigated 180° periodic stripe domains in $PbTiO_3$ thin films with thickness ranging between 1.6 and 42 nm, while Ref. 9 studied 90° stripe domains in single crystal $BaTiO_3$ thin lamellae with thickness varying between 70 and 530 nm. One may also wonder how the *morphology* of the stripe domains evolves when varying the film's thickness along the Kittel law. For instance, it is still not clear what happens to the vortex kind of dipole arrangement (that is predicted to occur in the 180° stripes for ultrathin films,[10,11] and that is characterized by dipoles easily rotating across the stripes in order to form a kind of vortex structure) when increasing the film's thickness. Finally, it is worthwhile to determine if metastable states also consisting of periodic stripe domains, but with periods different from those predicted by the Kittel law, can occur in thin films.

The aim of this letter is to use a first-principles-based method to investigate the validity of the Kittel law for the recently discovered periodic 180° stripe domains in ferroelectric ultrathin films[8] as well as to provide energetic and atomistic insight about such domains. As opposed to the conventional phenomenological methods based on continuum theory,[9,12] our method can simulate ultrathin films with domain widths of only few unit cells without using adjustable empirical parameters (which are difficult to be determined experimentally,[13] and that can lead to different simulation results[14]).

More precisely, we study $Pb(Zr_{0.4}Ti_{0.6})O_3$ films that are grown along the [001] direction (which is chosen to be the z axis) and are Pb–O terminated at all surfaces. They are modeled by $L_x \times L_y \times L_z$ supercells, where L_x and L_y are the numbers of unit cells along the periodic x and y axes, respectively, and L_z is the number of finite (001) B layers along the *nonperiodic* z axis. The total energy of such supercells is used in Monte Carlo (MC) simulations and is written as

$$\varepsilon_{\text{tot}}(\{\mathbf{u}_i\},\{\sigma_i\},\{\mathbf{v}_i\},\eta) = \varepsilon_{H_{\text{eff}}}(\{\mathbf{u}_i\},\{\sigma_i\},\{\mathbf{v}_i\},\eta) + \beta\sum_i \langle \mathbf{E}_{\text{dep}}\rangle Z^* \mathbf{u}_i, \quad (1)$$

where $\mathbf{u}_i$ is the local soft mode in the unit cell i of the film. The MC simulations typically run over 40 000 sweeps to ensure that the simulated systems reach their lowest possible free-energy state. The $\{\sigma_i\}$ arrangement characterizes the atomic configuration of the alloy.[15] The $\{\mathbf{v}_i\}$ are inhomogeneous strain-related variables and η is the homogeneous strain tensor.[16] The inplane lattice matching between the (001) film and the substrate is simulated by freezing $\eta_1 = \eta_2 = \delta$ and $\eta_6 = 0$ (in Voigt notation)—with δ being the value forcing the film to adopt the in-plane lattice constant of the substrate.[11]

The first and second terms of Eq. (1) represents the (alloy effective Hamiltonian) intrinsic energy of the film under *ideal open-circuit* (OC) conditions and the effect of residual depolarizing field E_{dep} on physical properties, respectively. The expression and first-principles-derived parameters of $\varepsilon_{H\text{eff}}$ are those given in Refs. 15 and 17 for $Pb(Zr_{0.4}Ti_{0.6})O_3$ (PZT) *bulk*, except for the dipole-dipole interactions for which the formula derived in Refs. 18 and 19 for thin film under ideal OC conditions is used. Such electrical boundary conditions lead to a *maximum* depolarizing field (denoted by $\langle E_{\text{dep}}\rangle$) inside the film, when the dipoles point along the [001] direction. $\langle E_{\text{dep}}\rangle$ is *exactly* derived at an atomistic level, following the procedure introduced in Ref. 18. The β parameter is then used to control the degree of *screening* of $\langle E_{\text{dep}}\rangle$: $\beta=0$ corresponds to ideal OC conditions,

[a]Electronic mail: blai@uark.edu

Phase Transitions,
Vol. 80, Nos. 4–5, April–May 2007, 385–413

The nature of ferroelectricity under pressure

IGOR A. KORNEV* and LAURENT BELLAICHE

Physics Department, University of Arkansas, Fayetteville, Arkansas 72701, USA

(*Received 22 August 2006; in final form 30 March 2007*)

Advances in first-principles computational approaches have, over the past fifteen years, made possible the investigation of physical properties of ferroelectric systems. In particular, such approaches have led to a *microscopic* understanding of the occurrence of ferroelectricity in perovskite oxides at ambient pressure. In this article, we report *ab initio* studies on the effect of hydrostatic pressure on the ferroelectricity in perovskites and related materials. We found that, unlike common belief, these materials exhibit ferroelectricity at high enough pressure. We also explain, in detail the (unusual) nature of this ferroelectricity.

Keywords: Ferroelectric materials; Ferroelectricity; Phonos; Soft models

1. Introduction

ABO_3 perovskites form one of the most important classes of materials because they can exhibit a broad range of properties, e.g., superconductivity, magnetism, ferroelectricity, piezoelectricity, dielectricity and multiferroism. Such properties can be varied – and thus optimized to generate various devices with great performance and diverse functionalities – thanks to many factors. Examples of such factors are external magnetic and electrical fields, atomic substitution, chemical ordering and pressure.

In a classic paper, Samara *et al.* [1] were able to explain the effect of hydrostatic pressure on displacive phase transitions associated with soft zone-center transverse optic (TO) and zone-boundary phonons. Among the most striking pressure effects is the decrease of the transition temperature with pressure and ultimate vanishing of ferroelectricity [1]. As was shown, the vanishing of ferroelectricity with pressure can be readily understood from the well-known soft-mode theory [2] where the soft mode frequency depends on the short-range and Coulomb interactions. In this case, the vanishing of ferroelectricity is associated with a much more rapid increase of the short-range interactions than the long-range interactions with increasing pressure. As a result, the harmonic soft-mode frequency becomes less negative with increasing pressure. It is interesting to note that for the zone boundary modes the roles of the short-range and long-range forces are reversed, which leads to an enhancement

*Corresponding author. Email: ikornev@uark.edu

Phase Transitions
ISSN 0141-1594 print/ISSN 1029-0338 online
http://www.tandf.co.uk/journals
DOI: 10.1080/01411590701228117

Asymmetric screening of the depolarizing field in a ferroelectric thin film

S. Prosandeev[1,2] and L. Bellaiche[1]
[1]*Physics Department, University of Arkansas, Fayetteville, Arkansas 72701, USA*
[2]*Institute of Physics, Rostov State University, Rostov on Don 344090, Russia*
(Received 13 April 2007; revised manuscript received 4 May 2007; published 31 May 2007)

A first-principles-based approach is developed to mimic the (asymmetric) screening of the depolarizing field at the top surface of ferroelectric ultrathin films. Varying the magnitude of this one-side screening (i) results in the formation of different kinds of periodic nanostripe domain patterns, including original ones that are highly asymmetric and that can be thought of as connecting (and generalizing) the traditional Landau-Lifshitz and Kittel models of dipolar domains, and (ii) leads to a change in the domain's period, suggesting that the asymmetric screening of the depolarizing field is responsible for the existence of two recently observed nanostripe phases.

DOI: 10.1103/PhysRevB.75.172109 PACS number(s): 68.55.−a, 77.22.Ej, 77.80.Bh, 77.80.Dj

Stripe domains in ferromagnetic and ferroelectric systems are of technological importance because the properties of such systems depend strongly on the dipole arrangement. They are also of great fundamental interest because, among other things, their morphology reveals the balance between competitive interactions. The first theory of stripe domain structures was developed by Landau and Lifshitz in 1935 for magnetic systems.[1] In this model, the dipoles at the surfaces lie in plane, while the dipoles inside the film are parallel or antiparrel to the film's orientation (to be referred to as the z axis). This results in a closure domain pattern (that does not produce any macroscopic field outside the film) with 90° domain walls. The stability of this kind of stripe domain is due to the anisotropy of the lattice, with the easiest axis being along the z axis, overcoming the energetic cost of having domain walls. Later on, Kittel[2] suggested another pattern for stripe domains in magnetic thin films, in which all dipoles (including the ones at the surface) point either along the $+z$ or $-z$ direction. Such pattern produces a (stray) magnetic field outside the film that results in a costly magnetostatic energy. Such a solution is thus only stable for "uniaxial" thin films, i.e., having a very large anisotropy that overcomes the magnetostatic energy. The traditional Landau-Lifshitz and Kittel models both lead to the annihilation of the so-called demagnetizing and/or depolarizing field inside the film, and both predict that the stripe pattern of a given film under a given mechanical boundary condition has a unique domain period (that solely depends on the thickness of the film). Recently, 180° periodic stripe domain structures, with remarkably small periods (of the order of nanometers), were observed in ultrathin ferroelectric films.[3] The morphology of such stripes were not determined because this represents a major experimental challenge. On the other hand, a rather surprising result was found; namely, that these stripes can have two different periods for the same film but for different temperatures. It was then suggested that the existence of these two periods (that roughly differ by a ratio of $\sqrt{2}$) is related to the asymmetry of the experimental setup; namely, that the top (free) surface and the bottom (substrate/film) interface do not provide the same quantitative screening (if any) of the depolarizing field and that this asymmetry is somehow temperature dependent.[3] One may want to know if this suggestion is indeed correct, and one may also wonder if other stripe patterns (that is, deviating from the traditional Landau-Lifshitz and Kittel pictures) can result from this asymmetric screening. (Note that Ref. 4 strongly hints that varying the magnitude of the asymmetric screening of the depolarizing field can indeed affect domain width. However, the authors of Ref. 4 assumed that the Kittel model always applies when describing the domain configuration, which may have prevented them from discovering other stripe patterns.) Obviously, first-principles-based methods constitute a powerful tool to answer such questions because of their accuracy and deep microscopic insight. However, such methods have "only" been developed and/or used so far (to the best of our knowledge) to tackle problems related to a *symmetric* screening of the depolarizing field,[5–9] that is, when both surfaces similarly contribute to the domain's morphology.

The aims of this study are twofold. First, we wish to develop a first-principles-based approach allowing an asymmetric screening of the depolarizing field. Secondly, we want to use such a method to provide answers to the aforementioned questions. As we will see, such asymmetric screening can result in other stripe domain patterns and can indeed explain the experimental observations of Ref. 3.

Here, we consider a (001) $PbZr_{1-x}Ti_xO_3$ (PZT) thin film sandwiched by a nongrounded metallic plate, from the top side, and by a nonconducting substrate, from the bottom side. The film is PbO terminated. The distance between the top BO layer (where B atoms are either Ti or Zr) of the thin film and the metallic plate is denoted as R_{met}, and is allowed to vary. A "dead layer" (separating the top PbO surface and the metallic plate) can thus exist in our simulation, with its thickness being denoted by D and being equal to $R_{met}-\frac{a}{2}$ (where a is the five-atom unit-cell parameter). Here, this dead layer is assumed to possess a dielectric permittivity equal to unity. Specifically, the Ti composition and the thickness of the film are chosen to be $x=0.6$ and 48 Å, respectively. Such film is mimicked by a $6\times48\times12$ supercell that is periodic along the x and y directions but finite along the z axis. (The x, y, and z axes lie along the [100], [010], and [001] directions, respectively.) Its total energy is written as

$$E_{tot}(\{\mathbf{p_i}\},\{\mathbf{v_i}\},\{\sigma_i\},\hat{\eta}) = E_{mat}(\{\mathbf{p_i}\},\{\mathbf{v_i}\},\{\sigma_i\},\hat{\eta}) + E_{surf}(\{\mathbf{p_i}\},\{\mathbf{v_i}\}) + E_{scr}(\{\mathbf{p_i}\}), \quad (1)$$

JOURNAL OF MATERIALS SCIENCE 41 (2006) 137–145

Properties of ferroelectric ultrathin films from first principles

IGOR A. KORNEV*
Physics Department, University of Arkansas, Fayetteville, Arkansas 72701, USA; Novgorod State University, Russia
E-mail: ikornev@uark.edu

HUAXIANG FU, LAURENT BELLAICHE
Physics Department, University of Arkansas, Fayetteville, Arkansas 72701, USA

Advances in first-principles computational approaches have, over the past ten years, made possible the investigation of basic physical properties of simple ferroelectric systems. Recently, first-principles techniques also proved to be powerful methods for predicting finite-temperature properties of solid solutions in great details. Consequently, *bulk* perovskites are rather well understood nowadays. On the other hand, one task still remains to be accomplished by *ab-initio* methods, that is, an accurate description and a deep understanding of ferroelectric *nanostructures*. Despite the fact that nanometer scale ferroelectric materials have gained widespread interest both technologically and scientifically (partly because of novel effects arising in connection with the reduction of their spatial extension), first-principles-based calculations on ferroelectric nanostructures are rather scarce. For instance, the precise effects of the substrate, growth orientation, surface termination, boundary conditions and thickness on the finite-temperature ferroelectric properties of *ultrathin films* are not well established, since their full understandings require (i) microscopic insights on nanoscale behavior that are quite difficult to access and analyze via experimental probes, and (ii) the development of new computational schemes. One may also wonder how some striking features exhibited by some bulk materials evolve in the corresponding thin films. A typical example of such feature is the morphotropic phase boundary of various solid solutions, where unusual low-symmetry phases associated with a composition-induced rotation of the spontaneous polarization and an enhancement of dielectric and piezoelectric responses were recently discovered. In this paper, recent findings resulting from the development and use of numerical *first-principles-based* tools on ferroelectric ultrathin films are discussed.

1. Introduction

Ferroelectric materials are of unique importance for a variety of existing and potential device applications. Examples include piezoelectric transducers and actuators, nonvolatile ferroelectric memories, and dielectrics for microelectronics and wireless communication [1–3]. An important class of ferroelectric materials are the perovskites ABO_3. The perovskite crystal structure ABO_3 can be regarded as a three-dimensional network of corner sharing BO_6 octahedra, with the B ions in the center of the octahedra. In a cubic perovskite, the A site is twelvefold surrounded by oxygen ions. As the temperature is reduced, many of these compounds undergo a phase transition and develop a switchable spontaneous electric polarization, thus becoming ferroelectric. Most of the perovskite compounds that are of greater interests are not simple systems, but rather complex solid solutions with the general formula $A(B', B'')O_3$, i.e., with two kinds of B atoms

*Author to whom all correspondence should be addressed.
0022-2461
DOI: 10.1007/s10853-005-5962-0

Finite-temperature properties of $(Ba,Sr)TiO_3$ systems from atomistic simulations

Laura Walizer, Sergey Lisenkov, and L. Bellaiche
Physics Department, University of Arkansas, Fayetteville, Arkansas 72701, USA
(Received 19 January 2006; published 11 April 2006)

An effective Hamiltonian approach is developed to mimic finite-temperature properties of $(Ba_xSr_{1-x})TiO_3$ perovskite systems. It is found that this atomistic approach is overall quite accurate to qualitatively *and* quantitatively reproduce the experimental composition-temperature phase diagram of the *disordered solid solutions* (especially, for compositions x larger than 25%), when allowing one single parameter to deviate from its first-principles-derived value. Interestingly, such approach also yields predictions that are in good agreement with direct first-principles calculations for $BaTiO_3/SrTiO_3$ *superlattices*. The proposed approach is thus promising to investigate phenomena in any perovskite system made of Ba, Sr, Ti, and O atoms, independently of the overall composition and atomic arrangement.

DOI: 10.1103/PhysRevB.73.144105 PACS number(s): 77.84.Dy, 81.30.Bx, 77.80.Bh, 31.15.Ar

I. INTRODUCTION

Ferroelectric perovskite $(A'A'')BO_3$ [or $A(B'B'')O_3$] alloys are of growing importance for a variety of device applications[1,2] either when grown as solid solutions or in the form of $A'BO_3/A''BO_3$ (or $AB'O_3/AB''O_3$) superlattices. Such systems are also of large fundamental interest, mostly in order to reveal the microscopic effects responsible for their properties. A deep knowledge of ferroelectric alloys at an atomistic level has the potential to result in original and/or enhanced macroscopic properties. Accurate atomistic simulations are thus needed to understand the properties of perovskite alloys in general, and to guide the discovery of "wunderbar" materials, in particular. Within the last six years, three different kinds of atomistic simulations have been developed and used for perovskite alloys. One approach is the shell model that has been applied to disordered $(Ba_xSr_{1-x})TiO_3$ (BST) and $K(Ta_{1-x}Nb_x)O_3$ solid solutions as well as to $KTaO_3/KNbO_3$ superlattices.[3–6] In particular, the shell model qualitatively reproduces the experimental composition-temperature phase diagram of BST. However, it remains unknown if such an approach can also yield subtle alloy phenomena, such as the existence of the low-temperature monoclinic phase discovered in the phase diagram of $Pb(Zr_{1-x}Ti_x)O_3$ alloys for a narrow range of composition.[7] On the other hand, it has been shown that such unusual low-symmetry phase can be very well reproduced by another atomistic technique, namely the bond-valence model.[8] However, we are not aware of any study demonstrating that this latter model can mimic well superlattices as well as properties of ferroelectric alloys at intermediate or high temperatures (i.e., not only at low temperatures). Similarly, there is (at least) one limitation for the third kind of atomistic simulations, the alloy effective Hamiltonian method, which has been rather successful for describing properties of Pb-based systems. The limitation of this method is that any alloy effective Hamiltonian scheme developed so far is only technically applicable to a single composition or for a narrow compositional range around a specific concentration.[9–15] As a result, this prevents, e.g., the investigation of the *whole* composition-temperature phase diagram of disordered alloys, unless one develops a large number of effective Hamiltonians—each corresponding to a different overall composition.

The aim of the paper is to show that it is possible to develop a single alloy effective Hamiltonian method that can predict finite-temperature properties of solid solutions for the whole composition range as well as properties of superlattices having different overall concentrations. Here, we focus on perovskite systems made of Ba, Sr, Ti, and O atoms because of (1) the technological importance of BST solid solutions,[16] and (2) the numerous experimental and direct first-principles data that are already available in the literature for such systems (see, e.g., Refs. 3 and 17–19 and references therein), and that we can compare them to check the accuracy of our model.

This paper is organized as follows. Section II describes in detail the presently proposed effective Hamiltonian scheme. In Sec. III, we show and discuss the predictions for disordered BST solid solutions and $BaTiO_3/SrTiO_3$ superlattices obtained by this scheme. Finally, we present our conclusions in Sec. IV.

II. METHODS

Our scheme is based on the construction of an alloy effective Hamiltonian from first-principles calculations, with the total energy E being written as a sum of two different main terms

$$E(\{\mathbf{u}_i\},\eta_H,\{\eta_I\},\{\sigma_j\},\{\eta_{loc}\}) = E_{\text{ave}}(\{\mathbf{u}_i\},\eta_H,\{\eta_I\}) + E_{\text{loc}}(\{\mathbf{u}_i\},\{\eta_I\},\{\sigma_j\},\{\eta_{loc}\}), \quad (1)$$

where E_{ave}, as in Refs. 9–13, is the total energy associated with the hypothetical *simple* $\langle A\rangle BO_3$ system resulting from the use of the virtual crystal approximation[20–22] (VCA) to mimic $(Ba_{0.5}Sr_{0.5})TiO_3$; E_{loc} gathers terms associated with alloying effects going beyond the VCA approximation; $\mathbf{u}_i$ is the local soft mode (which is centered on B atoms) in unit cell i; η_H and $\{\eta_I\}$ are the *homogeneous* and *inhomogeneous* strain tensor[23] associated with the virtual $\langle Ba_{0.5}Sr_{0.5}\rangle TiO_3$ system, respectively; $\{\sigma_j\}$ characterizes the atomic configuration, that is, $\sigma_j=+1$ or -1 corresponds to the presence of a Ba or Sr atom, respectively, at the A-lattice site j of the

Phase Diagram of Pb(Zr, Ti)O_3 Solid Solutions from First Principles

Igor A. Kornev,[1] L. Bellaiche,[1] P.-E. Janolin,[2] B. Dkhil,[2] and E. Suard[3]

[1]*Physics Department, University of Arkansas, Fayetteville, Arkansas 72701, USA*

[2]*Laboratoire Structures, Propriétés et Modélisation des Solides, Ecole Centrale Paris, CNRS-UMR8580, Grande Voie des Vignes, 92295 Châtenay-Malabry Cedex, France*

[3]*Institut Laue-Langevin, 6 rue Jules Horowitz, BP 156 38042, Grenoble Cedex, France*

(Received 14 July 2006; published 13 October 2006)

A first-principles-derived scheme that incorporates ferroelectric and antiferrodistortive degrees of freedom is developed to study finite-temperature properties of $Pb(Zr_{1-x}Ti_x)O_3$ solid solution near its morphotropic phase boundary. The use of this numerical technique (i) resolves controversies about the monoclinic ground state for some Ti compositions, (ii) leads to the discovery of an overlooked phase, and (iii) yields three multiphase points that are each associated with four phases. Additional neutron diffraction measurements strongly support some of these predictions.

DOI: 10.1103/PhysRevLett.97.157601 PACS numbers: 77.80.Bh, 61.12.Ld, 77.84.Dy, 81.30.Bx

The ferroelectric $Pb(Zr_{1-x}Ti_x)O_3$ (PZT) system is an example of perovskite solid solutions that are of high technological relevance because of their widespread use in piezoelectric transducers and actuators [1]. Its phase diagram in a narrow compositional region centered at $x = 0.50$ and denoted as the morphotropic phase boundary (MPB) [2] also makes PZT of large fundamental importance. For instance, recent measurements have discovered an unexpected ferroelectric (FE) monoclinic phase [3] that leads to high electromechanical coefficients [4,5] and acts as a structural bridge between the well-known FE tetragonal and rhombohedral phases [3,5]. Moreover, another overlooked monoclinic phase has been recently observed [6–9], in which the usually competing [10] ferroelectric distortions and antiferrodistortive (AFD) motions (which are associated with the oxygen octahedra rotation) *coexist*. However, many controversies still surround this latter monoclinic phase, such as its exact space group, the axis about which the oxygen octahedra rotate, and even if it is a minority phase rather than the long-range ground state [6–9].

In view of these findings, one may also wonder if *other* surprises—such as other overlooked phase(s) or multiphase points (which are unusual thermodynamic features [11])—are still in store for PZT. Some features could indeed have been missed because of (i) the difficulties in growing and characterizing at various temperatures the many samples with tiny compositional differences and (ii) the current lack of theoretical tools that are able to accurately compute finite-temperature properties of perovskite alloys. For instance, the two sole first-principles-based finite-temperature schemes [5,12] that yield a monoclinic phase in the phase diagram of disordered PZT have some shortcomings: the model of Ref. [5] gives Curie temperatures that are $\simeq 60\%$ larger than measurements and does not include AFD motions, while we are not aware of any study reporting the accuracy of the bond-valence model of Ref. [12] for transition temperatures in PZT.

The purpose of this Letter is threefold: (1) to develop a numerical scheme able to accurately compute finite-temperature properties of perovskite solid solutions and that incorporates both FE and AFD motions; (2) to apply such a scheme to resolve the controversies discussed above, as well as to reveal some striking, overlooked effects in the MPB of PZT; and (3) to confirm experimentally some of these discoveries, via neutron diffractions.

Our numerical scheme is based on the generalization of the first-principles-derived alloy effective Hamiltonian of Ref. [5] to include AFD effects in addition to FE degrees of freedom. The total energy is thus written as a *sum* of two main terms, $E_{FE}(\{\mathbf{u}_i\}, \{\eta_H\}, \{\eta_I\}, \{\sigma_j\})$ and $E_{AFD\text{-}C}(\{\mathbf{u}_i\}, \{\eta_H\}, \{\eta_I\}, \{\sigma_j\}, \{\omega_i\})$, where E_{FE} is the energy provided in Ref. [5], while $E_{AFD\text{-}C}$ gathers AFD motions and their couplings in solid solutions. $\mathbf{u}_i$ is the local soft mode (which is directly proportional to the dipole) in unit cell i; $\{\eta_H\}$ and $\{\eta_I\}$ are the homogeneous and inhomogeneous strain tensors [13], respectively; $\sigma_j = +1$ or -1 corresponds to the presence of a Zr or Ti atom, respectively, at the B-lattice site j of the $Pb(Zr_{1-x}Ti_x)O_3$ system. Finally, $\{\omega_i\}$ is a (B-centered) vector characterizing the direction and magnitude of the AFD motions in unit cell i. For instance, ω_i parallel to $\mathbf{z}$ corresponds to a rotation of the oxygen octahedra about the z axis. For $E_{AFD\text{-}C}$, we propose the following expression that contains five major terms:

Controlling Toroidal Moment by Means of an Inhomogeneous Static Field: An *Ab Initio* Study

S. Prosandeev,[1,2] I. Ponomareva,[1] I. Kornev,[1] I. Naumov,[1] and L. Bellaiche[1]
[1]*Physics Department, University of Arkansas, Fayetteville, Arkansas 72701, USA*
[2]*Rostov State University, Rostov on Don, 344090, Russia*
(Received 9 February 2006; revised manuscript received 6 April 2006; published 16 June 2006)

A first-principles-based approach is used to show (i) that stress-free ferroelectric nanodots under open-circuit-like electrical boundary conditions maintain a vortex structure for their local dipoles when subject to a transverse inhomogeneous static electric field, and, more importantly, (ii) that such a field leads to the solution of a fundamental and technological challenge: namely, the efficient control of the direction of the macroscopic toroidal moment. The effects responsible for such striking features are revealed and discussed.

DOI: 10.1103/PhysRevLett.96.237601 PACS numbers: 77.80.Bh, 77.22.Ej, 77.84.Dy

The unique properties of ferroelectric and ferromagnetic solids are widely used in many important applications. Interestingly, these properties can dramatically change when going from bulks to nanostructures [1–3]. For instance, it has been recently discovered that zero-dimensional (0D) ferroelectrics can have a vortex structure for their dipoles below a critical temperature [4,5]. Such an unusual vortex resembles the curling state exhibited by magnetic dots above a certain size [1,6] and leads to the activation of a macroscopic toroidal moment, which involves the cross product between the $\mathbf{r}_i$ vectors locating the i unit cells and their local electrical dipoles $\mathbf{p}_i$, i.e., it is defined as $\mathbf{G} = \frac{1}{2N}\sum_i \mathbf{r}_i \times \mathbf{p}_i$, where the sum runs over the N unit cells of the 0D system.

The possibility of switching the direction of the toroidal moment opens exciting opportunities for nanomemory devices [4,7], nanomotors, nanotransducers, nanoswitchers, nanosensors, etc. However, a practical control of the $\mathbf{G}$ toroidal moment is rather challenging, mostly due to the fact that electric toroids directly interact with the *curl* of $\mathbf{E}$ but not with an uniform electric field alone [8]. Moreover, a nonvanishing *curl* of $\mathbf{E}$ can *only* be produced (according to Maxwell equations) by a temporal change of the magnetic field, $-d\mathbf{B}/dt$, but the magnitude of the magnetic field necessary to switch the electric toroidal moment is impractical. Furthermore, even if this large magnetic field was reachable, it would disturb a volume of the sample much larger than the nanodot size. As a result, manipulating the toroidal moment of a *single* nanodot, separately from the toroidal moment of the other dots of the sample, will become impossible—which will thus seriously limit the benefits of using toroids for creating the next generation of "wunderbar" devices. (One also needs to be able to "read" the chirality of the vortex of a single nanodot via, e.g., the field produced by its dipoles [4].)

The aims of this Letter is twofold: (1) to report first-principles-based simulations demonstrating that there is an original and efficient way to control the electric toroidal moment of a single nanodot, namely, by using an inhomogeneous static electric field; and (2) to reveal, and understand, the reasons for such control.

Here, we use the first-principles-based Monte Carlo scheme of Ref. [9] to study a $12 \times 12 \times 12$ stress-free cubic dot that is under open-circuit electrical boundary conditions and that is made of $Pb(Zr_{0.4}Ti_{0.6})O_3$ (PZT)—with the surfaces being Pb-O terminated. This scheme generalizes to 0D systems the alloy effective Hamiltonian method proposed in Ref. [10] for bulks, by (i) substituting the dipole-dipole interaction of infinite three-dimensional systems by the corresponding interaction in 0D materials [5]; and (ii) incorporating surface-induced atomic relaxations that are caused by the vacuum surrounding the dot—with the governing parameters having been fitted to first-principles calculations on Pb-O terminated PZT thin films [11]. We consider a transverse inhomogeneous electric field arising from charges located away from the studied dot, and incorporate the interaction between the dipoles in the dot and this field in the total energy provided by the effective Hamiltonian method. The temperature is decreased by small steps, and the x, y, and z axis are chosen along the pseudocubic [100], [010], and [001] directions, respectively.

Figure 1 shows the two setups that we considered, as well as the resulting inhomogeneous field and ground-state dipole pattern in the dot. In practice, such setups and inhomogeneous fields can be generated by, e.g., piezoforce-microscopy tip(s), nanowires, switching ferroelectric dots, or other original methods.

Let us first discuss the setup of Fig. 1(a). The dipolar source of the field is made of two opposite charges of 2×10^{-17} C distant of 15 primitive unit cells along the x axis from the center of the investigated dot—resulting in a field magnitude of about 2×10^8 V/m in the center of this dot. One interesting result of Fig. 1(a) is that the studied dot under this inhomogeneous field maintains a vortex structure at low temperature. The interactions between the dipoles of the dot under open-circuit conditions and the inhomogeneous field are thus not strong enough to overcome the depolarizing-field effects responsible for the existence of a toroidal moment in an isolated dot [4,5] [One can, in fact, "break" this vortex structure by applying fields with magnitude several times larger than the one

Electric-Field-Induced Domain Evolution in Ferroelectric Ultrathin Films

Bo-Kuai Lai, I. Ponomareva, I. I. Naumov, I. Kornev, Huaxiang Fu, L. Bellaiche, and G. J. Salamo

Physics Department, University of Arkansas, Fayetteville, Arkansas 72701, USA

(Received 21 July 2005; revised manuscript received 9 February 2006; published 5 April 2006)

The electric-field-induced evolution of the recently discovered periodic 180° nanostripe domain structure is predicted in epitaxial $Pb(Zr_{0.5}Ti_{0.5})O_3$ ultrathin films from first principles. This evolution involves (1) the lateral growth of majority dipole domains at the expense of minority domains with the overall stripe periodicity remaining unchanged, (2) the creation of surface-avoiding *nanobubbles*, and (3) the formation of a single monodomain state. Analogies and differences (i) with ferroelectric thin films made of $BaTiO_3$ and (ii) with ferromagnetic thin films under magnetic field are discussed.

DOI: 10.1103/PhysRevLett.96.137602 PACS numbers: 77.22.Ej, 68.55.−a, 77.80.Bh, 77.84.Dy

Ferroelectric thin films are receiving an enormous amount of attention because of their technological promise in leading toward miniaturized and efficient devices [1]. An ongoing intensive fundamental effort has also been made to determine if (and understanding how) properties of these low-dimensional systems can differ from those of the corresponding three-dimensional bulk. As a result, recent studies revealed striking unusual features that are related to a particular characteristic of thin films, namely, their internal depolarizing fields. An example of such features is the prediction of a minimal critical thickness below which no ferroelectricity can exist [2]. Another example is the occurrence of an unusual dipole pattern [3,4], which consists of 180° stripe domains that, unlike domains in bulks, are periodic (and thus propagate throughout the *entire* material) with its periodicity being exceptionally small, that is, on the order of a few nanometers. Despite its obvious technological and fundamental importance, we are not aware of any study revealing how this peculiar stripe pattern evolves—and depends on the inherent parameters of the film—when applying the external factor that lies at the heart of many ferroelectric devices, namely, an external homogenous electric field. In particular, one may wonder if a phenomenon seen in ferromagnetic films under magnetic fields also occurs in ferroelectric films under electric fields, that is, the formation of so-called bubbles [5]. The discovery of such bubbles would make ferroelectric thin films of even broader interest, and would rise the questions of similitude or difference between the morphology, size, shape, and formation mechanism of bubbles in ferromagnetic versus ferroelectric thin films.

The aim of this Letter is to reveal from first principles, as well as to provide unprecedented detailed atomistic features of, the stripe domains' evolution in $Pb(Zr_{0.5}Ti_{0.5})O_3$ (PZT) ultrathin films under external electric fields. Such evolution does involve ferroelectric bubbles—as well as other features—that possess some striking differences (of technological promise) with respect to magnetic bubbles.

As in Ref. [3], the $Pb(Zr_{0.5}Ti_{0.5})O_3$ films are simulated to be grown along the [001] direction (which is chosen to be the z axis) and assumed to be Pb-O terminated at all surfaces. They are modeled by $40 \times 24 \times m$ supercells that are periodic along the x and y axes (which are chosen along the [100] and [010] pseudocubic directions, respectively) and where m is the number of finite (001) B layers along the *nonperiodic* z axis. The total energy of such supercells is used in Monte Carlo (MC) simulations, which typically run over 100 000 sweeps, and is written as

$$\varepsilon_{\text{tot}}(\{\boldsymbol{u}_i\},\{\sigma_i\},\{\boldsymbol{v}_i\},\eta) = \varepsilon_{\text{Heff}}(\{\boldsymbol{u}_i\},\{\sigma_i\},\{\boldsymbol{v}_i\},\eta) + \beta\Sigma_i\langle\boldsymbol{E}_{\text{dep}}\rangle\cdot Z^*\boldsymbol{u}_i - \Sigma_i\boldsymbol{E}\cdot Z^*\boldsymbol{u}_i, \quad (1)$$

where $\boldsymbol{u}_i$ is the local soft mode in the unit cell i of the film—whose product with the effective charge Z^* yields the local electrical dipole in this cell. The $\{\sigma_i\}$ arrangement characterizes the atomic configuration of the alloy [6]. The $\{\boldsymbol{v}_i\}$'s are the inhomogeneous strain-related variables inside these films [7]. η is the homogeneous strain tensor, which is particularly relevant to mechanical boundary conditions since *epitaxial* (001) films are associated with the freezing of three of the six components of η (in Voigt notation), which are $\eta_6 = 0$ and $\eta_1 = \eta_2 = \delta$, with δ being the value forcing the film to adopt the in-plane lattice constants of the chosen substrate [3,8,9]. $\varepsilon_{\text{Heff}}$ is the (alloy effective Hamiltonian) intrinsic energy of the ferroelectric film. Its expression and first-principles-derived parameters are those given in Refs. [6,10] for $Pb(Zr_{0.5}Ti_{0.5})O_3$ *bulk*, except for the dipole-dipole interactions for which we implemented the formula derived in Refs. [11,12] for thin film under ideal open-circuit (OC) conditions. Such electrical boundary conditions naturally lead to the existence of a *maximum* depolarizing field (to be denoted by $\langle\boldsymbol{E}_{\text{dep}}\rangle$) inside the film, when the dipoles point along the [001] direction. $\langle\boldsymbol{E}_{\text{dep}}\rangle$ is *exactly* derived at an atomistic level, following the procedure introduced in Ref. [11]. The second term of Eq. (1) mimics a *screening* of $\langle\boldsymbol{E}_{\text{dep}}\rangle$ thanks to the β parameter. More precisely, the residual depolarizing field, resulting from the combination of the first and second term of Eq. (1), has a magnitude equal to $(1-\beta)|\langle\boldsymbol{E}_{\text{dep}}\rangle|$. In other words, $\beta = 0$ corresponds to ideal OC conditions,

Influence of the growth direction on properties of ferroelectric ultrathin films

I. Ponomareva* and L. Bellaiche†
Department of Physics, University of Arkansas, Fayetteville, Arkansas 72701, USA
(Received 26 June 2006; published 3 August 2006)

A first-principles-based approach is developed and used to investigate $Pb(Zr_{0.4}Ti_{0.6})O_3$ ultrathin films having different growth directions and subject to different boundary conditions. A wide variety of dipole patterns is found, including ferroelectric phases absent in the bulk and different periodic stripe nanodomains. Moreover, a large enhancement of dielectricity is found in ultrathin films exhibiting a growth direction that differs from a possible direction of the polarization in the corresponding bulk. A set of two general and simple rules is provided to analyze and understand all these features.

DOI: 10.1103/PhysRevB.74.064102 PACS number(s): 77.84.Dy, 68.55.−a, 77.22.Ej, 77.80.Bh

I. INTRODUCTION

Ferroelectric thin films are of high interest[1–12] because of their potential applications in miniaturized devices. Many of their features, such as the dependence of their dipole patterns on boundary conditions and size thickness, are now rather well established.[4–8,11] However, an overwhelming majority of past studies focused on films grown along [001]. As a result, the influence of the *growth direction* on their properties is poorly understood. For instance, Ref. 13 observed that $Pb(Zr_{1-x}Ti_x)O_3$ films surprisingly adopt different macroscopic ferroelectric phases when changing the growth direction from [001] to [111]. Similarly, Ref. 14 revealed that $Pb(Zr_{0.35}Ti_{0.65})O_3$ thin films grown along [111] exhibit, below a certain thickness, a ferroelectric phase differing from the one of the bulk. Reference 15 further reports 90° domains in $PbZr_{0.25}Ti_{0.75}O_3$ film grown along [111], which strikingly differs from the 180° domains discovered in [001] $PbTiO_3$ films.[5] Furthermore, some experiments indicated that properties—such as fatigue endurance and piezoelectricity—can be improved when using a growth direction different from [001]. The microscopic reasons behind such puzzling effects are unknown. The situation is even worse for *ultrathin* films because we are not aware of any work studying the effect of growth direction on their properties, despite their promises to yield unusual phenomena, such as a critical thickness below which ferroelectricity can disappear[4] or the appearance of stripe domains with a remarkably small period.[5]

The aim of this paper is twofold: (i) to demonstrate, via the development and use of a first-principles-based approach, that the growth direction in ferroelectric ultrathin films can lead to original features, such as an enhancement of dielectric responses or different complex dipole patterns, and (ii) to analyze and understand such features via the formulation of two simple rules.

This article is organized as follows. Section II describes the theoretical method we developed and used to tackle the two items indicated above. Section III reports our predictions for different electrical and mechanical boundary conditions, as well as for different films' thickness. Finally, Sec. IV provides a brief summary.

II. METHODOLOGY

We theoretically study thin films made of $Pb(Zr_{0.4}Ti_{0.6})O_3$ (PZT), for which the bulk polarization points along ⟨001⟩ and which lies *outside* the morphotropic phase boundary[16,17] (to prevent the dipoles from easily rotating). Our qualitative predictions should thus also apply to $PbTiO_3$ films. We investigate three common[5,13–15,18,19] growth orientations: namely, [001], [110], and [111]. The films all have Pb-O-terminated surfaces and are represented by supercells that are *finite* along the growth direction, to be denoted as the z' direction, and repeated periodically along two in-plane x' and y' directions. The total energy is written as $\mathcal{E}_{Heff}(\mathbf{p}_i, \mathbf{v}_i, \eta, \sigma_i) + \beta\Sigma_i\langle\mathbf{E}_{dep}\rangle\cdot\mathbf{p}_i$, where $\mathbf{p}_i$ is the local dipole at site i of the supercell and $\mathbf{v}_i$ are inhomogeneous-strain-related variables around this site i. η is the homogeneous strain tensor while σ_i represents the alloy atomic configuration[16]—which is randomly chosen. The expression and first-principles-derived parameters of $\mathcal{E}_{Heff}$ are those given in Refs. 16 and 20 for PZT *bulk*, except for the dipole-dipole interactions for which the expressions derived in Ref. 21 for two-dimensional (2D) nanostructures *under ideal open-circuit conditions* are used. Such conditions naturally lead to a maximum depolarizing field (denoted by $\langle\mathbf{E}_{dep}\rangle$) inside the film when the dipoles point along the growth direction. We mimic a *screening* of $\langle\mathbf{E}_{dep}\rangle$ via the β coefficient. More precisely, the residual depolarizing field has a magnitude equal to $(1-\beta)\ |\langle\mathbf{E}_{dep}\rangle|$. In other words, $\beta=1$ and $\beta=0$ correspond to ideal short-circuit (SC) and open circuit (OC) electrical boundary conditions, respectively, while a value of β in between corresponds to a more realistic situation.[4] Technically, $\langle\mathbf{E}_{dep}\rangle$ is calculated via the atomistic approach of Ref. 22. Different *mechanical* boundary conditions are also simulated thanks to the homogeneous strain η.[7,23] For example, during the simulation associated with an epitaxial strain in the (x',y') planes, four components of η—in the $x'y'z'$ coordinate system—are kept fixed (namely, $\eta_{x'y'}=\eta_{y'x'}=0$ and $\eta_{x'x'}=\eta_{y'y'}=\delta$, with δ characterizing the lattice mismatch between PZT and a chosen substrate) while the other components relax. On the other hand, *all* the components of the strain tensor are allowed to relax for *stress-free* systems. [Note that we do not consider any strain *gradient* mostly because we do not anticipate (based on experimental evidence[5]) that such effect should occur for the films' thicknesses considered here.]

The novelty of our approach with respect to the numerical scheme of Refs. 16 and 20 mostly lies in the fact that the atomic sites' coordinates, the matrices appearing in the

Symmetry breaking at the nanoscale and diffuse transitions in ferroelectrics: A comparative study of $PbSc_{1/2}Nb_{1/2}O_3$ and $PbZr_{0.6}Ti_{0.4}O_3$

Jorge Íñiguez[1] and L. Bellaiche[2]
[1]*Institut de Ciencia de Materials de Barcelona (ICMAB-CSIC), Campus de la UAB, 08193 Bellaterra (Barcelona), Spain*
[2]*Physics Department, University of Arkansas, Fayetteville, Arkansas 72701, USA*
(Received 19 January 2006; published 13 April 2006)

We use a first-principles-based approach on periodic nanometric supercells to compare the properties of $Pb(Sc_{1/2}Nb_{1/2})O_3$ (PSN), a ferroelectric with relaxor-like characteristics, and $Pb(Zr_{0.6}Ti_{0.4})O_3$ (PZT), a normal ferroelectric. Unlike in PZT, we find a breaking of the macroscopic symmetry at the nanoscale and easier polarization fluctuations in PSN, both caused by large internal electric fields. Such features lead to a broad dielectric response and a polarization tail in PSN. A discussion about the possible consequences of such findings for real (i.e., macroscopic) materials is also provided.

DOI: 10.1103/PhysRevB.73.144109 PACS number(s): 61.43.Bn, 77.22.Ch, 77.80.−e, 77.84.Dy

I. INTRODUCTION

Relaxor ferroelectrics are characterized by a broad, frequency-dependent dielectric response and the freezing-in of local (nanoscale) polarizations at the so-called Burns temperature—which is well above the dielectric response maximum.[1,2] Determining the origin of these intriguing effects has been a challenge to scientists since the discovery of relaxor ferroelectrics more than fifty years ago.[3] Three main (phenomenological) models have been proposed to explain relaxor behavior. The first one states that relaxor properties arise from quenched, randomly distributed, internal electric fields that lead to the formation of *noninteracting* ferroelectric domains of nanometric size.[4,5] The second model proposes that relaxors exhibit a glassylike state with randomly distributed, *interacting*, polar microregions.[6,7] The third one is the so-called spherical-random-bond-random-field model,[8] where both random interactions between polar nanometric regions and internal electric fields are considered.

These models have been essential to advance our understanding of relaxors. However, they are necessarily very simple (in order to be solvable), and the correspondence between the assumptions of the models (e.g., quenched electric fields and polar nanoregions) and the actual atomistic details of the materials is questionable. Elucidating the microscopic mechanisms responsible for relaxor behavior thus remains an open question. Interestingly, first-principles techniques can provide a deep microscopic insight into materials. On the other hand, such *ab initio* methods are usually applicable to relatively small supercells, which makes them challenging to use to mimic and understand real relaxors.

In this article we investigate periodic nanometric supercells made of $Pb(Sc_{1/2}Nb_{1/2})O_3$ (PSN) relaxor and $PbZr_{0.6}Ti_{0.4}O_3$ (PZT) normal ferroelectrics, by using an atomistic first-principles-based approach. Our goals are twofold. First, we want to reveal if PSN and PZT already differ at the nanoscale, and what are the microscopic reasons for such a difference (if any). Secondly, we wish to start a discussion on how such a difference (if any) may be related to the properties of the real macroscopic materials.

This paper is organized as follows. Section II briefly describes the method used in this work. In Sec. III, we show and analyze our predictions for periodic *nanometric* supercells. In particular, we will see that, unlike in PZT, large internal electric fields in PSN break the macroscopic symmetry at the nanoscale and facilitate polarization fluctuations between different minima. Such features yield a broad dielectric response (which is a relaxor characteristic) and a polarization tail (which is reminiscent of a diffuse phase transition) in PSN. Section IV provides a discussion about the possible consequences that such nanoscale findings may have on microscopic and macroscopic properties of real relaxorlike materials. Finally, we present our conclusions in Sec. V.

II. METHOD

Here we use the *atomistic* first-principles-based effective Hamiltonians that have been successful in treating complex ferroelectric alloys.[9,10] Within these approaches, the total energy of $A(B',B'')O_3$ solid solutions is written as a sum of two terms: E_{ave}, which describes the interactions in a virtual crystal $AB^{ave}O_3$, where B^{ave} is defined by averaging the potentials of atoms B' and B'',[11] and E_{loc}, which describes how the actual distribution of B-cations affects the energetics of the local soft modes $\mathbf{u}_i$ (defined in each cell i and proportional to the local dipoles) and the local strain variables. We will be mainly concerned with the term in E_{loc} that has the form:

$$E_{loc,e}(\{\mathbf{u}_i\},\{\sigma_j\}) = -\sum_i Z^* \mathbf{u}_i \cdot \epsilon_i[\{\sigma_j\}]. \quad (1)$$

$\sigma_j=1$ (respectively, -1) if there is a B' (respectively, B'') cation in cell j; ϵ_i is the internal field at cell i, which depends on the surrounding B-cation distribution;[9] Z^* is the Born effective charge associated with the local mode. All the parameters of the total energy, including the internal fields, are obtained from first-principles calculations on small cells.

We solve the effective Hamiltonian by the Monte Carlo (MC) technique to compute the properties of two qualitatively different ferroelectric alloys. The first system is $Pb(Sc_{1/2}Nb_{1/2})O_3$, which has a fixed stoichiometry so that charge neutrality is preserved. PSN—when grown in its dis-

Phase Transitions,
Vol. 79, Nos. 1–2, January–February 2006, 123–134

Taylor & Francis
Taylor & Francis Group

Polar and chemical order in relation with morphotropic phase boundaries and relaxor behaviour in bulk and nanostructured PSN–PT

R. HAUMONT*†, J. CARREAUD†, P. GEMEINER†, B. DKHIL†, C. MALIBERT†§, A. AL-BARAKATY¶, L. BELLAICHE¶ and J. M. KIAT†‡

†Laboratoire Structures, Propriétés et Modélisation des Solides, Ecole Centrale Paris, CNRS-UMR8580, Grande Voie des Vignes, 92295 Châtenay-Malabry Cedex, France
‡Laboratoire Léon Brillouin, CE Saclay CNRS-UMR12, 91991 Gif-Sur-Yvette Cedex, France
§Lab. d'Etudes des Milieux Nanométriques, Université d'Evry, 91000 Evry Val d'Essonne, France
¶Department of Physics, University of Arkansas, Fayetteville, Arkansas 72701, USA

(*Received 7 July 2005; accepted 25 December 2005*)

We have recently evidenced the existence of a complex path of polarisation rotation via two monoclinic phases in the giant-piezoelectric materials PSN–PT that is similar to the PMN–PT system. In this article we have presented the state of knowledge on the PSN–PT system and have given new results showing the close connection between the local inhomogeneous chemical order of Sc/Nb/Ti cations and the stability of different ferroelectric phases. The notion of morphotropic phase boundaries is discussed in relation with the gradual appearance of long-range polar order with increasing Ti content in PSN–PT. Comparison with the films and nanopowders/ceramics has also been made.

Keywords: Monoclinic phase; PSN–PT system; Nanostructure

1. Introduction

Among lead-based ferroelectric relaxors a special interest is devoted to $PbSc_{1/2}Nb_{1/2}O_3$ (PSN) because of the degree of ordering of Sc and Nb ions that strongly influences the dielectric behaviour. This ordering can be controlled by thermal treatment due to a high-temperature order–disorder transformation ([1] and references herein). This compound has been recognised as that revealing the strong dielectric relaxation and – contrary to $PbMg_{1/3}Nb_{2/3}O_3$ (PMN) – with the ferroelectric transition from the cubic to rhombohedral phase (R3m). Introduction of lead titanate (PT) makes this compound very attractive as that with very high dielectric permittivity (figure 1) and electromechanical coupling factor k_p [2–4] and makes it the best relaxor-PT ceramic material for large-k applications.

*Corresponding author. Email: raphael.haumont@lpces.u-psud.fr

Phase Transitions
ISSN 0141-1594 print/ISSN 1029-0338 online © 2006 Taylor & Francis
http://www.tandf.co.uk/journals
DOI: 10.1080/01411590600555917

Properties of Ferroelectric Nanodots Embedded in a Polarizable Medium: Atomistic Simulations

S. Prosandeev[1,2] and L. Bellaiche[1]

[1]*Physics Department, University of Arkansas, Fayetteville, Arkansas 72701, USA*
[2]*Institute of Physics, Rostov State University, Rostov on Don 344090, Russia*

(Received 22 June 2006; published 20 October 2006)

An atomistic approach is used to investigate finite-temperature properties of ferroelectric nanodots that are embedded in a polarizable medium. Different phases are predicted, depending on the ferroelectric strengths of the material constituting the dot and of the system forming the medium. In particular, novel states, exhibiting a coexistence between two kinds of order parameters or possessing a peculiar order between dipole vortices of adjacent dots, are discovered. We also discuss the origins of these phases, e.g., depolarizing fields and medium-driven interactions between dots.

DOI: 10.1103/PhysRevLett.97.167601 PACS numbers: 77.80.Bh, 61.46.−w, 71.15.Nc, 77.22.Ej

Ferroelectric nanostructures are of current high interest, because of their technological promise in leading toward miniaturized devices [1] and because of their potential in resulting in new phenomena. For instance, it was recently predicted that *isolated* nanodots of ferroelectrics can have a vortex structure for their dipoles below a critical temperature [2–4]. Such a vortex does not create any polarization but rather generates a macroscopic toroidal moment that involves the cross product between the $\mathbf{r}_i$ vectors locating the i unit cells and their local electrical dipoles $\mathbf{p}_i$—i.e., it is defined as $\mathbf{G} = \frac{1}{2N}\sum_i \mathbf{r}_i \times \mathbf{p}_i$, where the sum runs over the N unit cells of the nanodot. Being able to switch the direction of $\mathbf{G}$ opens exciting opportunities for nanomemory devices [2,5].

Interestingly, the possibility for the dipoles to form a vortex structure has been omitted in previous studies (see, e.g., Refs. [6–8] that used an effective medium approximation) aimed at determining the properties of ferroelectric or paraelectric nanoparticles that are *embedded* in a polarizable medium. As a result, original features may have been overlooked in these composite systems. For instance, one may wonder if novel states occur in such two-component materials. In particular, can dipole vortices in dots immersed in a polarizable medium coexist with a spontaneous polarization (unlike in isolated dots [2,3])? Similarly, how do toroidal moments of neighboring dots organize themselves (e.g, are they lying along parallel or antiparallel directions?)? It would also be worthwhile to determine the dependency of these novel states (if any) on the ferroelectric strengths of the materials forming the dot and medium and to reveal their governing mechanisms. The aim of this Letter is to address the issues mentioned above, by performing atomistic simulations.

Our atomistic scheme is based on the construction of an effective Hamiltonian, with the total energy E being written as a sum of two main terms:

$$E(\{\mathbf{u}_i\},\{\eta_H\},\{\eta_I\},\{\sigma_j\}) = E_{\text{ave}}(\{\mathbf{u}_i\},\{\eta_H\},\{\eta_I\}) + E_{\text{loc}}(\{\mathbf{u}_i\},\{\eta_I\}), \quad (1)$$

where E_{ave}—as in Refs. [9,10]—is the total energy associated with the hypothetical *simple* $A<B>O_3$ system resulting from the use of the virtual crystal approximation (VCA) [11] to mimic $A(B',B'')O_3$ compounds; E_{loc} gathers alloying terms going beyond the VCA approximation; $\mathbf{u}_i$ is the local soft mode (directly related to the electrical dipole) in unit cell i; $\{\eta_H\}$ and $\{\eta_I\}$ are the *homogeneous* and *inhomogeneous* strain tensors, respectively [12]; $\{\sigma_j\}$ characterizes the atomic configuration; that is, $\sigma_j = 1$ (-1) if there is a B' (B'') cation at the B-lattice site j of the $A(B',B'')O_3$ materials. For E_{ave}, we use the analytical expression proposed in Ref. [12] for simple ABO_3 systems. For E_{loc}, we use the following expression:

$$E_{\text{loc}}(\{\mathbf{u}_i\},\{\eta_I\},\{\sigma_j\}) = \sum_{ij}[Q_{j,i}\sigma_j\mathbf{e}_{ji}\cdot\mathbf{u}_i + R_{j,i}\sigma_j\mathbf{f}_{ji}\cdot\mathbf{v}_i] + \sum_i \Delta\kappa(\sigma_i)u_i^2, \quad (2)$$

where the sums over i and j run over unit cells and mixed sublattice sites, respectively. $\{\mathbf{v}_i\}$ are dimensionless local displacements which are related to the inhomogeneous strain variables inside each cell [12]. $Q_{j,i}(\sigma_j)$ and $R_{j,i}(\sigma_j)$ characterize the strengths of the alloying-induced intersite interactions. $\mathbf{e}_{ji}$ is a unit vector joining the site j to the center of the soft-mode vector $\mathbf{u}_i$, and $\mathbf{f}_{ji}$ is a unit vector joining the site j to the origin of the displacement $\mathbf{v}_i$. Practically, we included contributions up to the third neighbors for $Q_{j,i}(\sigma_j)$ and over the first-neighbor shell for $R_{j,i}(\sigma_j)$. Note that, for systems made of $AB''O_3$ dots embedded in a $AB'O_3$ medium, these contributions play a role only near the dots' surfaces—because of the analytical expression of the first two terms in Eq. (2). The last term in Eq. (2), which involves the $\Delta\kappa(\sigma_i)$ parameters, characterizes the on site contribution of alloying. It is an original contribution since it was not included in the alloy effective Hamiltonians of Refs. [9,10]. We incorporate such a term here—which is consistent with the first-principles results of Ref. [13]—because it provides an easy way to artificially adjust the "ferroelectric strength" of $AB'O_3$ and

Isostructural phase transitions in GaN/ScN and InN/ScN superlattices

V. Ranjan, S. Bin-Omran, and L. Bellaiche
Physics Department, University of Arkansas, Fayetteville, Arkansas 72701, USA

Ahmad Alsaad
Jordan University of Science and Technology, Department of Physical Sciences, P.O. Box 3030, Irbid, Jordan
(Received 27 January 2005; published 3 May 2005)

We predict the existence of pressure-induced isostructural phase transitions (IPTs) in GaN/ScN and InN/ScN superlattices from first principles. The IPTs in these superlattices are anomalous in the sense that they are associated with trivial order parameters and generate a dramatic change in many physical quantities. Furthermore, the *order* of the phase transition is found to be dependent on the superlattice period and on the nontransition-metal cation. We also reveal the reason behind, and consequences of, these unusual dependencies and IPTs.

DOI: 10.1103/PhysRevB.71.195302 PACS number(s): 61.50.Ks, 64.60.−i, 64.70.Kb, 71.20.Nr

I. INTRODUCTION

The so-called *isostructural* phase transitions (IPTs) are particularly remarkable, partly because of the difficulty in characterizing and understanding them. For example, the fact that such peculiar phase transitions leave the crystal symmetry unchanged makes the choice of the order parameter—which is the preliminary step for the theoretical description of a phase transition[1]—a nontrivial task. Order parameters that have been proposed in the literature for IPTs are rather unusual and vary from a function involving defects concentrations[2] to atomic positions changing in disordered and/or subtle fashion,[3,4] via an electronic-induced change in compressibility[1] and a tiny modification in bond angle.[4,5] Similarly, observing IPTs, especially, if they are of second-order, is usually challenging, because many properties are only slightly affected by these transitions.[3] These difficulties and the relative rarity of IPTs are the two main reasons why these latter are in overall much less studied and thus less understood than the "more usual" symmetry-breaking phase transitions.

The aim of this paper is to report first-principles calculations predicting that GaN/ScN and InN/ScN superlattices undergo a pressure-induced isostructural phase transition that is anomalous in the sense (1) it is associated with "*trivial*" order parameters, (2) it leads to a *dramatic* change in various properties, and (3) the *character* of the transition depends on the period of the superlattice, as well as, on the nontransition-metal cation. Our simulations also reveal driving forces responsible for these anomalous features.

The organization of this article is as follows. The computational method we have adopted for the calculations is described in Sec. II. We present our results in Sec. III. Finally conclusions are given in Sec. IV.

II. METHODOLOGY

The primitive lattice vectors of the parent compounds GaN, InN, and ScN, in their most stable hexagonal form,[6–8] are given by

$$\mathbf{a}_1 = a\left(\frac{1}{2}\mathbf{x} - \frac{\sqrt{3}}{2}\mathbf{y}\right),$$

$$\mathbf{a}_2 = a\left(\frac{1}{2}\mathbf{x} + \frac{\sqrt{3}}{2}\mathbf{y}\right),$$

$$\mathbf{a}_3 = c\mathbf{z}. \tag{1}$$

where a and c are the in-plane and out-of-plane lattice parameters, respectively, and where c/a is the axial ratio. The unit vectors along the Cartesian axes are denoted as $\mathbf{x}$, $\mathbf{y}$, and $\mathbf{z}$. The primitive unit cell for such systems contains four atoms: two N atoms located at $\mathbf{r}_1$ and $\mathbf{r}_2$, and two cations of the same type (e.g., Ga) located at $\mathbf{r}_3$ and $\mathbf{r}_4$, with

$$\mathbf{r}_1 = 0$$

$$\mathbf{r}_2 = \frac{2}{3}\mathbf{a}_1 + \frac{1}{3}\mathbf{a}_2 + \frac{1}{2}\mathbf{a}_3,$$

$$\mathbf{r}_3 = u\mathbf{a}_3,$$

$$\mathbf{r}_4 = \frac{2}{3}\mathbf{a}_1 + \frac{1}{3}\mathbf{a}_2 + \left(\frac{1}{2} + \mathbf{u}\right)\mathbf{a}_3. \tag{2}$$

Three parameters, a, c/a, and the internal parameter u which determines the relative position of atoms inside the unit cell, are thus needed to fully characterize the binary hexagonal parents. Our previous local-density-approximation (LDA) calculations predicted that (1) $c/a=1.631$ and $u=0.376$ for GaN, and (2) $c/a=1.620$ and $u=0.378$ for InN (Ref. 8), which agree very well with measurements.[9] The resulting ground-state, in both GaN and InN, is thus the wurtzite phase, is associated with the polar $P6_3mc$ (C_{6v}) space group and is *four*-times coordinated. On the other hand, we recently predicted that the equilibrium value of u and c/a are dramatically different in hexagonal ScN, namely 0.5 and ≈ 1.207, respectively.[6,7] This specific combination of lattice parameters leads to a layered structure, denoted by

Ferroelectricity of Perovskites under Pressure

Igor A. Kornev,[1,*] L. Bellaiche,[1] P. Bouvier,[2] P.-E. Janolin,[3] B. Dkhil,[3] and J. Kreisel[4]

[1]*Physics Department, University of Arkansas, Fayetteville, Arkansas 72701, USA*

[2]*Laboratoire d'Electrochimie et de Physicochimie des Matériaux et des Interfaces, CNRS, BP 75, 38402 St. Martin d'Hères Cedex, France*

[3]*Laboratoire Structures, Propriétés et Modélisation des Solides, CNRS-UMR8580, Ecole Centrale Paris, 92290 Châtenay-Malabry, France*

[4]*Laboratoire des Matériaux et du Génie Physique, ENS de Physique de Grenoble, B.P.46, 38402 St. Martin d'Hères, France*

(Received 9 August 2005; published 31 October 2005)

Ab initio simulations and experimental techniques are combined to reveal that, unlike what was commonly accepted for more than 30 years, perovskites and related materials *enhance* their ferroelectricity as hydrostatic pressure increases above a critical value. This unexpected high-pressure ferroelectricity is different in nature from conventional ferroelectricity because it is driven by an original electronic effect rather by long-range interactions.

DOI: 10.1103/PhysRevLett.95.196804 PACS numbers: 77.80.Bh, 62.50.+p, 77.84.Dy

ABO_3 perovskites form one of the most important classes of materials because they can exhibit a broad range of properties, e.g., superconductivity, magnetism, ferroelectricity, and multiferroism. Such properties can be varied—and thus optimized to generate various devices with great performance and diverse functionalities—thanks to many factors. Examples of such factors are external magnetic and electrical fields, atomic substitution, chemical ordering, and pressure.

Indeed, a famous 30-year-old Letter [1] demonstrated that hydrostatic pressure P reduces, and even annihilates for high enough value, ferroelectricity (FE) in perovskites [2,3]. Such reduction can be understood when recalling that the occurrence of "conventional" FE results from a delicate balance between long-range Coulomb ionic interactions favoring ferroelectric distortions and short-range electronic effects preferring the undistorted paraelectric cubic structure [4,5]. This balance can be tipped towards FE by small covalent effects—especially, the hybridization between the d orbitals of the B transition metal and the O $2p$ states—that weaken short-range repulsions [6]. A simple and widely used theory indicates that short-range repulsions increase more rapidly than long-range attractions *as pressure increases*, leading to the reduction of FE [1].

The aims of this Letter are threefold. First of all, we discover, by combining theoretical and experimental techniques, that such reduction indeed occurs at low pressure *but does not hold at high pressure*, since the "classical" $PbTiO_3$ material is found to adopt a nonmonotonous behavior with pressure. As a result, an increase in P above a critical value *enhances* its ferroelectricity. The second aim of this Letter is to reveal that high-pressure FE is dramatically different from conventional FE (occurring at low P) since the former is electronically—rather than ionically—driven. Finally, we found that such high-pressure ferroelectricity is a general phenomenon since it exists in other perovskites, as well as other materials. Playing with pressure may thus lead to the design of devices with enhanced or new capabilities.

We conducted calculations at 0 K within the density functional theory and the pseudopotential method with the following electrons being treated as valence in $PbTiO_3$: Pb $5s$, Pb $5p$, Ti $3s$, Ti $3p$, Ti $3d$, Ti $4s$, O $2s$, and O $2p$. Our results are qualitatively independent on technical details such as the used exchange-correlation functional [7–9], pseudopotential types [10,11], kinetic energy cutoff (that was varied between 40 Ry and 120 Ry), or softwares [12–14]. We performed: (1) total energy calculations (with full relaxation) to determine the evolution of some phases as a function of P up to ~120 GPa [3], and (2) phonon calculations of a specific structure [15].

On an experimental point of view, high-pressure Raman scattering and x-ray diffraction were carried out at room temperature in a gasketed diamond anvil cell on pure $PbTiO_3$ samples. Nitrogen or argon served as the pressure-transmitting medium which ensured a hydrostatic environment and the pressure was calibrated using the standard ruby fluorescence method. Depolarized Raman spectra up to 44 GPa of a powder sample were performed in backscattering geometry using a 514.53 nm-excitation line from an Ar^+ ion laser focused to a spot of 2–4 μm. The scattered light was analyzed using a T64000 Jobin-Yvon spectrometer and collected with a charge coupled device. The x-ray diffraction data collections up to 48 GPa were performed twice on two 20 μm-single crystals using the rotating crystal technique at ID30 high-pressure beam line at the European Synchrotron Radiation Facility [16]. More than 50 nonequivalent Bragg reflections ($2\theta > 24°$) were recorded on an image plate detector with a focused monochromatic wavelength of $\lambda = 0.3738$ Å. A silicon

Combined theoretical and experimental study of the low-temperature properties of $BaZrO_3$

A. R. Akbarzadeh,[1] I. Kornev,[1] C. Malibert,[2,3] L. Bellaiche,[1] and J. M. Kiat[2,4]
[1]*Physics Department, University of Arkansas, Fayetteville, Arkansas 72701, USA*
[2]*Laboratoire Structures, Propriétés et Modélisations des Solides, Ecole Centrale Paris, 92295 Châtenay-Malabry Cedex, France*
[3]*Laboratoire d'Etudes des Milieux Nanométriques, Université d'Evry Val d'Essonne, 91000 Evry, France*
[4]*Laboratoire Léon Brillouin, CE Saclay, 91191 Gif-sur-Yvette Cedex, France*
(Received 11 March 2005; revised manuscript received 8 August 2005; published 2 November 2005)

Low temperature properties of $BaZrO_3$ are revealed by combining experimental techniques (x-ray diffraction, neutron scattering and dielectric measurements) with theoretical first-principles-based methods (total energy and linear response calculations within density functional theory, and effective Hamiltonian approaches with and without zero-point vibrations). Unlike most of the perovskite systems, $BaZrO_3$ does not undergo any (long-range-order) structural phase transition and thus remains cubic and paraelectric down to 2 K, even when neglecting zero-point vibrations. On the other hand, these latter pure quantum effects lead to a negligible thermal dependency of the cubic lattice parameter below ≈40 K. They also affect the permittivity of $BaZrO_3$ by inducing an overall saturation of the real part of the dielectric response, for temperatures below ≈40 K. Two fine structures in the real part, as well as in the imaginary part, of the dielectric response are further observed around 50–65 K and 15 K, respectively. Microscopic origins (e.g., unavoidable defects and oxygen octahedra rotation occurring at a local scale) of such anomalies are suggested. Finally, possible reasons for the facts that some of these dielectric anomalies have not been previously reported in the better studied $KTaO_3$ and $SrTiO_3$ incipient ferroelectrics are also discussed.

DOI: 10.1103/PhysRevB.72.205104 PACS number(s): 77.22.Gm, 61.50.−f, 61.10.Nz, 61.12.Ex

I. INTRODUCTION

$BaZrO_3$ is a ceramic oxide of the perovskite family structure with a large lattice constant, high melting point, small thermal expansion coefficient, low dielectric loss and low thermal conductivity (see, e.g., Refs. 1–13 and references therein). These aforementioned properties make $BaZrO_3$ (i) a very good candidate to be used as an inert crucible in crystal growth techniques,[7,11] (ii) an excellent material for wireless communications[1,10] and (iii) a very good substrate in thin film deposition.[1,3] $BaZrO_3$ is also one of the two parent compounds of the (Pb-free and thus environmental-friendly) $Ba(Zr,Ti)O_3$ solid solutions, which is promising for manufacturing high Q materials with a variety of applications in microwave industry.[13]

Interestingly, properties of $BaZrO_3$ have been measured as long as 40 years ago, as well as very recently,[1–3] but only at room or higher temperature (to the best of our knowledge). Similarly, we are not aware of any calculation (either from phenomenological theory or first-principles calculations) predicting the dielectric properties of $BaZrO_3$. As a result, low-temperature dielectric properties of $BaZrO_3$ have never been investigated, despite the fact that many unusual effects are known to occur in some perovskite materials between 0 and 50 K. One drastic example of such effects is the (temperature-independent) plateau and large values of the real part of the dielectric response in $KTaO_3$ and $SrTiO_3$, which arise from the quantum-induced suppression of ferroelectricity in these materials. Other examples are the anomalous peaks observed around 10-50 K for the imaginary part of the dielectric response in $KTaO_3$, $K(Ta,Nb)O_3$, $(Pb,La)TiO_3$:Cu,[14,15] and $SrTiO_3$,[15,16] that are neither associated with structural phase transition nor do have a corresponding peak in the real part of the dielectric response (which conflicts with the well-established Kramers-Kronig relations[17]).

The aim of this article is to investigate the low-temperature behavior of $BaZrO_3$ from measurements and first-principles-based simulations. We report several unusual features in the real and imaginary parts of the dielectric responses while *no* long-range ferroelectric, antiferroelectric or antiferrodistortive structural phase transition occurs in $BaZrO_3$ down to 2 K. Discussions and similarities or differences between $BaZrO_3$ and the (better-studied) $KTaO_3$ and $SrTiO_3$-related materials are also indicated to better understand the low-temperature dielectric anomalies reported in several perovskites.

This article is organized as follows. Section II describes the experimental and theoretical methods we used to investigate $BaZrO_3$. Section III reports the measurements and predictions for structural and dielectric properties. Finally, Secs. IV and V provide a discussion and conclusion, respectively.

II. METHODOLOGY

A. Experimental procedures

Powder samples of $BaZrO_3$ were synthesized by solid state reaction by calcination at 1400 K and sintering at 1600 K starting from stoichiometric amounts of the corresponding oxides ($BaCO_3$, ZrO_2). The synthesized samples were well crystallized and no presence of parasitic phases was evidenced by x-ray diffraction (XRD) and chemical analysis. The final fired density is around 88–90 %, the typical grain size is ≈10 μm and the size distribution is typically 10% of the mean grain size. The temperature dependence of the di-

Low-dimensional ferroelectrics under different electrical and mechanical boundary conditions: Atomistic simulations

I. Ponomareva,* I. I. Naumov,† and L. Bellaiche‡
Department of Physics, University of Arkansas, Fayetteville, Arkansas 72701, USA
(Received 7 September 2005; published 21 December 2005)

Ferroelectric nanodots and infinite wires of $Pb(Zr_{0.4}Ti_{0.6})O_3$ alloy under different boundary conditions are investigated via Monte Carlo simulations using an atomistic first-principles-based effective Hamiltonian. These nanosystems all exhibit a spontaneous polarization that points along a nonperiodic direction, for situations close to short-circuit electrical boundary conditions and independently of the epitaxial strain. On the other hand, unusual dipole patterns arise in these systems when they are under open-like circuit conditions. The dependency of these patterns on the nanostructure's dimensionality and strain is further revealed and explained.

DOI: 10.1103/PhysRevB.72.214118 PACS number(s): 77.22.Ej, 77.80.Bh, 77.84.Dy

I. INTRODUCTION

Intense effort has been recently made in synthesizing, characterizing, and/or simulating ferroelectric nanostructures (FENs) because of their technological and fundamental promise (see, e.g., Refs. 1–17 and references therein). Among the different possible classes of FENs, the [two-dimensional-like (2D-like)] thin films are, by far, the ones that have been the most investigated. As a result, their properties begin to be rather well determined and understood. On the other hand, studies on zero-dimensional-like (0D-like) and one-dimensional-like (1D-like) FENs are rather scarce, despite their potential in resulting to interesting phenomena. For instance, Refs. 8 and 9 predicted that nanodots, nanodisks, and nanorods all exhibit a vortex structure for their electrical dipoles—leading to a nonzero toroid moment of polarization rather than a net polarization—when under specific boundary conditions, namely, stress-free and open circuit. In our minds, what is crucially missing nowadays is to know and understand how properties of 0D-like and 1D-like FEN depend on mechanical and electrical boundary conditions—which is a feature solely known in ferroelectric thin films.[7,12,11] As a matter of fact, such boundary conditions most likely have a dramatic effect on the FENs properties and can vary from one experimental setup to another, depending (i) on the used substrate, (ii) if the FENs are embedded in a insulating versus metallic host, or (iii) if the FENs are placed in a reactive atmosphere able to modify the FENs surfaces composition.

The main aim of this paper is to fill up this gap by investigating ferroelectric nanodots and nanowires under different electrical and mechanical boundary conditions. Our systematic study not only reveals unusual striking dipole patterns of these ferroelectric nanostructures, but also allows one to understand how and why the different classes of low-dimensional ferroelectrics (e.g., dots, wires, films) can differ or look alike when under similar boundary conditions.

II. METHODOLOGY

We decided to focus on dots and wires made of (disordered) $Pb(Zr_{0.4}Ti_{0.6})O_3$ solid solutions for mostly two reasons. First of all, such alloys are technologically important. Second, our chosen Ti composition allows us to explore how mechanical and electrical boundary conditions should, typically (e.g., as in the $PbTiO_3$ simple system), affect electrical dipoles in low-dimensional ferroelectrics. In other words, we purposely avoid investigating lead-zirconate-titanate (PZT) alloys with smaller Ti concentration because (i) anomalous features (such as the easiness of rotating the spontaneous polarization) occur in PZT bulks for Ti content ranging between $\approx$46 and $\approx$51 %,[18] and (ii) the rather unusual antiferrodistortive rotation of the oxygen octahedra can be activated, and compete with ferroelectricity, in $Pb(Zr_{1-x}Ti_x)O_3$ bulks with x smaller than $\approx$50%.[19]

In this paper, the x-, y- and z-axes are chosen along the pseudocubic [100], [010], and [001] directions, respectively. The nanostructures are represented by supercells that are either finite in any direction, in the case of dots, or repeated periodically *along the z direction*, in the case of nanowires. We typically use supercells of 48 Å length (12 unit cells) in any nonperiodic direction. Moreover, two different supercells of 12 and 24 unit cells, respectively, along the z-periodic direction have been chosen to mimic the (same) infinite wire, in order to check the dependency of its properties on the supercell choice. The total energy of such supercells is written as

$$\mathcal{E}_{Heff}(\mathbf{p_i}, \mathbf{v_i}, \eta, \sigma_i) + \beta \sum_i \langle \mathbf{E}_{dep} \rangle \mathbf{p_i} \quad (1)$$

where $\mathbf{p_i}$ is the local dipole at site i of the supercell and $\mathbf{v_i}$ are inhomogeneous-strain-related variables around this site i. η is the homogeneous strain tensor while σ_i represents the atomic configuration of the alloy.[20] The expression and first-principles-derived parameters of (the alloy effective Hamiltonian) $\mathcal{E}_{Heff}$ energy are those given in Ref. 20 for PZT *bulk*, except for the dipole-dipole interactions for which we use the analytical expressions derived in Ref. 21 for nanostructures *under ideal open-circuit (OC) conditions*. Such dipole-dipole interactions depend on the dimensionality of the system; that is, their expressions differ for the case of dots (that are finite along any Cartesian direction) and wires (that are infinitely periodic along a single Cartesian direction). The second term

PHYSICAL REVIEW B 72, 140102(R) (2005)

Atomistic treatment of depolarizing energy and field in ferroelectric nanostructures

I. Ponomareva, I. I. Naumov, I. Kornev, Huaxiang Fu, and L. Bellaiche
Department of Physics, University of Arkansas, Fayetteville, Arkansas 72701, USA
(Received 11 August 2005; revised manuscript received 22 September 2005; published 24 October 2005)

An *atomistic* approach allowing an accurate and efficient treatment of depolarizing energy and field in *any* low-dimensional ferroelectric structure is developed. Application of this approach demonstrates the limits of the widely used continuum model (even) for simple test cases. Moreover, implementation of this approach within a first-principles-based model reveals an unusual phase transition—from a state exhibiting a spontaneous polarization to a phase associated with a toroid moment of polarization—in a ferroelectric nanodot for a critical value of the depolarizing field.

DOI: 10.1103/PhysRevB.72.140102 PACS number(s): 77.22.Ej, 77.80.Bh, 77.84.Dy

Ferroelectric nanostructures (FEN) are of increasing technological and fundamental interest because of the need in miniaturization of devices, as well as, the appearance of new phenomena (see, e.g., Refs. 1–6, and references therein). Unscreened polarization-induced charges at the surfaces of FEN generate a depolarizing field that is responsible for striking properties. Examples are the existence of a critical thickness below in which no ferroelectricity can appear,[3] and the observation and prediction of laminar stripe nanodomains[2,4] as well as the formation of polarization vortex.[5,6] Interestingly, and despite its huge importance, we are not aware of any model being able to *exactly* calculate the depolarizing field and energy in *any* low-dimensional ferroelectric. For instance, the widely used continuum model (1) neglects the atomistic nature of materials, (2) is technically applicable only in the limit of large enough systems, and (3) cannot predict the depolarizing energy and/or field in the realistic cases of inhomogeneously polarized samples.

In this report we (i) demonstrate that it is possible to derive a scheme allowing the exact *atomistic* computation of the depolarizing energy and field in any low-dimensional FEN; (ii) use this scheme to check the accuracy of the continuum model for some simple test cases; (iii) report an unusual phase transition between two different kinds of order parameters in a ferroelectric nanodot that is driven by the depolarizing field.

To calculate the depolarizing energy in low-dimensional ferroelectrics, one first needs to realize that a system under perfect open-circuit (OC) electrical boundary conditions exhibits a *maximum* depolarizing field (if the polarization lies along a nonperiodic direction), while ideal short-circuit (SC) electrical boundary conditions leads to a complete screening of charges at the FEN surfaces that fully annihilates any depolarizing field. As a result, the depolarizing energy and field experienced by the FEN should involve a *difference* between the dipole-dipole interactions associated with these two extreme electrical boundary conditions. We shall write the energy of the dipole-dipole interaction in *any* system in the form

$$\mathcal{E}_{dip}^{(D)} = \frac{1}{2V}\sum_{\alpha\beta,ij} Q_{\alpha\beta,ij}^{(S,D)} p_\alpha(\mathbf{r}_i) p_\beta(\mathbf{r}_j), \tag{1}$$

where $D=3,2,1$ stands for a system periodic in 3, 2, and 1 directions, respectively; $D=0$ corresponds to nonperiodic systems, and the sum runs over the atomic sites i and j that differ from each other and belong to a *supercell* (to be denoted by S) mimicking the system. Such a supercell is infinitely repeated along the periodic directions, if any. For instance, thin films are modeled by supercells that are repeated in two dimensions while the direction associated with the growth direction of the film is nonperiodic. For dots, the supercell is not repeated. V is the volume of the supercell, $\boldsymbol{p}(\boldsymbol{r}_i)$ the dipole moment at the site i, and $\alpha=x,y,z$ denotes the Cartesian components. The quantity $Q^{(S,D)}$ depends on both the chosen supercell (S) and the periodicity of the system (D).

The elements of the Q matrix for systems periodic in three,[7] two (x and y), one (z) directions[22] and nonperiodic systems are given by

$$Q_{\alpha\beta,ij}^{(S,3)} = \frac{4\pi}{V}\sum_{\mathbf{G}\neq 0}\frac{1}{G^2}\exp\left(-\frac{G^2}{4\lambda^2}\right)G_\alpha G_\beta \cos(\mathbf{G}\cdot\mathbf{r}_{ij}) - \frac{4\lambda^3\delta_{\alpha\beta}\delta_{ij}}{3\sqrt{\pi}},$$

$$Q_{\alpha\beta,ij}^{(S,2)} = \frac{2\pi}{A}\sum_{\mathbf{G}}\left\{G\cos(\mathbf{G}\cdot\boldsymbol{\rho}_{ij})\left[\frac{1}{\sqrt{4\pi}}\Gamma\left(-\frac{1}{2},\frac{G^2}{4\lambda^2}\right)\delta_{\alpha z}\delta_{\beta z} + \frac{1}{G^2}\operatorname{erfc}\left(\frac{G}{2\lambda}\right)G_\alpha G_\beta\right] + G\exp(-G|z_{ij}|)\left[\left(\frac{G_\alpha G_\beta}{G^2} - \delta_{\alpha z}\delta_{\beta z}\right)\cos(\mathbf{G}\cdot\boldsymbol{\rho}_{ij}) - \frac{G_\alpha\delta_{\beta z}}{G}\sin(\mathbf{G}\cdot\boldsymbol{\rho}_{ij})\frac{z_{ij}}{|z_{ij}|}\right]\right\} - \frac{4\lambda^3\delta_{\alpha\beta}\delta_{ij}}{3\sqrt{\pi}},$$

$$Q_{\alpha\beta,ij}^{(S,1)} = \frac{2}{a}\sum_{\mathbf{G}} G^2\cos(\mathbf{G}\cdot z_{ij})\left\{K_0(G\rho_{ij})\delta_{\alpha z}\delta_{\beta z} + \frac{\delta_{\alpha x}\delta_{\beta x}+\delta_{\alpha y}\delta_{\beta y}}{G\rho_{ij}}K_1(G\rho_{ij}) - \frac{1}{\rho_{ij}^2}K_2(G\rho_{ij})\rho_{\alpha,ij}\rho_{\beta,ij}\right\} - \frac{2}{a}\sum_{\mathbf{G}} G\sin(\mathbf{G}\cdot z_{ij})K_1(G\rho_{ij})\rho_{ij}^{-1}G_\alpha\rho_{\beta,ij} + \frac{1}{a^3}(\delta_{\alpha x}\delta_{\beta x}$$

APPLIED PHYSICS LETTERS 86, 132904 (2005)

Phase diagrams of epitaxial $BaTiO_3$ ultrathin films from first principles

Bo-Kuai Lai,[a] Igor A. Kornev, L. Bellaiche, and G. J. Salamo
Physics Department, University of Arkansas, Fayetteville, Arkansas 72701

(Received 12 November 2004; accepted 5 February 2005; published online 22 March 2005)

Using a first-principles-based scheme, we determine the qualitative and quantitative effects of surface/interface, thickness and electrical boundary conditions on the temperature-misfit strain phase diagrams of epitaxial (001) $BaTiO_3$ ultrathin films. The microscopic reasons leading to such effects are also revealed. © *2005 American Institute of Physics*. [DOI: 10.1063/1.1890480]

The potential of ferroelectric thin films for applications such as dynamic random access memories,[1] nonvolatile random access memories,[2] and integrated devices[3] has attracted a lot of research attention. Interestingly, when going from bulk to thin films, many factors (e.g., strain, thickness, electrode, surface termination, interface roughness, and charge transfer at the free surface and interface)[4–10] can dramatically affect material properties. The *experimental* evaluation of the effect of each factor on physical properties is difficult because the properties of real thin films are a *combined* result of these factors. As a result, theoretical study is important since it can untangle these factors and provide fundamental insights into the behavior of thin films.

For example, Pertsev *et al.*[11] predicted the temperature-"misfit strain" phase diagrams for epitaxial and single-domain (001) $PbTiO_3$ and $BaTiO_3$ thin films using a phenomenological method. Five crystallographic phases were obtained: the *p* phase ($Px=Py=Pz=0$) at high temperatures; the *c* phase ($Px=Py=0, Pz\neq 0$) at high compressive strains; the *aa* phase ($Px=Py\neq 0, Pz=0$) at high tensile strains; and the *ac* ($Px=Pz\neq 0, Py=0$) and *r* phases ($Px=Py\neq 0, Pz\neq 0$) at low temperatures and low strains. Here, *Px*, *Py* and *Pz* are the Cartesian components of the spontaneous polarization along the [100], [010], and [001] pseudocubic directions, respectively. The same method was also used to study periodic two-domain structures, but with a different set of parameters.[12] Recently, Dieguez *et al.*[13] pointed out that the different sets of parameters used in Refs. 11 and 12 actually yield different low temperature phase behaviors, and thus decided to use *ab initio* approaches to avoid such dependency on experimentally deduced parameters. Their resulting temperature-misfit strain phase diagram for epitaxial (001) $BaTiO_3$ films mostly differs from the one of Ref. 11 by two features: the *ac* phase is now absent, and the phase diagram is symmetric with respect to zero misfit strain.

These two pioneering studies of Refs. 11 and 13 have led to a better understanding of epitaxial thin films. However, their use of *periodic bulks*, with mechanical constraints, to mimic epitaxial *films* has prevented them from investigating the effect of two important factors on physical properties of thin films, namely the existence of a *surface/interface* and the film *thickness*. Similarly, both works assume ideal short-circuit (SC) electrical conditions (that is, a vanishing total internal electric field), whereas real thin films likely exhibit a nonvanishing depolarizing field—even when sandwiched between metallic electrodes.[10] The aim of this letter is to reveal the role of the surface/interface, thickness, and electrical boundary conditions on the temperature-misfit strain phase diagram of (001) epitaxial $BaTiO_3$ ultrathin films, by using a first-principles-derived method.

Similar to the approach used in Refs. 11 and 13, our $BaTiO_3$ thin films are simulated to be grown along the ⟨001⟩ direction (*z* axis) and assumed to be Ba–O terminated at all surfaces/interfaces. They are modeled by (large and z-elongated) $10\times10\times40$ periodic supercells that contain a few number of (001) B layers (to be denoted by *m*) sandwiched by nonpolar systems (representing, e.g., air, nonferroelectric substrates, metallic electrodes, etc,...). Here, we typically choose $m=5$ or 7, implying that these nonpolar regions are quite large. As a result, we obtain well-converged results for the film's properties, and the film thickness is automatically accounted for in our simulations. Following Ref. 8, the total energy of such a supercell is used in Monte Carlo simulations and is written as

$$E_{tot}(\{\mathbf{u}_i\},\{\mathbf{v}_i\},\eta) = E_{Heff}(\{\mathbf{u}_i\},\{\mathbf{v}_i\},\eta) + \beta\Sigma_i 2\Pi(Z^{*2}/a^3\varepsilon_\infty) \times\langle u_{j,z}\rangle_s u_{i,z}, \quad (1)$$

where E_{Heff} is the (effective Hamiltonian) intrinsic energy of the ferroelectric film. Its expression and first-principles-derived parameters are those given in Refs. 14 and 15, respectively, for bulk $BaTiO_3$.[16] $\{\mathbf{u}_i\}$ are the local ferroelectric distortions from paraelectric symmetry in unit cells *i* of the film—which are directly proportional to the electrical polarization and whose components along the *z* axis are denoted as $u_{i,z}$. $\{\mathbf{v}_i\}$ are the inhomogeneous strain-related variables inside these films, whereas η is the homogeneous strain tensor. *Epitaxial* (001) films are associated with the freezing of three of the six η components (in Voigt notation), i.e., $\eta_6=0$ and $\eta_1=\eta_2=\delta$, with δ being the value forcing the film to adopt an in-plane lattice constant equal to the one of the chosen in Ref. 13. $\{\mathbf{u}_i\}$ and $\{\mathbf{v}_i\}$ are forced to vanish outside the films whereas the second term of Eq. (1) mimics the effects on properties of partial or full screening of polarization-induced charges at surfaces. It is directly proportional to a β parameter that characterizes the strength of the $\mathbf{E_d}$ *total* electric field inside the film. $\beta=0$ corresponds to ideal open-circuit conditions with $\mathbf{E_d}$ adopting its maximum magnitude, whereas an increase in β lowers this magnitude. The value of β corresponding to ideal SC conditions (to be denoted by β_{SC}) is 0.69 and 0.732 for thin films with $m=7$ and 5, respectively, for $10\times10\times40$ periodic supercells.[8] This second term is also dependent on the Born effective charge (Z^*), the lattice constant (a), the electronic dielectric constant of $BaTiO_3$ (ε_∞), as well as the average of the *z*

[a]Electronic mail: blai@uark.edu

Morphotropic phase boundary of heterovalent perovskite solid solutions: Experimental and theoretical investigation of $PbSc_{1/2}Nb_{1/2}O_3$-$PbTiO_3$

R. Haumont
Laboratoire Structures, Propriétés et Modélisation des Solides, Ecole Centrale Paris, CNRS-UMR8580, Grande Voie des Vignes 92295, Chatenay-Malabry Cedex, France

A. Al-Barakaty
Department of Physics, University of Arkansas, Fayetteville, Arkansas 72701, USA

B. Dkhil
Laboratoire Structures, Propriétés et Modélisation des Solides, Ecole Centrale Paris, CNRS-UMR8580, Grande Voie des Vignes 92295, Chatenay-Malabry Cedex, France

J. M. Kiat
Laboratoire Structures, Propriétés et Modélisation des Solides, Ecole Centrale Paris, CNRS-UMR8580, Grande Voie des Vignes 92295, Chatenay-Malabry Cedex, France, and Laboratoire Leon Brillouin, CE Saclay CNRS-UMR12, 91991 Gif-Sur-Yvette Cedex, France

L. Bellaiche
Department of Physics, University of Arkansas, Fayetteville, Arkansas 72701, USA
(Received 23 July 2004; revised manuscript received 22 October 2004; published 31 March 2005)

X-ray and neutron diffraction techniques are combined with first-principles-based simulations to derive and understand the structural properties of $Pb(Sc,Nb,Ti)O_3$ (PSN-PT) near its morphotropic phase boundary (MPB). An analysis of our measurements yields, at room and low temperatures, an overall tetragonal T—monoclinic M_C—monoclinic M_B—rhombohedral R path (when adopting the notations of Vanderbilt and Cohen, Phys. Rev. B **63**, 94108 (2001) for the monoclinic phases) as the Ti composition decreases across the MPB. A composition- and temperature-dependent significant mixing between some of these phases is also measured and reported here. The overall T-M_C-M_B-R path, which has also been proposed for $Pb(Mg,Nb,Ti)O_3$ [A. K. Singh and D. Pandey, Phys. Rev. B **67**, 64102 (2003)] is rather complex since it involves a *change* in the polarization path: this polarization first rotates in a (100) plane for the T-M_C part of the path and then in a (1–10) plane for the M_B-R part of the path. Moreover, a comparison between these measurements and first-principles-based calculations raises the possibility that this complex path, and the associated M_C and M_B phases, can only occur if the samples exhibit a deviation from a perfectly homogeneous and disordered situation, e.g. possess nanoscale chemically-ordered regions. If not, homogeneously disordered PSN-PT is predicted to exhibit at low temperature the same polarization path as $Pb(Zr,Ti)O_3$, that is T-monoclinic M_A-R which involves a "single" polarization rotation in a (1–10) plane. Nanoscale inhomogeneity may thus play a key role on the macroscopic properties of PSN-PT, in particular, and of other heterovalent complex solid solutions, in general, near their MPB.

DOI: 10.1103/PhysRevB.71.104106 PACS number(s): 81.30.Bx, 77.84.Dy, 61.10.−i, 61.12.−q

I. INTRODUCTION

Insulating perovskite solid solutions are of tremendous technological importance because of their exceptional piezoelectric and dielectric responses.[1,2] To date, the largest electromechanical and dielectric responses have been found in $PbTiO_3$-based alloys—e.g., $Pb(Zr,Ti)O_3$ (PZT), $Pb(Mg,Nb,Ti)O_3$ (PMN-PT) and $Pb(Zn,Nb,Ti)O_3$ (PZN-PT)—in a region of relatively narrow composition range, denoted the morphotropic phase boundary (MPB). This region separates a R rhombohedral state for low Ti concentration from a tetragonal T phase at a higher Ti content. The enhancement of piezoelectricity and dielectricity occurring in the MPB has been shown, experimentally and theoretically, to be linked to the existence of low-symmetry phase(s) that can be seen as structurally bridging the well-known R and T phases via the rotation of the spontaneous polarization.[3–18]

Interestingly, the precise symmetry, and the number and mixing of these intermediate structures seem to vary from one kind of material to another. As a matter of fact, it is now well established that the so-called monoclinic M_A phase[13] is the sole low-symmetry phase existing in the MPB of PZT (when focusing on polarizations, i.e. when neglecting antiferrodistortive displacements) at atmospheric pressure and under no external electric field.[5,11] On the other hand, PMN-PT has been reported to follow, in overall, a T—monoclinic M_C—monoclinic M_B-R path once decreasing the Ti concentration across the MPB.[6] Such a path is quite complex and involves a change of plane in which the polar-

J. Phys. IV France 128 (2005) 55–60
© EDP Sciences, Les Ulis
DOI: 10.1051/jp4:2005128009

Study of potassium-sodium-niobate alloys: A combined experimental and theoretical approach

I. Attia[1,2], L. Bellaiche[1], P. Gemeiner[2], B. Dkhil[2] and B. Malic[3]

[1] Physics Department University of Arkansas Fayetteville, AR 72701, USA
[2] Laboratoire Structures, Propriétés et Modélisation des Solides, CNRS-UMR 8580, Ecole Centrale Paris Grande Voie des vignes, 92925 Châtenay-Malabry, France
[3] Josef Stefan Institute Jamova 39, 1000 Ljubljana, Slovenia

Abstract. Experimental and theoretical techniques are combined to investigate properties of the environmentally-friendly and technologically-promising $(K_{0.5}Na_{0.5})NbO_3$ (KNN) solid solutions. Two long-range ferroelectric phases of orthorhombic and tetragonal symmetry are reported above 250K. Furthermore, our dielectric measurements, X-ray data and simulations suggest an unusual formation of rhombohedral clusters within an orthorhombic matrix at lower temperature.

1. INTRODUCTION

As a result of the concerns raised by the toxicity of lead, new regulations have been taken in Europe in order to protect health and environment. The development of lead-free or low-lead content materials with properties similar to those occurring in Pb-based compounds has then become a goal of major importance.

In particular, the potassium-sodium niobate alloy $(K_{1-x}Na_x)NbO_3$ (usually denoted as KNN), after being investigated in the seventies, has gained a renewed interest. As a matter of fact, this solid solution, for compositions close to 50% and when mixed with a few amount of $LiNbO_3$, was very recently found to exhibit d_{33} piezoelectric coefficients as high as 200-235 pC/N, k_{33} electromechanical coefficients higher than 40%, as well as Curie temperatures in the range of 725-783K [1]. Furthermore, on a fundamental point of view, the composition-temperature phase diagram of KNN is rather complex (and thus also worth of interest) mainly because of a possible competition and/or coexistence between ferroelectric and antiferrodistortive degrees of freedom [2]. It is thus possible that some structural phases (especially of low-symmetry and at low-temperature) have been overlooked in the past, due to the challenge in precisely characterizing them. As in $Pb(Zr,Ti)O_3$, such phases (if any) may be responsible for the large electromechanical responses recently discovered in KNN-based systems [1].

The aim of the present work is to study in detail properties of KNN having an overall 50% Na composition as a function of temperature, by combining experimental and numerical techniques.

1.1 Experimental methods

The samples were prepared from sodium potassium tartrate tetrahydrate $KO_2CCH(OH)CH(OH)CO_2Na.4H_2O$ (99.5% Fluka) and niobium oxide Nb_2O_5 (99.9% Aldrich). After mixing in stoechiometric proportions in acetone, powders were first calcined at 1180K during 4 hours and uniaxial cold pressed and sintered at 1100°C for 12 hours in air.

Dielectric measurements at various frequencies using a Hewlett-Packard4192A impedance meter were performed as a function of temperature with cooling and heating runs of 2K/min. A cryofurnace with a precision better than 0.1K was used for temperatures typically ranging between 100K to 450K while a furnace with a precision better than 1K was used for the high temperature range 300K-873K.

Properties of GaN/ScN and InN/ScN superlattices from first principles

V. Ranjan, S. Bin-Omran, David Sichuga, Robert Sean Nichols, and L. Bellaiche
Physics Department, University of Arkansas, Fayetteville, Arkansas 72701, USA

Ahmad Alsaad
Jordan University of Science & Technology, Department of Physical Sciences, P.O Box 3030, Irbid, Jordan
(Received 27 April 2005; published 4 August 2005)

First-principles calculations have been carried out to reveal structural, electromechanical, electronic, and lattice dynamical properties of GaN/ScN and InN/ScN superlattices—made by alternating *hexagonal* layers of GaN, or InN, with *hexagonal* layers of ScN—for different periods and overall compositions. These nitride systems belong to two different structural classes (having different coordination number), depending on the overall composition. For Sc compositions larger than 50%, each atom has nearly five nearest neighbors. On the other hand, Sc-deficient superlattices adopt a ground state that is nearly fourfold coordinated. This change of structure, and the change in composition or period within the same structure, considerably affect the piezoelectric response, the electronic band gap in magnitude as well as in character (indirect versus direct), and the phonon spectra. We also discussed the relevance of some of these predictions for designing future technological applications.

DOI: 10.1103/PhysRevB.72.085315 PACS number(s): 71.20.Nr, 61.66.Dk, 77.65.−j, 63.20.Dj

I. INTRODUCTION

Gallium nitride and indium nitride have been extensively studied in the last ten years for fundamental and technological reasons, as well as for the differences they exhibit with respect to more conventional III-V semiconductors (such as GaAs, InAs, or AlAs). For instance, the ground state of both GaN and InN is the so-called wurtzite structure—which belongs to the hexagonal symmetry class, is polar and four-times coordinated—that differs from the cubic and nonpolar zinc-blende phase that "usual" III-V semiconductors adopt. Nitrogen is also known to form rather short bonds with Ga or In (e.g., the length of these bonds in GaN and InN is about 80% of those occurring in GaAs and InAs, respectively), which results in exceptionally small atomic volumes in these nitride semiconductor compounds. Consequently, they exhibit a large magnitude of the forbidden gap (e.g., $E_g > 3$ eV in GaN), a considerable hardness, and high thermal conductivity. Some of these properties make the nitrides technologically useful (see Ref. 1 and references therein). As a matter of fact, nitride semiconductors have led to the development of future short-wavelength (green, blue, and ultraviolet) electroluminescence devices.[2–4]

Furthermore, there has also been a long interest in another III-V nitride system, namely ScN. For instance, Travaglini *et al.*[5] performed optical reflectivity measurements on ScN and compared them with the results of the first-principles electronic structure calculations by Monnier *et al.*[6] More recently, first-principles calculations were performed and experiments were carried out[7,8] to determine the band structure of the ScN in its ground-state structure. They predict ScN to be a semiconductor. While most of the previous studies on ScN focused on the ground-state structure (that is, the rock-salt phase[9]), we recently reported the discovery of another stable phase in ScN. Such phase is metastable and is a layered hexagonal (nonpolar) phase that is five-times coordinated,[10] and that we denoted as *h*-ScN (to follow the notation given to a similar phase found in MgO in Ref. 11). Moreover, we further predicted that applying a compressive in-plane strain on *h*-ScN can result in a very high piezoelectric response, as well as a tuning of the electronic band gap in the entire visible range.[12] In other words, it can lead to multifunctionality.

Interestingly, studies dedicated to *solid solutions* made by alloying ScN with GaN or InN are rather scarce,[13–15] while these materials have the potential to yield optimized properties or striking features.[12] For instance, in a recent work we found that superlattices made by alternating n layers of ScN with n layers of GaN (or InN)—that is, superlattices having an overall Sc concentration of 50%—exhibit a rare phenomenon. More precisely, they undergo an *isostructural* phase transition (from a wurtzite-derived to a *h*-derived phase) when applying a hydrostatic pressure. Such peculiar phase transition was also found to considerably affect piezoelectric, dielectric, and dynamical properties.[15]

The aim of this paper is to predict (and understand) various properties of solid solutions made by alloying hexagonal ScN with hexagonal GaN and InN, *as a function of composition*. More precisely, we have carried first-principles calculations to investigate structural, piezoelectric response, optical and phonon spectrum of (ScN)/(GaN) and (ScN)/(InN) superlattices for different overall compositions and different periods. We focused on short-period superlattices rather than disordered systems for two main reasons. First of all, the accuracy needed to accomplish our aim "forced" us to select first-principles methods as the numerical tool of choice, which forbids us to investigate large systems because their studies would require a large cost in computer time and memory. Second, short-period superlattices have indeed been grown in nitride semiconductors,[16] in general, and in GaN/ScN,[13] in particular.

This paper is organized as follows. Section II indicates the methodology we have used for our calculations. In Sec. III, we show and discuss the properties of these superlattices.

Available online at www.sciencedirect.com
ScienceDirect
Current Opinion in Solid State and Materials Science 9 (2005) 114–121
Current Opinion in Solid State & Materials Science

Modelling of nanoscale ferroelectrics from atomistic simulations

I. Ponomareva, I. Naumov, I. Kornev, H. Fu, L. Bellaiche *

Physics Department, University of Arkansas, Fayetteville, AR 72701, USA

Received 20 November 2005; accepted 8 May 2006

Abstract

The recent development and use of atomistic approaches have revealed the occurrence of original features in zero- and one-dimensional ferroelectric systems, and have also indicated how properties of such nanostructures dramatically depend on boundary conditions.

Keywords: Ferroelectric nanostructures; Atomistic simulations; First-principles techniques; Nanodomains

1. Introduction

Ferroelectric nanostructures (FENs) are receiving a lot of attention for technological reasons, e.g., the need in devices miniaturization [1] and their potential for applications such as dynamic random access memories [2], nonvolatile random access memories [3] and integrated devices [4]. Such low-dimensional systems are also attractive from a fundamental point of view by, e.g., determining if – and understanding how – their properties can differ from those of the corresponding (three-dimensional) bulk system.

Properties of perovskite thin and ultrathin films – that are two-dimensional systems – are now rather well understood thanks to an intense experimental and theoretical effort (see, e.g., Refs. [5,6] and references therein). On the other hand, studies on 0D-like and 1D-like FENs are rather scarce mostly because of the difficulty in growing, characterizing and modelling them [7–18]. Interestingly, such nanosystems should be exquisitely sensitive to many factors, such as their morphology and boundary conditions because: (i) the strong Coulomb interactions that give rise to ferroelectricity are drastically modified in the presence of surfaces and interfaces; (ii) a ferroelectric state is significantly affected by the mechanical boundary conditions due to a strong electrostrictive coupling; (iii) the fields arising either from space charge or from depolarization also interact strongly and directly with the ferroelectric order parameter. Thus, by altering the properties of ferroelectrics in unexpected ways, nanostructuring may result in both new science and new functional devices. Accurate atomistic simulations can thus be useful to provide local insights on nanoscale behavior that are difficult to access via experimental probes, and to guide synthesis of materials with new or improved properties.

The purposes of the present review are twofold: (1) to provide a description of different numerical atomistic schemes allowing the computation of properties of 0D and 1D FENs; (2) to summarize the understanding of these low-dimensional systems that has been gained in the last 3 years thanks to these numerical schemes.

2. Methodology

2.1. Dipole–dipole interaction in ferroelectric nanostructures under open-circuit conditions

One important issue associated with ferroelectric nanostructures is how to precisely compute their dipole–dipole interactions when they are under open-circuit electrical boundary conditions. As a matter of fact, at the exception of 0D systems that form the sole type of nanostructure having a *finite* number of atomic sites, the dipole–dipole interaction energy in other low-dimensional systems can *not* be

* Corresponding author.
E-mail address: laurent@uark.edu (L. Bellaiche).

1359-0286/$ - see front matter © 2006 Elsevier Ltd. All rights reserved.
doi:10.1016/j.cossms.2006.05.003

Letters to Nature

Nature **432**, 737-740 (9 December 2004) | doi:10.1038/nature03107; Received 7 June 2004; Accepted 7 October 2004

Unusual phase transitions in ferroelectric nanodisks and nanorods

Ivan I. Naumov, L. Bellaiche and Huaxiang Fu

1. Department of Physics, University of Arkansas, Fayetteville, Arkansas 72701, USA

Correspondence to: Huaxiang Fu Email: **hfu@uark.edu** (mailto:hfu@uark.edu)

Bulk ferroelectrics undergo structural phase transformations at low temperatures, giving multi-stable (that is, multiple-minimum) degenerate states with spontaneous polarization. Accessing these states by applying, and varying the direction of, an external electric field is a key principle for the operation of devices such as non-volatile ferroelectric random access memories[1] (/nature/journal/v432/n7018/full/nature03107.html#B1) (NFERAMs). Compared with bulk ferroelectrics, low-dimensional finite ferroelectric structures promise to increase the storage density of NFERAMs 10,000-fold[2] (/nature/journal/v432/n7018/full/nature03107.html#B2). But this anticipated benefit hinges on whether phase transitions and multi-stable states still exist in low-dimensional structures. Previous studies have suggested that phase transitions are impossible in one-dimensional systems[3], (/nature/journal/v432/n7018/full/nature03107.html#B3) [4], (/nature/journal/v432/n7018/full/nature03107.html#B4) [5] (/nature/journal/v432/n7018/full/nature03107.html#B5), and become increasingly less likely as dimensionality further decreases[3], (/nature/journal/v432/n7018/full/nature03107.html#B3) [4], (/nature/journal/v432/n7018/full/nature03107.html#B4) [5], (/nature/journal/v432/n7018/full/nature03107.html#B5) [6] (/nature/journal/v432/n7018/full/nature03107.html#B6). Here we perform *ab initio* studies of ferroelectric nanoscale disks and rods of technologically important $Pb(Zr,Ti)O_3$ solid solutions, and demonstrate the existence of previously unknown phase transitions in zero-dimensional ferroelectric nanoparticles. The minimum diameter of the disks that display low-temperature structural bistability is determined to be 3.2 nm, enabling an ultimate NFERAM density of 60×10^{12} bits per square inch—that is, five orders of magnitude larger than those currently available[7] (/nature/journal/v432/n7018/full/nature03107.html#B7). Our results suggest an innovative use of ferroelectric nanostructures for data storage, and are of fundamental value for the theory of phase transition in systems of low dimensionality.

PHYSICAL REVIEW B 70, 220102(R) (2004)

Properties of $Pb(Zr,Ti)O_3$ ultrathin films under stress-free and open-circuit electrical boundary conditions

Emad Almahmoud, Yulia Navtsenya, Igor Kornev, Huaxiang Fu, and L. Bellaiche
Physics Department, University of Arkansas, Fayetteville, Arkansas 72701, USA
(Received 3 September 2004; published 17 December 2004)

A first-principles-based scheme is developed to simulate properties of (001) PbO-terminated $Pb(Zr_{1-x}Ti_x)O_3$ thin films that are under stress-free and open-circuit boundary conditions. Their low-temperature spontaneous polarization never vanishes down to the minimal thickness, and continuously rotates between the in-plane ⟨010⟩ and ⟨110⟩ directions when varying the Ti composition around $x=0.50$. Such rotation dramatically enhances piezoelectricity and dielectricity. Furthermore, the order of some phase transitions changes when going from bulk to thin films.

DOI: 10.1103/PhysRevB.70.220102 PACS number(s): 77.55.+f, 77.80.Bh, 77.65.Bn, 77.22.Ch

Ferroelectric thin films are currently of enormous technological interest, mostly because of the need for miniaturization in devices.[1] Many fundamental questions are still unanswered and/or unsettled in these low-dimensional systems. For instance, whether or not there is a critical thickness below which no ferroelectricity can occur is still under debate.[2–6] Similarly, the precise effects of surface on properties of thin films are opened for discussion.[5,7–10] One may also wonder how the striking features exhibited by some bulk materials may evolve in the corresponding thin films. Typical examples of such features are the unusual low-symmetry phases (associated with a composition-induced rotation of the spontaneous polarization and with an enhancement of dielectric and piezoelectric responses), recently discovered in the morphotropic phase boundary (MPB) of various alloys.[11–15]

One reason behind this lack of knowledge is that thin (and particularly ultrathin) films are difficult to synthesize in a good quality form, and their characterization is by no means straightforward. Similarly, realistically simulating thin films is a theoretical challenge. For instance, while phenomenological and *ab initio*-based models have already provided a deep insight into thin films (see Refs. 2 and 16–18 and references therein), such models do not usually incorporate some subtle surface-related phenomena, e.g., charge transfer and modification of ferroelectric interactions near the surface. On the other hand, direct first-principles techniques can easily include such effects.[3,7–10] However, their large computational cost currently prevents them from being used to study complex phenomena and/or complex systems (e.g., thin films made of disordered solid solutions), especially at finite temperature. The atomistic approach of Ref. 5 is a promising technique for investigating thin films at finite temperature, but its level of accuracy depends on the surface termination,[5] which emphasizes that mimicking well surface effects on physical properties is tricky.

The aims of this Rapid Communication are twofold: first, to present a first-principles-derived approach allowing accurate predictions of finite-temperature properties of complex ferroelectric thin films, under stress-free and open-circuit boundary conditions; second, to use this approach to better understand thin films by providing answers to the questions mentioned above.

Here, we extend the *ab initio* effective Hamiltonian scheme proposed in Ref. 12 to mimic thin films that (1) are made of $Pb(Zr,Ti)O_3$ (PZT); (2) are grown on a substrate along the [001] direction; and (3) have vacuum above them. More precisely, the total energy E_{tot} of such low-dimensional systems is written as

$$\begin{aligned} E_{tot}(\{\mathbf{u}(i)\},\{\mathbf{v}(i)\},\eta,\{\sigma_i\}) &= E_{mat}(\{\mathbf{u}(i)\},\{\mathbf{v}(i)\},\eta,\{\sigma_i\}) + P\sum_j u_z(j) + T\sum_j v_z(j) \\ &+ S\sum_j \sum_{\alpha=x,y} u_\alpha(j)[u_\alpha(j+\hat{\alpha}) + u_\alpha(j-\hat{\alpha})], \end{aligned} \quad (1)$$

where $\mathbf{u}(i)$ are the (B-centered) local soft modes in unit cells i of the film, and are directly proportional to the electrical polarization, $\mathbf{v}(i)$ are inhomogeneous strains around the i site, while η is the homogeneous strain tensor. $\{\sigma_i\}$ characterizes the alloy configuration.[12] E_{mat} represents the intrinsic ferroelectric and elastic interactions *inside* the film, with its analytical expression and first-principles-derived parameters being those of PZT *bulks*.[12] Only four (out of 26) parameters are composition dependent in E_{mat}: they are those associated with the so-called local-mode self-energy.[12] The last three terms of Eq. (1) mimic explicit interactions between this film and the vacuum, with the j index running over all the B sites that are the closest to the free surface. $u_x(j)$, $u_y(j)$, and $u_z(j)$ denote the (x, y and z) Cartesian component of $\mathbf{u}(j)$ along the pseudocubic [100], [010], and [001] directions, respectively. α runs over the x and y axes (i.e., it does not include the growth direction). $u_\alpha(j+\hat{\alpha})$ [respectively, $u_\alpha(j-\hat{\alpha})$] is the α component of the local mode centered on the B site that is the closest from the j site that is parallel (respectively, antiparallel) to the α axis. The P and T parameters quantify how vacuum affects the out-of-plane components (u_z and v_z) of the local modes and inhomogeneous strains near the surface, respectively. S characterizes the change, with respect to the bulk, of the short-range interaction between the in-plane components of the local modes near the surface. The P, T, and S parameters are determined from first-principles calculations on a PbO-terminated (001) 17-atom slab (corresponding to 3 B-O and 4 A-O atomic layers) of a PZT alloy, as

Atomistic simulations of the incipient ferroelectric $KTaO_3$

A. R. Akbarzadeh,[1] L. Bellaiche,[1] Kevin Leung,[2] Jorge Íñiguez,[3,4,5] and David Vanderbilt[3]
[1]*Physics Department, University of Arkansas, Fayetteville, Arkansas 72701, USA*
[2]*Sandia National Laboratories, Mail Stop 1421, Albuquerque, New Mexico 87185, USA*
[3]*Department of Physics and Astronomy, Rutgers University, Piscataway, New Jersey 08854-8019, USA*
[4]*NIST Center for Neutron Research, National Institute of Standards and Technology, Gaithersburg, Maryland 20899-8562, USA*
[5]*Department of Materials Science and Engineering, University of Maryland, College Park, Maryland 20742-2115, USA*
(Received 22 December 2003; published 17 August 2004)

A parameterized effective Hamiltonian approach is used to investigate $KTaO_3$. We find that the experimentally observed anomalous dielectric response of this incipient ferroelectric is well reproduced by this approach, once quantum effects are accounted for. Quantum fluctuations suppress the paraelectric-to-ferroelectric phase transition; it is unnecessary to introduce defects to explain the dielectric behavior. The resulting quantum-induced local structure exhibits off-center atomic displacements that display *longitudinal, needle-like correlations* extending a few lattice constants.

DOI: 10.1103/PhysRevB.70.054103 PACS number(s): 77.84.−s, 78.20.Bh, 81.30.Dz

I. INTRODUCTION

Numerous experimental and theoretical studies have been carried out on the perovskite $KTaO_3$ over the last 40 years (see, e.g., Refs. 1–12, and references therein), making this material one of the most-studied "incipient ferroelectrics." The main reason for this interest is that the dielectric constant of $KTaO_3$ increases continuously with decreasing temperature down to ~10 K, but then saturates to a plateau at a large value (≈4000) at lower temperatures while remaining paraelectric and cubic all the way down to 0 K.[2,3] These anomalous low-temperature features are usually thought to be caused by the suppression of a paraelectric-to-ferroelectric phase transition by zero-point quantum fluctuations[2,3] (hence, the name "incipient ferroelectric" or "quantum paraelectric" used to describe $KTaO_3$ and other materials, such as $SrTiO_3$, exhibiting similar unusual dielectric and structural properties). Surprisingly, this generally accepted picture is apparently *not* supported by various first-principles calculations, using the density-functional theory (DFT) either in its local-density approximation (LDA),[13] or generalized-gradient approximation (GGA),[14,15] form since these simulations all predict that $KTaO_3$ should be paraelectric at $T=0$ even when neglecting zero-point motion.[4–6] This raises the possibility that LDA and GGA are not accurate enough to adequately reproduce the qualitative properties of incipient ferroelectrics. An alternate explanation for this discrepancy between first-principles calculations and experiments is that the simulations assume a perfect material while real samples may contain defects such as oxygen vacancies and Fe^{+3} ions,[2,3,7,8] that might lead to the observed anomalous properties of $KTaO_3$. In fact, the interpretation of various experiments,[9,10] still remains controversial as to whether they are attributable to extrinsic effects (i.e., defects induced) or intrinsic off-center atomic displacements. Furthermore, while previous studies invoke the existence of *ferroelectric microregions* inside the *macroscopically-paraelectric* $KTaO_3$ system to explain some of its properties,[9,11] there has never been any *direct* determination of the size and shape of these proposed polar regions, to the best of our knowledge. For instance, the pioneering work of Ref. 9 made several assumptions in their analysis of low-temperature Raman spectra—such as isotropy of these microregions—to extract a characteristic size ≃16 Å for these polar regions.

We use large-scale atomistic simulations to shed light on the aforementioned long-standing problems. We report calculations on $KTaO_3$ using a parameterized effective Hamiltonian approach. Our main findings are that (i) LDA and GGA are indeed not accurate enough to reproduce the observed anomalous properties of $KTaO_3$, even qualitatively; (ii) these properties *can* be understood *without the need of introducing defects*, if quantum fluctuations are present to suppress the paraelectric-to-ferroelectric transition; (iii) the low-temperature local structure of $KTaO_3$ is characterized by off-center atomic displacements that are *longitudinally correlated, in a needle-like (and thus anisotropic) way, with a correlation length spanning a few five-atom unit cells.*

The remainder of this paper is organized as follows. In Sec. II, we give a brief description of the methods we have used. Section III discusses the results on dielectric susceptibility and microscopic properties of $KTaO_3$. Finally, Sec. IV concludes the paper.

II. METHODOLOGY

We use the effective Hamiltonian (H_{eff}) approach developed in Ref. 16 to investigate finite-temperature properties of $KTaO_3$. Within this approach, the total energy E_{tot} is a function of three types of local degrees of freedom: (1) the $\mathbf{u}_i$ (B-site centered) local soft-mode amplitude in each i five-atom cell, describing the local polarization in each cell; (2) the v_i (A-site centered) inhomogeneous strain variables; and (3) the homogeneous strain tensor. E_{tot} contains 18 parameters and 5 different contributions: a local-mode self energy, a long-range dipole-dipole interaction, a short-range interaction between local modes, an elastic energy, and an interaction between the local modes and strains.[16] This effective Hamiltonian approach has been successfully used to model,

PHYSICAL REVIEW B 70, 220102(R) (2004)

Properties of $Pb(Zr,Ti)O_3$ ultrathin films under stress-free and open-circuit electrical boundary conditions

Emad Almahmoud, Yulia Navtsenya, Igor Kornev, Huaxiang Fu, and L. Bellaiche
Physics Department, University of Arkansas, Fayetteville, Arkansas 72701, USA
(Received 3 September 2004; published 17 December 2004)

A first-principles-based scheme is developed to simulate properties of (001) PbO-terminated $Pb(Zr_{1-x}Ti_x)O_3$ thin films that are under stress-free and open-circuit boundary conditions. Their low-temperature spontaneous polarization never vanishes down to the minimal thickness, and continuously rotates between the in-plane $\langle 010\rangle$ and $\langle 110\rangle$ directions when varying the Ti composition around $x=0.50$. Such rotation dramatically enhances piezoelectricity and dielectricity. Furthermore, the order of some phase transitions changes when going from bulk to thin films.

DOI: 10.1103/PhysRevB.70.220102 PACS number(s): 77.55.+f, 77.80.Bh, 77.65.Bn, 77.22.Ch

Ferroelectric thin films are currently of enormous technological interest, mostly because of the need for miniaturization in devices.[1] Many fundamental questions are still unanswered and/or unsettled in these low-dimensional systems. For instance, whether or not there is a critical thickness below which no ferroelectricity can occur is still under debate.[2–6] Similarly, the precise effects of surface on properties of thin films are opened for discussion.[5,7–10] One may also wonder how the striking features exhibited by some bulk materials may evolve in the corresponding thin films. Typical examples of such features are the unusual low-symmetry phases (associated with a composition-induced rotation of the spontaneous polarization and with an enhancement of dielectric and piezoelectric responses), recently discovered in the morphotropic phase boundary (MPB) of various alloys.[11–15]

One reason behind this lack of knowledge is that thin (and particularly ultrathin) films are difficult to synthesize in a good quality form, and their characterization is by no means straightforward. Similarly, realistically simulating thin films is a theoretical challenge. For instance, while phenomenological and *ab initio*-based models have already provided a deep insight into thin films (see Refs. 2 and 16–18 and references therein), such models do not usually incorporate some subtle surface-related phenomena, e.g., charge transfer and modification of ferroelectric interactions near the surface. On the other hand, direct first-principles techniques can easily include such effects.[3,7–10] However, their large computational cost currently prevents them from being used to study complex phenomena and/or complex systems (e.g., thin films made of disordered solid solutions), especially at finite temperature. The atomistic approach of Ref. 5 is a promising technique for investigating thin films at finite temperature, but its level of accuracy depends on the surface termination,[5] which emphasizes that mimicking well surface effects on physical properties is tricky.

The aims of this Rapid Communication are twofold: first, to present a first-principles-derived approach allowing accurate predictions of finite-temperature properties of complex ferroelectric thin films, under stress-free and open-circuit boundary conditions; second, to use this approach to better understand thin films by providing answers to the questions mentioned above.

Here, we extend the *ab initio* effective Hamiltonian scheme proposed in Ref. 12 to mimic thin films that (1) are made of $Pb(Zr,Ti)O_3$ (PZT); (2) are grown on a substrate along the [001] direction; and (3) have vacuum above them. More precisely, the total energy E_{tot} of such low-dimensional systems is written as

$$\begin{aligned} E_{tot}(\{\mathbf{u}(i)\},\{\mathbf{v}(i)\},\eta,\{\sigma_i\}) &= E_{mat}(\{\mathbf{u}(i)\},\{\mathbf{v}(i)\},\eta,\{\sigma_i\}) + P\sum_j u_z(j) + T\sum_j v_z(j) \\ &+ S\sum_j \sum_{\alpha=x,y} u_\alpha(j)[u_\alpha(j+\hat{\alpha}) + u_\alpha(j-\hat{\alpha})], \end{aligned} \quad (1)$$

where $\mathbf{u}(i)$ are the (B-centered) local soft modes in unit cells i of the film, and are directly proportional to the electrical polarization. $\mathbf{v}(i)$ are inhomogeneous strains around the i site, while η is the homogeneous strain tensor. $\{\sigma_i\}$ characterizes the alloy configuration.[12] E_{mat} represents the intrinsic ferroelectric and elastic interactions *inside* the film, with its analytical expression and first-principles-derived parameters being those of PZT *bulks*.[12] Only four (out of 26) parameters are composition dependent in E_{mat}: they are those associated with the so-called local-mode self-energy.[12] The last three terms of Eq. (1) mimic explicit interactions between this film and the vacuum, with the j index running over all the B sites that are the closest to the free surface. $u_x(j)$, $u_y(j)$, and $u_z(j)$ denote the (x, y and z) Cartesian component of $\mathbf{u}(j)$ along the pseudocubic [100], [010], and [001] directions, respectively. α runs over the x and y axes (i.e., it does not include the growth direction). $u_\alpha(j+\hat{\alpha})$ [respectively, $u_\alpha(j-\hat{\alpha})$] is the α component of the local mode centered on the B site that is the closest from the j site that is parallel (respectively, antiparallel) to the α axis. The P and T parameters quantify how vacuum affects the out-of-plane components (u_z and v_z) of the local modes and inhomogeneous strains near the surface, respectively. S characterizes the change, with respect to the bulk, of the short-range interaction between the in-plane components of the local modes near the surface. The P, T, and S parameters are determined from first-principles calculations on a PbO-terminated (001) 17-atom slab (corresponding to 3 B-O and 4 A-O atomic layers) of a PZT alloy, as

Ultrathin Films of Ferroelectric Solid Solutions under a Residual Depolarizing Field

Igor Kornev, Huaxiang Fu, and L. Bellaiche
Physics Department, University of Arkansas, Fayetteville, Arkansas 72701, USA
(Received 17 March 2004; published 5 November 2004)

A first-principles-derived approach is developed to study the effects of depolarizing electric fields on the properties of $Pb(Zr, Ti)O_3$ ultrathin films for different mechanical boundary conditions. A rich variety of ferroelectric phases and polarization patterns is found, depending on the interplay between strain and the amount of screening of surface charges. Examples include triclinic phases, monoclinic states with in-plane and/or out-of-plane components of the polarization, homogeneous and inhomogeneous tetragonal states, as well as peculiar laminar nanodomains.

DOI: 10.1103/PhysRevLett.93.196104 PACS numbers: 68.55.–a, 77.22.Ej, 77.80.Bh, 77.84.Dy

Ferroelectric thin films are of increasing technological interest because of the need in miniaturization of devices [1]. An intriguing problem in these films concerns their polarization patterns. For instance, the various following patterns have been recently predicted or observed: out-of-plane *monodomains* [2–5], 180° out-of-plane *stripe domains* [5,6], 90° multidomains that are oriented *parallel* to the film [7], and *microscopically paraelectric* phases [4]. The fact that dramatically different patterns have been reported for similar *mechanical* boundary conditions supports a concept discussed in Refs. [4,8], namely, that they arise from different *electrical* boundary conditions. More precisely, real thin films are likely neither in ideal open-circuit (OC) conditions, for which unscreened polarization-induced surface charges can generate a large depolarizing electric field along the growth direction [9], nor in ideal short-circuit (SC) conditions, which are associated with a vanishing internal field resulting from the full screening of surface charges, but rather experience a situation in between. The *amount* of surface charges' screening in thin films can vary from one experimental setup to another, possibly generating *different* polarization patterns [4,5].

Phenomenological and atomistic models have provided deep insight into thin films, but "only" for ideal OC or SC conditions (see Refs. [6,7,10], and references therein). First-principles calculations with electrical conditions falling between these two extremes have been performed, but the small used supercell size may have prevented the prediction of domains [4]. Finally, experimentally extracting the magnitude of the internal field is a challenging task. A precise correlation between the amount of screening of surface charges and the morphology of the polarization pattern, and how this correlation depends on mechanical boundary conditions, are thus still lacking nowadays despite their importance. *Atomic-scale* details of multidomains—and their formation mechanism—are also scarce in ferroelectric thin films. One may also wonder if some uncompensated depolarizing fields can yield ferroelectric phases that do *not* exist in the corresponding bulk material. Candidates for these latter anomalies are films made of alloys with a composition lying near their morphotropic phase boundary (MPB), because of the easiness of rotating their polarization [11].

In this Letter, we develop a first-principles-based scheme to investigate the effects of uncompensated depolarizing fields on the properties of $Pb(Zr_{1-x}Ti_x)O_3$ (PZT) films near their MPB, for different mechanical boundary conditions. Answers to the problems summarized above are provided. We find a rich variety of ferroelectric phases, including unusual triclinic and monoclinic states. We also observe complex nanodomains and reveal their formation and atomic characteristics.

We model PZT thin films that (i) are grown along the [001] direction (to be chosen along the z axis), (ii) are "sandwiched" between nonpolar systems (mimicking, e.g., air, vacuum, electrodes, and/or nonferroelectric substrates), (iii) have Pb-O terminated surfaces, and (iv) have a 50% overall Ti composition. Such structures are modeled by large periodic supercells that are elongated along the z direction and that contain a few number of B layers to be denoted by m, with the atoms being randomly distributed inside each layer. Typically, we use $10 \times 10 \times 40$ periodic supercells with m around 5. The nonpolar regions outside the film are thus altogether $40 - m$ lattice constant thick along the growth direction, which allows well-converged results for the film properties [6]. The total energy of such supercells is used in Monte Carlo simulations, and is written as

$$E_{Heff}(\{\mathbf{u}_i\}, \{\mathbf{v}_i\}, \eta, \{\sigma_i\}) - \sum_i \beta 2\pi \frac{Z^2}{a^3 \epsilon_\infty} \langle u_{j,z} \rangle_s u_{i,z}, \quad (1)$$

where E_{Heff} is the energy of the ferroelectric film *per se*. Its expression and first-principles-derived parameters are those given in Ref. [11] for bulk PZT. $\mathbf{u}_i$ are the local soft modes in unit cells i of the PZT film whose components along the z axis are denoted as $u_{i,z}$. $\mathbf{v}_i$ are inhomogeneous strain-related variables inside these films, while η is the homogeneous strain tensor. The form of η is relevant to stress-free (all the components of η fully relax) versus

Ferroelectricity in Barium Titanate Quantum Dots and Wires

Huaxiang Fu and L. Bellaiche
Department of Physics, University of Arkansas, Fayetteville, Arkansas 72701, USA
(Received 1 August 2003; published 18 December 2003)

Properties of $BaTiO_3$ colloidal quantum dots and wires are simulated using a first-principles-based approach. Large atomic off-center displacements (that are robust against capping matrix materials) are found to exist in very small (<5 nm) dots. We further determine the size dependences of electrical and electromechanical responses in the studied nanostructures, as well as provide microscopic understanding of these responses.

DOI: 10.1103/PhysRevLett.91.257601 PACS numbers: 77.80.-e, 77.65.-j, 61.46.+w

Intense experimental effort has been made recently in synthesizing and understanding ferroelectric (FE) nanostructures—e.g., $BaTiO_3$ dots [1], rods [2], wires [3], and nanotubes [4], and $Pb(Zr, Ti)O_3$ thin films [5,6] and nanoparticles [7]—mainly because of their promise in increasing FE nonvolatile-memory density thousands fold by reading and writing into *individual nanoparticles* [3,8,9]. Furthermore, these FE nanostructures are also critical in light of miniaturizing piezoelectric transducers and actuators, ultrasonic devices, and medical imaging detectors [10,11]. From a fundamental point of view, ferroelectricity is caused by atomic off-center displacements, resulting from a delicate balance between long-range (LR) Coulomb interaction and short-range (SR) covalent interaction [12]. In nanostructures, both interactions—and thus their balance—are altered with respect to the bulk, since the LR interaction is truncated due to lack of periodicity, while the SR one is significantly modified near the surface boundary. Consequently, it is commonly believed [13–16] that ferroelectricity in nanostructures would disappear entirely (i.e., there is no ferroelectric off-center instability) below a critical size. This belief has recently received support from a theoretical study on $BaTiO_3$ *thin films* [17]. For FE nanoparticles, while measurements of lattice structures (rather than polarization) are available only at large sizes (~500 Å, Refs. [14,15]), the critical size of ferroelectricity (if any) is unknown [1–3,7]. In fact, it is not even clear whether there are any ferroelectric displacements in FE dots and/or whether these displacements are aligned to form long-range ferroelectric phases. Similarly, virtually nothing is known about the electrical and mechanical responses of FE nanoparticles to electric fields.

The purpose of this Letter is to investigate, from first principles, the ferroelectric properties of $BaTiO_3$ colloidal nanoparticles—and, in particular, to answer whether there is ferroelectricity in FE nanoparticles *and* how these particles respond to applied electric fields. These properties are found to be unusual and differ from what is commonly believed.

Here, we further develop and use a first-principles-derived effective-Hamiltonian approach [18,19] coupled with Monte Carlo simulations. (Ideally, one would like to use direct first-principles density-functional theory, but this is currently computationally impracticable.) The effective Hamiltonians of Refs. [18,19], which are derived from first principles and possess a comparable accuracy, have been successfully applied to many FE materials, including simple $BaTiO_3$ [20], $PbTiO_3$ [21], and $KNbO_3$ [22] systems, and complex $Pb(Zr, Ti)O_3$ [19] and $Pb(Sc, Nb)O_3$ [23] solid solutions. In this approach, local modes $\{\mathbf{u}_i\}$ (i is the cell index) describe the ferroelectric instability in individual 5-atom cells; $\mathbf{u}_i$ are associated with local electrical dipoles $\mathbf{P}_i$ via $\mathbf{P}_i = Z^*\mathbf{u}_i$ (where Z^* is the effective charge of the local mode).

Compared to the original method detailed in Ref. [18], two new developments are made here in order to be able to study FE nanoparticles: (i) No supercell periodic boundary conditions are imposed, and the LR dipole-dipole interaction is performed in real-space (inside the nanoparticles) rather than in reciprocal space. Our simulations with open-boundary condition precisely mimic the experimental situations [3,5,6] in which polarizations in FE wires and films are probed by noncontact electrostatic forces without metallic electrodes. By contrast, the calculations of $BaTiO_3$ *thin films* in Ref. [17] assume a short-circuit boundary condition with metallic electrodes surrounding the films. Also note that, in our real-space implementation without artificial periodicity for finite systems, the potential field generated by *every* dipole in the nanoparticles—including the depolarization field produced by the charges (i.e., uncompensated dipoles) at nanoparticle surfaces—is precisely computed and properly accounted for. (ii) Existence of the vacuum surrounding nanoparticles will cause *surface-induced* atomic relaxations and cell-shape changes (thus affecting both local modes and local inhomogeneous strains) near the nanoparticle surfaces. To account for the effect of atomic relaxations on local modes, an interaction between local modes at surfaces and the vacuum (denoted as mode-vacuum interaction) is added in the

First-Principles Determination of Electromechanical Responses of Solids under Finite Electric Fields

Huaxiang Fu and L. Bellaiche

Physics Department, University of Arkansas, Fayetteville, Arkansas 72701, USA

(Received 28 March 2003; published 30 July 2003)

We describe a first-principles, easy-to-implement, and efficient approach for determining the structural geometry of insulating solids under finite electric fields. This method consists of simultaneously minimizing the field-induced total ionic forces and the electric free energy. Moreover, we present a theory to analyze its predictions that provides a microscopic understanding of electromechanical responses in materials. We illustrate this approach by computing piezoelectric and dielectric responses of two rather different compounds, namely, ferroelectric $PbTiO_3$ and semiconductor GaN.

DOI: 10.1103/PhysRevLett.91.057601 PACS numbers: 77.65.-j, 77.84.Bw, 78.20.Bh

Converting electricity to mechanical energies, via the application of an electric field in piezoelectric materials, is a process of both technological and fundamental interest [1–3]. For this process, the determination and microscopic understanding of the d_{ij} piezoelectric coefficients — which characterize the response of strains η_i ($i = 1, 2, \ldots, 6$ using Voigt notation) to an electric field $\mathcal{E}$ via $\eta_i = \sum_j d_{ij}\mathcal{E}_j$ — is critical in light of discovering new materials having the promise to drastically improve the resolution and range of piezoelectric transducers and actuators. Measuring these coefficients in experiments is straightforward using Sawyer-Tower circuits [4]. On the other hand, unlike the calculation of the *inverse* piezoelectric coefficients e_{ij} [5,6], the use of first-principles density-functional theory (DFT) [7] to compute the piezoelectric responses d_{ij} of solids *under finite electric fields* proved to be exceptionally difficult [8,9]. More specifically, the difficulty lies in that an infinite solid in a static electric field has no ground state. Therefore, energy minimization cannot be directly performed using the variational principle that underlies the time-independent DFT.

The past few years have witnessed an intense activity in seeking methods able to mimic electric-field effects in solids within the DFT. Several approaches have been developed. (i) The approach of Ref. [10] uses periodic real-space supercells, so that charges do not "run away" and that the system still has an energy minimum. This method is straightforward to implement, and was applied to compute the *electronic* response (i.e., electronic screening) to external electric fields. (ii) The scheme proposed in Ref. [8] — that uses field-dependent Wannier functions to prevent charge tunneling — was implemented in a non-self-consistent tight-binding model [8], as well as in self-consistent DFT calculations [11]. (iii) Another method, based on low-order DFT perturbative expansions of thermodynamic energy as a function of electric fields, has been recently developed [12]. This approach takes advantage of the fact that the problem of studying electromechanical responses in solids can be converted to the search of structural geometry under a constrained polarization [12], if one assumes a first-order expansion of energy in which the electric field is only coupled to the zero-field polarization. A simple and less powerful "constrained-polarization" technique was developed and used in Ref. [13]. (iv) Finally, a scheme yielding field-dependent Bloch functions at the local minimum of free energy, and using conjugate-gradient method, has been proposed and successfully developed in Ref. [14]. A similar scheme but implemented within the Car-Parrinello *ab initio* molecular-dynamics method was independently developed in Ref. [15].

In this Letter, we propose and successfully apply an alternative approach that (i) allows an accurate structural minimization of solids under finite electric fields, and thus computation of piezoelectric and dielectric coefficients; (ii) is easily implementable in *any* DFT code; (iii) is computationally efficient; and (iv) naturally leads to the understanding of why some materials, and not others, exhibit large electromechanical responses.

The proposed method starts from the expression (within DFT) of the free energy (F) of an insulator under a uniform finite electric field:

$$F(\mathbf{R}, \eta, \mathcal{E}) = U_{\mathrm{KS}}[\mathbf{R}(\mathcal{E}), \eta(\mathcal{E})] - \mathbf{P}(\mathbf{R}, \eta, \mathcal{E}) \cdot \mathcal{E}, \quad (1)$$

where F, the Kohn-Sham internal energy U_{KS}, and the macroscopic polarization $\mathbf{P}$ for each unit cell all depend on atomic positions $\mathbf{R}$, strain η, and electric field $\mathcal{E}$. Note that the electric field $\mathcal{E}$ in Eq. (1) is the *screened* macroscopic field inside the material [9]. Equation (1) implies that the total force $\mathbf{Q}^i_{\mathrm{tot}}$ acting on ion i is simply $\mathbf{Q}^i_{\mathrm{tot}} = \mathbf{Q}^i_{\mathrm{HF}} + Z^*_i(\mathbf{R}, \eta, \mathcal{E})\mathcal{E}$, where $\mathbf{Q}^i_{\mathrm{HF}}$ is the (usual) Hellmann-Feynman force, and Z^*_i is the Born effective-charge tensor of ion i. *When the system is at its field-induced local minimum*, the total force $\mathbf{Q}^i_{\mathrm{tot}}$ on each ion i should vanish, or, equivalently, the Hellmann-Feynman force should thus satisfy

$$\mathbf{Q}^i_{\mathrm{HF}} = -Z^*_i(\mathbf{R}, \eta, \mathcal{E})\mathcal{E}, \qquad \text{for any ion } i. \quad (2)$$

 0031-9007/03/91(5)/057601(4)$20.00

Effects of Atomic Short-Range Order on the Properties of Perovskite Alloys in their Morphotropic Phase Boundary

A. M. George,[1] Jorge Íñiguez,[2] and L. Bellaiche[1]

[1]*Physics Department, University of Arkansas, Fayetteville, Arkansas 72701, USA*

[2]*Department of Physics and Astronomy, Rutgers University, Piscataway, New Jersey 08854-8019, USA*

(Received 1 April 2003; published 24 July 2003)

The effects of atomic *short-range* order on the properties of $Pb(Zr_{1-x}Ti_x)O_3$ alloy in its morphotropic phase boundary (MPB) are predicted by combining first-principles-based methods and annealing techniques. Clustering is found to lead to a compositional expansion of this boundary, while the association of unlike atoms yields a contraction of this region. Atomic short-range order can thus drastically affect properties of perovskite alloys in their MPB, by inducing phase transitions. Microscopic mechanisms responsible for these effects are revealed and discussed.

DOI: 10.1103/PhysRevLett.91.045504 PACS numbers: 81.30.Bx, 77.22.Ej, 77.80.Bh, 77.84.Dy

Complex insulating perovskite alloys, with the general formula $(A'A''\ldots)(B'B''\ldots)O_3$, are of great interest for a variety of device applications because of their anomalously large electromechanical responses [1–3]. Examples of such applications include piezoelectric transducers and actuators, as well as dielectrics for microelectronics and wireless communication.

Interestingly, many perovskite solid solutions, e.g., $Pb(Zr_{1-x}Ti_x)O_3$ (PZT), $[Pb(Zn_{1/3}Nb_{2/3})O_3]_{1-x}[PbTiO_3]_x$ (PZN–PT), $[Pb(Mg_{1/3}Nb_{2/3})O_3]_{1-x}[PbTiO_3]_x$ (PMN–PT), and $[Pb(Sc_{1/2}Nb_{1/2})O_3]_{1-x}[PbTiO_3]_x$ (PSN–PT), exhibit their largest electromechanical responses for compositions lying within the so-called morphotropic phase boundary (MPB). For more than 50 years this area was thought to *discontinuously* separate, in the temperature-composition plane, a rhombohedral (R) ferroelectric phase exhibiting an electric polarization along a $\langle 111\rangle$ direction from a tetragonal (T) ferroelectric structure having a polarization pointing along a $\langle 001\rangle$ direction. The recent discovery of a monoclinic ferroelectric phase in the MPB of PZT has completely changed this long-accepted picture [4], since this new phase acts as a structural bridge between the R and T phases [4,5]. Furthermore, the polarization in this low-symmetry phase continuously rotates when varying the composition [5,6], explaining why the MPB is the region of choice for optimization of piezoelectric and dielectric responses [5–8]. These recent findings have led to a flurry of investigations aimed at better understanding and characterizing the properties of the MPB in various perovskite alloys. In particular, other low-symmetry phases have also been subsequently discovered in PZN–PT, PMN–PT, and PSN–PT (see, for instance, Refs. [9–15]).

One remaining mystery of the MPB is about its compositional width. More precisely, rather different widths have been reported for the same solid solution, depending on the growth conditions [16]. Chemical short-range ordering (SRO) is often invoked for this variance between different measurements [16], since no long-range ordering occurs (to our knowledge) in the mixed sublattice of PZT and PMN–PT near their MPB. However, why and how SRO would affect the morphotropic phase boundary are two unresolved questions. One possible reason for this lack of knowledge is that the characterization of SRO is challenging and can only be accomplished via nonconventional experiment [17]. Another plausible reason is that mimicking these effects, via the use of computational schemes, requires high accuracy and handling of large supercells, which are two conditions that are not simultaneously met by either usual first-principles techniques or semiempirical approaches.

In this Letter, we take advantage of the accuracy, the possibility of using large supercells, and the microscopic insight provided by the first-principles-based approach of Ref. [5] to study the effect of SRO on the physical properties of PZT in its MPB. The use of this technique (i) proves that SRO does have a drastic effect on these properties, especially in the Ti-poor region of the MPB, (ii) further indicates that short-range association of like atoms has an opposite effect than short-range association of unlike atoms on the compositions delimiting the MPB, and (iii) reveals the microscopic mechanisms responsible for these features.

Short-range ordering in any $A(B'_{1-x}B''_x)O_3$ perovskite alloy can be characterized by the so-called Cowley parameters, defined as [18]

$$\alpha_j(x) = 1 - \frac{P(j)}{x}, \qquad (1)$$

where $P(j)$ is the probability of finding a B' (B'') atom being the jth nearest neighbor of a B'' (B') atom in the mixed B sublattice. Then, $\alpha_j(x) = 0$ for all j's represents a *truly disordered alloy* while $\alpha_j(x) > 0$ is associated with clustering, that is jth nearest neighbors are preferentially of the same atomic kind. The converse—a configuration for which $\alpha_j(x) < 0$—corresponds to *anticlustering*, that is, to a situation in which jth nearest neighbors are

Unusual Thermodynamic Properties and Nonergodicity in Ferroelectric Superlattices

Igor A. Kornev* and L. Bellaiche

Physics Department, University of Arkansas, Fayetteville, Arkansas 72701, USA

(Received 20 February 2003; published 12 September 2003)

The properties of $[Pb(Zr_{1-x_1}Ti_{x_1})O_3]_n/[Pb(Zr_{1-x_2}Ti_{x_2})O_3]_n$ superlattices, with a $2n$ period, are simulated using an *ab initio* based approach. The x_1 and x_2 compositions are chosen to be located across the morphotropic phase boundary of the corresponding disordered alloys, while the $(x_1 + x_2)/2$ average composition lies inside this boundary. These superlattices exhibit an unusual thermodynamic phase transition sequence, including a triclinic ground state. They also have the kind of peculiar free-energy landscape yielding nonergodicity. The effects responsible for these anomalies are discussed.

DOI: 10.1103/PhysRevLett.91.116103 PACS numbers: 68.65.Cd, 64.70.Kb, 77.80.Bh, 81.05.Zx

Ferroelectric heterostructures are of increasing technological interest because of their potential applications in advanced microsystems [1]. A particular type of heterostructure that has received recent attention is formed by superlattices, i.e., by compounds consisting of alternating layers made from different materials [2]. The properties of ferroelectric superlattices can be very different from those of their constituents, as a result of the complex nanostructure of these multilayer systems [3].

Another (currently unrelated) activity is taking place in ferroelectrics, namely, the investigation of the morphotropic phase boundary (MPB) of perovskite alloys [4]. This boundary was previously thought to discontinuously separate compositional regions of tetragonal and rhombohedral symmetry, for which the electrical polarization lies along a ⟨001⟩ and a ⟨111⟩ pseudocubic direction, respectively. The discovery of a monoclinic M_A phase in the MPB of $Pb(Zr_{1-x}Ti_x)O_3$ (PZT) solid solutions has drastically changed this picture [5]. [The notation for monoclinic phases is that of Ref. [6].] As a matter of fact, this M_A phase acts as a structural bridge between the tetragonal and rhombohedral phases, in the sense that the polarization in the M_A phase rotates between the pseudocubic ⟨001⟩ and ⟨111⟩ directions, as the Ti composition decreases within the MPB [7].

Independently of the two activities mentioned above, another research field is being intensively pursued. This field is the study of nonergodic systems, which are systems exhibiting properties that do not obey the usual Gibbs equilibrium statistical mechanics. Nonergodicity has been found in very diverse compounds, e.g., spin and structural glasses, granular systems, etc. [8]. Examples of observed behaviors associated with nonergodicity are an anomalous time dependency of macroscopic properties and/or a drastic dependency of such properties with thermal history [9]. The existence of various energetic minima that are separated by large barriers can drive a system to be nonergodic [10]. As a matter of fact, such a free-energy landscape can trap the system—for a long time at the experimental scale—in a particular valley, even if this valley is not the deepest one in energy. Consequently, the properties of such systems cannot be described by the Gibbs statistical averaging but rather require the use of new formalisms—e.g., the Edwards model—only involving the "blocked" configurations [10].

The aim of this Letter is twofold. First, we report that there is an unexplored class of ferroelectric superlattices that has unusual thermodynamic properties. This class is made by alternating layers of alloys having compositions lying just across their MPB. Second, we also predict that such layered systems can display nonergodicity.

More precisely, we theoretically investigate $[Pb(Zr_{1-x_1}Ti_{x_1})O_3]_n/[Pb(Zr_{1-x_2}Ti_{x_2})O_3]_n$ superlattices having (i) a $2n$ period, (ii) x_1 and x_2 compositions lying in the rhombohedral and tetragonal regions located just across the MPB of disordered PZT, and (iii) a $(x_1 + x_2)/2$ average composition yielding a monoclinic M_A phase in this MPB. These superlattices are chosen to be oriented along the [001] direction (see Fig. 1) and are denoted as $(nPZTx_1/nPZTx_2)$. Note that Ti and Zr atoms are randomly distributed within each (001) B plane under the constraint of fixed (x_1 or x_2) composition. We use

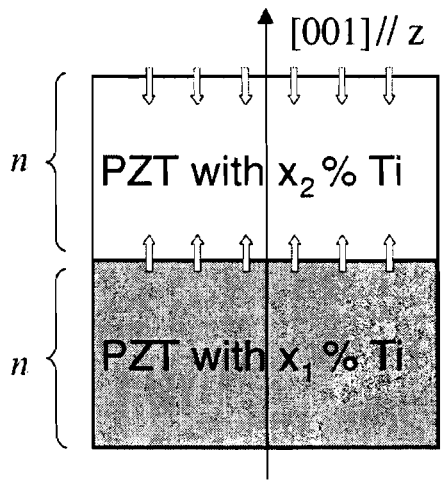

FIG. 1. Schematic illustration of the studied superlattices. n layers of PZT with a x_1 Ti concentration alternate with n layers of PZT with a x_2 Ti composition. The arrows indicate the strain field induced by the Ti and Zr size difference.

 0031-9007/03/91(11)/116103(4)$20.00

First-Principles Determination of Electromechanical Responses of Solids under Finite Electric Fields

Huaxiang Fu and L. Bellaiche

Physics Department, University of Arkansas, Fayetteville, Arkansas 72701, USA

(Received 28 March 2003; published 30 July 2003)

We describe a first-principles, easy-to-implement, and efficient approach for determining the structural geometry of insulating solids under finite electric fields. This method consists of simultaneously minimizing the field-induced total ionic forces and the electric free energy. Moreover, we present a theory to analyze its predictions that provides a microscopic understanding of electromechanical responses in materials. We illustrate this approach by computing piezoelectric and dielectric responses of two rather different compounds, namely, ferroelectric $PbTiO_3$ and semiconductor GaN.

DOI: 10.1103/PhysRevLett.91.057601 PACS numbers: 77.65.-j, 77.84.Bw, 78.20.Bh

Converting electricity to mechanical energies, via the application of an electric field in piezoelectric materials, is a process of both technological and fundamental interest [1–3]. For this process, the determination and microscopic understanding of the d_{ij} piezoelectric coefficients — which characterize the response of strains η_i ($i = 1, 2, \ldots, 6$ using Voigt notation) to an electric field $\mathcal{E}$ via $\eta_i = \sum_j d_{ij}\mathcal{E}_j$ — is critical in light of discovering new materials having the promise to drastically improve the resolution and range of piezoelectric transducers and actuators. Measuring these coefficients in experiments is straightforward using Sawyer-Tower circuits [4]. On the other hand, unlike the calculation of the *inverse* piezoelectric coefficients e_{ij} [5,6], the use of first-principles density-functional theory (DFT) [7] to compute the piezoelectric responses d_{ij} of solids *under finite electric fields* proved to be exceptionally difficult [8,9]. More specifically, the difficulty lies in that an infinite solid in a static electric field has no ground state. Therefore, energy minimization cannot be directly performed using the variational principle that underlies the time-independent DFT.

The past few years have witnessed an intense activity in seeking methods able to mimic electric-field effects in solids within the DFT. Several approaches have been developed. (i) The approach of Ref. [10] uses periodic real-space supercells, so that charges do not "run away" and that the system still has an energy minimum. This method is straightforward to implement, and was applied to compute the *electronic* response (i.e., electronic screening) to external electric fields. (ii) The scheme proposed in Ref. [8] — that uses field-dependent Wannier functions to prevent charge tunneling — was implemented in a non-self-consistent tight-binding model [8], as well as in self-consistent DFT calculations [11]. (iii) Another method, based on low-order DFT perturbative expansions of thermodynamic energy as a function of electric fields, has been recently developed [12]. This approach takes advantage of the fact that the problem of studying electromechanical responses in solids can be converted to the search of structural geometry under a constrained polarization [12], if one assumes a first-order expansion of energy in which the electric field is only coupled to the zero-field polarization. A simple and less powerful "constrained-polarization" technique was developed and used in Ref. [13]. (iv) Finally, a scheme yielding field-dependent Bloch functions at the local minimum of free energy, and using conjugate-gradient method, has been proposed and successfully developed in Ref. [14]. A similar scheme but implemented within the Car-Parrinello *ab initio* molecular-dynamics method was independently developed in Ref. [15].

In this Letter, we propose and successfully apply an alternative approach that (i) allows an accurate structural minimization of solids under finite electric fields, and thus computation of piezoelectric and dielectric coefficients; (ii) is easily implementable in *any* DFT code; (iii) is computationally efficient; and (iv) naturally leads to the understanding of why some materials, and not others, exhibit large electromechanical responses.

The proposed method starts from the expression (within DFT) of the free energy (F) of an insulator under a uniform finite electric field:

$$F(\mathbf{R}, \eta, \mathcal{E}) = U_{\mathrm{KS}}[\mathbf{R}(\mathcal{E}), \eta(\mathcal{E})] - \mathbf{P}(\mathbf{R}, \eta, \mathcal{E}) \cdot \mathcal{E}, \quad (1)$$

where F, the Kohn-Sham internal energy U_{KS}, and the macroscopic polarization $\mathbf{P}$ for each unit cell all depend on atomic positions $\mathbf{R}$, strain η, and electric field $\mathcal{E}$. Note that the electric field $\mathcal{E}$ in Eq. (1) is the *screened* macroscopic field inside the material [9]. Equation (1) implies that the total force $\mathbf{Q}^i_{\mathrm{tot}}$ acting on ion i is simply $\mathbf{Q}^i_{\mathrm{tot}} = \mathbf{Q}^i_{\mathrm{HF}} + Z^*_i(\mathbf{R}, \eta, \mathcal{E})\mathcal{E}$, where $\mathbf{Q}^i_{\mathrm{HF}}$ is the (usual) Hellmann-Feynman force, and Z^*_i is the Born effective-charge tensor of ion i. *When the system is at its field-induced local minimum*, the total force $\mathbf{Q}^i_{\mathrm{tot}}$ on each ion i should vanish, or, equivalently, the Hellmann-Feynman force should thus satisfy

$$\mathbf{Q}^i_{\mathrm{HF}} = -Z^*_i(\mathbf{R}, \eta, \mathcal{E})\mathcal{E}, \quad \text{for any ion } i. \quad (2)$$

 0031-9007/03/91(5)/057601(4)$20.00

Cationic-competition-induced monoclinic phase in high piezoelectric $(PbSc_{1/2}Nb_{1/2}O_3)_{1-x}$-$(PbTiO_3)_x$ compounds

R. Haumont,[1] B. Dkhil,[1] J. M. Kiat,[1,2] A. Al-Barakaty,[3] H. Dammak,[1] and L. Bellaiche[3]
[1]*Laboratoire Structures, Propriétés et Modélisation des Solides, Ecole Centrale Paris, CNRS-UMR8580, Grande Voie des Vignes 92295, Châtenay-Malabry Cedex, France*
[2]*Laboratoire Léon Brillouin, CE Saclay, CNRS-UMR12, 91191 Gif-sur-Yvette Cedex, France*
[3]*Department of Physics, University of Arkansas, Fayetteville, Arkansas 72701, USA*
(Received 16 December 2002; revised manuscript received 6 March 2003; published 30 July 2003)

A global picture for the structural evolution in the relaxor-ferroelectric solid solution $(PbSc_{1/2}Nb_{1/2}O_3)_{1-x}$-$(PbTiO_3)_x$ is proposed. Thanks to x-ray profile analysis and Rietveld neutron powder refinement, a monoclinic phase has been evidenced in the morphotropic region (i.e., $x \approx 0.43$). This lower-symmetry phase "bridges" the rhombohedral Ti-poor phase ($x \leq 0.26$) with the tetragonal Ti-rich phase ($x \geq 0.55$), in a similar way as in $PbMg_{1/3}Nb_{2/3}O_3$-$PbTiO_3$ or $Pb(Zn_{1/3}Nb_{2/3})O_3$-$PbTiO_3$. For weak titanium concentration, we observe a macroscopic rhombohedral state with local monoclinic symmetry resulting from the combination between Pb and Sc/Nb/Ti shifts along [001] and [111] directions, respectively. Cationic competition with Ti doping increases the coherence length of this short-range monoclinic phase, which becomes long range in the morphotropic region. This intermediate monoclinic phase is in complete agreement with our first-principles calculations which predict *Pm* or *Cm* space groups. It has been shown that these ones are very close to each other in the free-energy space, and a minor change of atomic distribution and/or a slight modification in composition or in stoichiometry is enough to alter the space group of the monoclinic ground state. Finally, in the Ti-rich region, the monoclinic ground state is destroyed in favor of a tetragonal phase.

DOI: 10.1103/PhysRevB.68.014114 PACS number(s): 61.50.−f

I. INTRODUCTION

One of the most interesting and studied groups of disordered compounds undergoing structural phase transitions are the so-called relaxors.[1] The main structural feature of relaxors is the random occupation of equivalent positions by different heterovalent ions. This chemical disorder results in the destruction of the normal ferroelectric phase transition and the appearance of physical properties similar to those of disordered magnets. The associated dielectric susceptibility exhibits an unusual response, strongly dependent on frequency and with very high values over a broad range of temperatures.[2] The relaxor state is then characterized by the frustration of local polarizations which can prevent long-range ferroelectric order from developing completely. Most of the relaxors are lead oxides belonging to the class of perovskites with either the general formula $Pb(B')_{1/3}(B'')_{2/3}O_3$ ($B'=Mg^{2+}$, Zn^{2+},...; $B''=Nb^{5+}$, Ta^{5+},...), i.e., 1:2-type compounds or $Pb(B')_{1/2}(B'')_{1/2}O_3$ ($B'=Sc^{3+}$, In^{3+},...; $B''=Nb^{5+}$, Ta^{5+},...), i.e., 1:1-type compounds.

In the case of 1:2-type compounds such as $PbMg_{1/3}Nb_{2/3}O_3$ (PMN), considered by most researchers to be the prototype of relaxors, the disorder results from the random occupation of the B site of the perovskite by two cations of different valences, namely, Mg^{2+} and Nb^{5+}. Charge neutrality imposes the Mg:Nb stoichiometry of 1:2, while the mixed-valence character of the B site produces random electric-field gradients and a locally broken translational symmetry.[3] Below a certain temperature, polar nanometric regions take place and freeze out.[4,5] No phase transition into a macroscopic ferroelectric phase occurs, the average structure remaining cubic down to 5 K.[6,7] But an induced ferroelectric phase can be realized by means of partial substitution,[8,9] external electric field,[10–12] or pressure.[13] Therefore existence or absence of phase transition is not a necessary condition for the relaxation phenomenon. Indeed, both 1:2- and 1:1-type ferroelectric relaxors such as $Pb(Zn_{1/3}Nb_{2/3})O_3$ (PZN) (Ref. 14) and $Pb(Sc_{1/2}Nb_{1/2})O_3$ (PSN),[15,16] respectively, undergo a spontaneous phase transition from a cubic to a rhombohedral phase.

PSN is of a special interest because the degree of ordering of Sc^{3+}- and Nb^{5+}-type ions can be controlled by thermal treatment, due to a high-temperature order-disorder transformation, which influences the dielectric behavior.[15–17] This feature provides promising directions for future experimental and theoretical research; indeed it has been shown from a first-principles-derived approach[18–21] that some specific arrangements between Sc^{3+} and Nb^{5+} (i) greatly enhance the electromechanical responses, (ii) lead to currently unobserved ground states of orthorhombic and monoclinic symmetries (while the disordered material adopts a well-known rhombohedral ground state), and (iii) can considerably shift the Curie temperature. In this heterovalent system, electrostatic interactions among Sc^{3+} and Nb^{5+} ions are then found to be very important. In addition, the stabilized structure is also conditioned by Pb^{2+} ions forming short Pb-O bonds.[18]

Recently, relaxor-based single crystals such as $(PbMg_{1/3}Nb_{2/3}O_3)_{1-x}$-$(PbTiO_3)_x$ (PMN-PT) and $(PbZn_{1/3}Nb_{2/3}O_3)_{1-x}$-$(PbTiO_3)_x$ (PZN-PT) have been reported to exhibit excellent piezoelectric properties, much better than the well-known $PbZr_xTi_{1-x}O_3$ (PZT) polycrystalline ceramics,[22] and have attracted attention for their potential in various applications.[23–25] Though clearly promising for transducers and actuators, their relatively low Curie tem-

Strained Hexagonal ScN: A Material with Unusual Structural and Optical Properties

V. Ranjan and L. Bellaiche
Physics Department, University of Arkansas, Fayetteville, Arkansas 72701, USA

Eric J. Walter
Department of Physics, College of William and Mary, Williamsburg, Virginia 23187, USA
(Received 14 March 2003; published 25 June 2003)

Local-density approximation calculations are performed to predict properties of compressively strained hexagonal ScN. This material is found to exhibit a large electromechanical response, a structural phase transition from a nonpolar to a polar structure, and a variation of the band gap in the entire visible light range when continuously changing the compressive strain. Microscopic effects responsible for these anomalies are revealed and discussed. Suggestions on how to practically grow ScN-based materials having such unusual properties are also provided.

DOI: 10.1103/PhysRevLett.90.257602 PACS numbers: 77.84.–s, 78.20.Bh, 78.30.Fs, 61.50.Ks

The optical properties of some semiconductors are of primary importance. For instance, the change in compositions of $(Ga_{1-x-y}In_xAl_y)N$ alloys or the change in the size of GaN quantum dots leads to photoluminescence in the entire visible spectrum [1,2], which is of considerable interest for the light-emitting device applications. A second class of compounds with fascinating properties is formed by *ferroelectrics*. These materials can undergo a structural phase transition between a nonpolar and a polar structure, when one varies the temperature [3]. This phase transition is associated with huge piezoelectric and dielectric responses, which explains why ferroelectrics are the materials of choice for applications—such as ultrasonic and sonar listening devices—based on an efficient conversion between electrical and mechanical signals [3].

Recently, Ref. [4] *suggested* that disordered hexagonal $(Sc_{1-x}Ga_x)N$ or $(Sc_{1-x}In_x)N$ alloys can bridge the semiconductor and the ferroelectric classes (i) by exhibiting a wide range of band gaps and (ii) by having large electromechanical responses, when varying x. This suggestion was based on the structural difference between hexagonal ScN and wurtzite GaN or InN, and has not yet been confirmed by either calculations or experiments.

The aim of this Letter is threefold. First, we want to *demonstrate* that hexagonal ScN-based materials can result in "smart" multifunctional compounds. Second, we wish to prove that varying another experimentally accessible parameter, namely, the strain rather than the composition, can lead to the simultaneous occurrence of features usually associated with semiconductors or ferroelectrics. Finally, our last goal is to provide suggestions on how to practically grow hexagonal ScN-based materials having such bridging properties.

Here, we report first-principles calculations that indeed show that compressively strained hexagonal ScN simultaneously exhibits (1) a large variation of the band gap in the technologically important light spectral region, (2) a phase transition leading to the appearance of a spontaneous electrical polarization, and (3) large electromechanical responses, when continuously varying the compressive strain. Our simulations also reveal the microscopic mechanisms responsible for the useful combination of these properties. These discoveries imply that simultaneously varying the composition *and* the strain in disordered hexagonal $(Sc_{1-x}Ga_x)N$ or $(Sc_{1-x}In_x)N$ alloys is a promising way to generate polar semiconductors with optimized electromechanical and optical properties.

Here, we use the density-functional theory, within the local-density approximation (LDA) [5–7], to investigate properties of hexagonal ScN. Other technical details of these calculations are given in Ref. [4]. We focus on hexagonal ScN whose primitive lattice vectors are $\mathbf{a}_1 = a[\frac{1}{2}\mathbf{x} - (\sqrt{3}/2)\mathbf{y}]$, $\mathbf{a}_2 = a[\frac{1}{2}\mathbf{x} + (\sqrt{3}/2)\mathbf{y}]$, and $\mathbf{a}_3 = c\mathbf{z}$, where a and c are the two lattice parameters, c/a is the axial ratio, and $\mathbf{x}$, $\mathbf{y}$, and $\mathbf{z}$ are the unit vectors along the three Cartesian axes. The primitive cell contains two Sc atoms, located at $\mathbf{r}_1 = \mathbf{0}$ and $\mathbf{r}_2 = \frac{2}{3}\mathbf{a}_1 + \frac{1}{3}\mathbf{a}_2 + \frac{1}{2}\mathbf{a}_3$, and two N atoms whose positions are given by $\mathbf{r}_3 = u\mathbf{a}_3$ and $\mathbf{r}_4 = \frac{2}{3}\mathbf{a}_1 + \frac{1}{3}\mathbf{a}_2 + (\frac{1}{2} + u)\mathbf{a}_3$, where u is the dimensionless internal parameter.

The minimization of the total energy with respect to *all* degrees of freedom yields [4] $a = a_{eq} = 3.66$ Å, $c/a = 1.207$ and $u = 0.5$, and leads to the structure displayed in Fig. 1(a). This hexagonal phase is a layered structure in which each (0001) plane contains the same amount of Sc and N atoms. This structure, which is referred to as the h phase in Refs. [4,8], also exhibits two other important features. First, this phase is paraelectric, as a result of its $P6_3/mmc$ space group. Second, it is nearly fivefold coordinated: a given Sc (N) atom forms short bonds $\simeq 2.11$ Å with *three* N (Sc) atoms belonging to the same basal plane but also forms slightly longer bonds $\simeq 2.21$ Å with *two* other N (Sc) atoms being in the (0001) planes below and above it, respectively.

One goal of this Letter is to go beyond the study of the equilibrium structure displayed in Fig. 1(a), by

Off-center atomic displacements in $BaTiO_3$ quantum dots

Huaxiang Fu and Laurent Bellaiche

Physics Department, University of Arkansas, Fayetteville, Arkansas 72701

Abstract. Structural properties of $BaTiO_3$ quantum dots are studied using a first-principles derived effective-Hamiltonian approach. Truncated long-range dipole-dipole interaction and modification of the short-range interaction due to the existence of vacuum are taken into account. Our calculations show that there are significant off-center atomic displacements in these dots; the amplitudes of such displacements are comparable with those occuring in bulk $BaTiO_3$. However, unlike in the bulk system, the net polarization in dots is found to be zero. Our results also show that the local displacements in the dots tend to flip across the distance of the entire dot, resulting in an unusual and complex pattern.

INTRODUCTION

As temperature decreases, bulk $BaTiO_3$ undergoes sequences of structural transitions[1]: from the paraelectric cubic phase to a tetragonal phase at 403K, then to an orthorhombic phase at 278K, and finally to a rhombohedral phase at 183K. Some of these phase transitions have an order-disorder character, as indicated by the existences of substantial atomic displacements at cubic phases and the broad Fourier spectrum over the Brillouin zone.[2] The microscopic mechanism that are responsible for the existence of ferroelectric phases are, in particular, the long-range (LR) dipole-dipole interaction and the short-range (SR) interatomic covalent coupling. The ferroelectric phases of bulk $BaTiO_3$ have now been understood, at a microscopic level, from both first-principles calculations[3] and effective Hamiltonian simulations.[2]

Compared to bulk materials, quantum dots (i.e., finite-size nanocrystals) do not have the imposed periodic boundary condition. As a result, the microscopic forces that determine the material phases are altered, and the delicated balance between the LR and SR interactions in bulk can be strongly modified with respect to the bulk case. It is therefore interesting to examine whether there are significant off-center displacements in dots, and whether these displacements will align themselves to form ferroelectric phases. Specifically, the following three differences exist between the bulk and dots: (1) The LR dipole interaction that is crucial to yield ferroelectric phases is truncated in dots. Unlike in bulk, the electrostatic potentials at different cells are thus not equal. (2) The SR interaction among the atoms near the boundary of dots are altered. The atomic displacements at the surfaces will thus be different from those inside the dots. (3) Depending on the sizes of dots, dielectric screening may be different from the bulk value, which will affect the LR dipole energy.

Here we study the off-center atomic displacements in $BaTiO_3$ dots using an effective

CP677, *Fundamental Physics of Ferroelectrics 2003*, edited by P. K. Davies and D. J. Singh

First-principles study of $(BiScO_3)_{1-x}$-$(PbTiO_3)_x$ piezoelectric alloys

Jorge Íñiguez,[1,*] David Vanderbilt,[1] and L. Bellaiche[2]
[1]*Department of Physics and Astronomy, Rutgers University, Piscataway, New Jersey 08854-8019, USA*
[2]*Physics Department, University of Arkansas, Fayetteville, Arkansas 72701, USA*
(Received 31 January 2003; revised manuscript received 17 April 2003; published 20 June 2003)

We report a first-principles study of a class of $(BiScO_3)_{1-x}$-$(PbTiO_3)_x$ (BS-PT) alloys recently proposed by Eitel *et al.* as promising materials for piezoelectric actuator applications. We show that (i) BS-PT displays very large structural distortions and polarizations at the morphotropic phase boundary (MPB) (we obtain a c/a of $\sim 1.05-1.08$ and $P_{tet} \approx 0.9$ C/m^2); (ii) the ferroelectric and piezoelectric properties of BS-PT are dominated by the onset of hybridization between Bi/Pb-6p and O-2p orbitals, a mechanism that is enhanced upon substitution of Pb by Bi; and (iii) the piezoelectric responses of BS-PT and $Pb(Zr_{1-x}Ti_x)O_3$ (PZT) at the MPB are comparable, at least as far as the computed values of the piezoelectric coefficient d_{15} are concerned. While our results are generally consistent with experiment, they also suggest that certain intrinsic properties of BS-PT may be even better than has been indicated by experiments to date. We also discuss results for PZT that demonstrate the prominent role played by Pb displacements in its piezoelectric properties.

DOI: 10.1103/PhysRevB.67.224107 PACS number(s): 77.65.Bn, 77.84.Dy, 61.66.Fn

I. INTRODUCTION

Perovskite alloys based on $PbTiO_3$ (PT) are of considerable interest for applications as piezoelectric actuator materials.[1,2] The phase diagrams of the most technologically important alloys are characterized by a morphotropic phase boundary (MPB) separating the PT-rich tetragonal phase, in which the polarization lies along a $\langle 001 \rangle$ direction, from the PT-poor rhombohedral phase, in which the polarization is along a $\langle 111 \rangle$ direction.[3] Because the structural transition between these two phases brings about a large electromechanical response, materials with a composition lying close to the MPB are the preferred ones for applications. Examples of such materials are $Pb(Zr_{1-x}Ti_x)O_3$ (PZT) or PZN-PT, in which PT is alloyed with $PbZrO_3$ (PZ) or $Pb(Zn_{1/3}Nb_{2/3})O_3$ (PZN), respectively.

Recently, attention has been drawn to a new class of materials in which PT is alloyed with Bi-based perovskites, the best-studied example being $(BiScO_3)_{1-x}$-$(PbTiO_3)_x$ (BS-PT).[4] The appeal of BS-PT is twofold: (i) it appears to have piezoelectric properties comparable to those of PZT and PZN-PT in quality, and (ii) its dielectric and piezoelectric properties should be more robust, over a wider temperature range, than those of PZT and PZN-PT. The physical reason behind (ii) is that the Curie temperature within the MPB composition range (T_C^{MPB}) is higher in BS-PT ($\sim 450\,^\circ$C) than in PZT ($\sim 400\,^\circ$C) or PZN-PT ($\sim 200\,^\circ$C), suggesting that BS-PT at room temperature will age more slowly, its properties will be more temperature independent, etc.[2,4] A possible drawback is that BS-PT is evidently not thermodynamically stable in the perovskite crystal structure over the entire range of composition. However, for application purposes it is only important that the perovskite structure can be obtained for compositions near the MPB, and this is indeed the case.

The authors of Ref. 4 synthesized BS-PT guided by an empirical crystal-chemistry rule suggesting that since Bi^{3+} is too small an ion to form a cubic perovskite with Sc^{3+}, it will have a strong tendency to move off-center from its high-symmetry position, yielding a high structural transition temperature. While perhaps overly simplistic, this reasoning is undoubtedly partially correct and is likely to be useful for materials engineering. However, it is unclear how to explain the large piezoelectric responses found in BS-PT based on ion-size considerations alone. The ferroelectric properties of materials such as PZT are known to be related to the partial covalency of some bonds,[5,6] and the situation in BS-PT should be similar. On the other hand, most of the relevant piezoelectric alloys have only Pb on the A site of their perovskite structure, and the chemistry of Pb is known to be very important to their properties.[7] The substitution of Pb by Bi in BS-PT is thus of particular interest in view of the good piezoelectric properties of this material.

We present here a first-principles study of BS-PT. We find that Bi plays a crucial role, and in particular that hybridization between Bi-6p and O-2p orbitals is the driving force for the ferroelectric instabilities of BS-PT, allowing for very large polarizations and responses. Our results are generally consistent with experiment, but they also suggest that the intrinsic ferroelectric and piezoelectric properties of BS-PT alloys might be even better than those measured experimentally to date.

We present our results in the form of a systematic comparison of the properties of BS-PT with those of PZT. Section II describes the first-principles methods employed. In Sec. III, we study the ferroelectric instabilities of pure BS, PT, and PZ, introducing some corresponding calculations on $BiYO_3$ (BY) as an aid to the discussion. In Sec. IV, we discuss the ferroelectric instabilities of the alloys and make contact with the experimental results, while Sec. V is devoted to the piezoelectric properties of the alloys near the MPB. We summarize and conclude in Sec. VI.

II. METHODS

The calculations were performed within a plane-wave implementation of the local-density approximation (LDA) to

PHYSICAL REVIEW B, VOLUME 65, 180301(R)

Optical phonons associated with the low-temperature ferroelectric properties of perovskite solid solutions

A. M. George,[1] Jorge Íñiguez,[1,2] and L. Bellaiche[1]
[1]*Physics Department, University of Arkansas, Fayetteville, Arkansas 72701*
[2]*Department of Physics and Astronomy, Rutgers University, Piscataway, New Jersey 08854-8019*
(Received 9 October 2001; published 19 April 2002)

A simple way of analyzing the atomic displacements in perovskite alloys is used to determine the optical phonons contributing to their low-temperature ferroelectric properties. This determination (i) leads to the identification of *three different kinds* of solid solutions, (ii) reveals why simple theoretical models can be used in some alloys and not in others, and (iii) explains why unusual phase transitions can occur in ordered ferroelectric solid solutions.

DOI: 10.1103/PhysRevB.65.180301 PACS number(s): 63.20.−e, 77.84.Dy, 77.80.Bh

At very low temperature, the different (five-atom) unit cells of *ferroelectric* and *simple* perovskite ABO_3 crystals all exhibit the same atomic displacements. As a result, the ferroelectric properties of such simple systems are fully associated with a *zone-center* optical phonon mode. On the other hand, ferroelectric perovskite $(A'A''\cdots)(B'B''\cdots)O_3$ *alloys* lack this translational symmetry, since different A and/or B sites can be occupied by different kinds of atoms. Such loss of symmetry implies that the $\mathbf{k}$ vectors of the simple cubic first Brillouin zone are not good quantum numbers to index the phonon spectrum of solid solutions. However, despite the formal illegitimacy of using physical concepts based on simple cubic translational invariance in solid solutions, recent *ab initio* calculations[1,2] have been able to accurately reproduce structural and piezoelectric properties of some ferroelectric perovskite alloys—namely, rhombohedral and tetragonal disordered $PbZr_{1-x}Ti_xO_3$ (PZT)—by using the virtual crystal approximation (VCA).[3] This VCA approach treats the ferroelectric alloy as a *simple* system and, as a result, only incorporates the effect of the reciprocal Γ point on the alloy low-temperature properties. On the other hand, Refs. 4,5 reported that the VCA approximation is unable to mimic ferroelectric features of other solid solutions such as the newly discovered monoclinic[6] PZT and disordered $PbSc_{0.5}Nb_{0.5}O_3$ (PSN).

It would thus be useful to quantify the degree of translational symmetry associated with the low-temperature ferroelectric properties of different alloy systems. Such a quantification would determine if some simple approximations can be used for some alloys and not for others. This analysis may also help in understanding why *atomic ordering* in solid solutions can lead to striking features as, for instance, recently predicted structural phase transitions and enhancement of electromechanical responses.[7–10] The aim of this paper is to better understand ferroelectric solid solutions by analyzing different systems with a simple procedure that enables such a quantification.

Here, we use the numerical scheme proposed in Ref. 4, which consists of constructing an alloy effective Hamiltonian from local-density approximation (LDA) calculations.[11,12] Details of this construction can be found in Refs. 4, 5, 8–10, and 13. The total energy provided by the alloy effective Hamiltonian is used in Monte Carlo simulations on $12\times12\times12$ supercells. The simulated temperature is kept fixed at a small value, namely, 5 K. 2×10^4 Monte Carlo sweeps are first performed to equilibrate the system, and then 2×10^4 sweeps are used to get the statistical averages. The outputs of the Monte Carlo procedure are the set of polar local soft modes $\{\mathbf{u}_i\}$, where i labels the cells, and the homogeneous strain tensor. Note that the $\mathbf{u}_i$ modes are directly related to the electrical polarization. The position in the first Brillouin zone of the optical phonons contributing to the low-temperature ferroelectric properties of the studied materials is then identified via the computation of the reciprocal-space $f_\mu(\mathbf{k})$ coefficients, defined as

$$f_\mu(\mathbf{k})=\beta\sum_i \exp(i\mathbf{k}\cdot\mathbf{R}_i)u_{i,\mu}, \qquad (1)$$

where $\mathbf{k}$ is a vector in the first Brillouin zone of the simple perovskite structure and $\mathbf{R}_i$ is the lattice vector associated with cell i. $u_{i,\mu}$ is the μ cartesian coordinate—i.e., $\mu=x,y$ or z—of the (real-space) local mode $\mathbf{u}_i$ centered on cell i.[14] β is a normalization coefficient yielding $\Sigma_k|f_\mu(\mathbf{k})|^2=1$. A value close to 1 for $|f_\mu(\mathbf{k})|^2$ at $\mathbf{k}=\mathbf{0}$ thus corresponds to the situation where only the Γ point contributes to the ferroelectric properties associated with the μ axis. On the other hand, a value significantly smaller than 1 for $|f_\mu(\mathbf{0})|^2$ implies the activation of optical phonons at off-center k points.[15] Note that, for each system studied, we use one snapshot among the thermally equilibrated Monte Carlo configurations to compute the coefficients defined in Eq. (1).

Table I shows the cartesian coordinates ($\langle u_x\rangle$, $\langle u_y\rangle$, and $\langle u_z\rangle$) of the supercell average of the local mode vectors, as well as the $|f_\mu(\mathbf{k})|^2$ coefficients at the Γ point, at 5 K and for three *disordered* solid solutions: (i) the PZT alloy with a Ti composition of 46%, for which the predicted ground state is ferroelectric and *rhombohedral*[4]—as indicated by the fact that $\langle u_x\rangle=\langle u_y\rangle=\langle u_z\rangle\neq0$; (ii) another PZT alloy with a Ti composition of 48% and crystallizing in the newly discovered *monoclinic* and so-called M_A phase[6,16]—for which $\langle u_z\rangle$ is larger than $\langle u_x\rangle$ and $\langle u_x\rangle=\langle u_y\rangle\neq0$,[17] and (iii) the PSN alloy that is predicted to adopt a ferroelectric rhombohedral ground state with an electrical polarization along the [111] direction, in agreement with experiments.[18,19] For comparison, Table I further provides similar information for the

PHYSICAL REVIEW B 66, 201203(R) (2002)

Properties of hexagonal ScN versus wurtzite GaN and InN

N. Farrer and L. Bellaiche
Physics Department, University of Arkansas, Fayetteville, Arkansas 72701

(Received 26 August 2002; revised manuscript received 1 October 2002; published 20 November 2002)

Local-density approximation calculations are performed to compare properties of hexagonal ScN with those of wurtzite GaN and InN. A nearly five-times coordinated hexagonal structure is found to be (meta)stable in ScN, unlike the wurtzite structure. Structural, dielectric, and optical properties of this stable hexagonal phase are predicted to be rather different from those of wurtzite GaN and InN. This implies that disordered hexagonal $Sc_{1-x}Ga_xN$ and $Sc_{1-x}In_xN$ alloys are very attractive both fundamentally and technologically.

DOI: 10.1103/PhysRevB.66.201203 PACS number(s): 61.50.Ah, 81.05.Zx, 77.84.Bw, 71.20.Nr

Interest in wurtzite nitride semiconductors—such as GaN, InN, AlN, and their alloys—has exploded in the past few years mainly because of their prospects in light-emitting device applications.[1,2] On the other hand, another nitride compound—that is, ScN—has attracted much less attention up to now, despite the fact that alloying ScN with GaN or InN could result in materials useful for band-gap engineering.[3,4]

Two kinds of recent studies conducted on ScN can be distinguished. First, theoretical and experimental investigations[5–7] mainly focused on the electronic band structure of ScN in its *rocksalt* ground state. All these works concluded that ScN is a semiconductor rather than a semimetal, as sometimes previously suggested.[8–10] Second, the pioneering study of Takeuchi[11] was aimed at investigating the stability of different phases *besides the rocksalt structure*. One particularly interesting prediction of Ref. 11 is the existence of a (meta)stable wurtzite structure in ScN. This finding can be important in light of growing technologically-promising $Sc_{1-x}Ga_xN$ and $Sc_{1-x}In_xN$ materials that would be true (hexagonal) *alloys* rather than an heterogeneous mixture between a rocksalt phase—ground state of ScN—and a wurtzite structure—ground states of both GaN and InN.

One aim of this Rapid Communication is to revisit the stability of the wurtzite phase in ScN. In particular, our calculations point out that the wurtzite structure is *unstable* in ScN. In contrast, we further predict that the hexagonal structure that has recently been found in MgO and which is nearly five-times coordinated,[12] is stable in ScN.

The second aim of this Rapid Communication is to show that the structural, dielectric, and optical properties of this hexagonal phase in ScN are rather different from those of wurtzite GaN and InN. Consequently, we expect that anomalous effects should occur in *hexagonal* $Sc_{1-x}Ga_xN$ and $Sc_{1-x}In_xN$ solid solutions when increasing the x composition. Examples of such effects are (1) a continuous evolution of the axial ratio from $\simeq 1.2$ to $\simeq 1.62$–1.63; (2) a change in the coordination number from $\simeq 5$ to $\simeq 4$; (3) a paraelectric-to-pyroelectric transition resulting in an enhancement of electromechanical responses; (4) a noticeable change in the cationic-averaged Born effective charge that is due to the fact that Sc is a transition-metal atom, unlike Ga or In; (5) a transition from an indirect to a direct band-gap semiconductor; and (6) the generation of materials with a wide range of band gap.

Here, we investigate the *class* of hexagonal phases for which the primitive lattice vectors of the direct Bravais lattice are,

$$\mathbf{a}_1 = a\left(\frac{1}{2}\mathbf{x} - \frac{\sqrt{3}}{2}\mathbf{y}\right),$$

$$\mathbf{a}_2 = a\left(\frac{1}{2}\mathbf{x} + \frac{\sqrt{3}}{2}\mathbf{y}\right),$$

$$\mathbf{a}_3 = c\mathbf{z}, \tag{1}$$

where a and c are the two different lattice parameters, and where c/a is the axial ratio. $\mathbf{x}$, $\mathbf{y}$, and $\mathbf{z}$ are the unit vectors along the Cartesian axes. The primitive unit cell contains four atoms: two atoms of type A (e.g., A=Sc) located at $\mathbf{r}_1$ and $\mathbf{r}_2$, and two atoms of type B (e.g., B=N) located at $\mathbf{r}_3$ and $\mathbf{r}_4$, with

$$\mathbf{r}_1 = \mathbf{0},$$

$$\mathbf{r}_2 = \frac{2}{3}\mathbf{a}_1 + \frac{1}{3}\mathbf{a}_2 + \frac{1}{2}\mathbf{a}_3,$$

$$\mathbf{r}_3 = u\mathbf{a}_3,$$

$$\mathbf{r}_4 = \frac{2}{3}\mathbf{a}_1 + \frac{1}{3}\mathbf{a}_2 + \left(\frac{1}{2} + u\right)\mathbf{a}_3, \tag{2}$$

where u is the dimensionless internal parameter. In the following, we will denote this class of hexagonal phases as h_c. Note that the wurtzite structure, which has a $6mm$ point group (in international notations) and for which $c/a = \sqrt{8/3}$ and $u = 0.375$ in its ideal form, belongs to h_c. Similarly, the structure, which is stable in BN,[13] whose point group is $6/mmm$ and for which $c/a \simeq 2.60$ and $u = 0.5$, is also contained in h_c.

We perform local-density approximation (LDA) (Ref. 14) calculations on the h_c class in ScN, using the Vanderbilt ultrasoft-pseudopotential scheme[15] with a plane-wave cutoff of 25 Ry. The $3s$, $3p$, $3d$, and $4s$ electrons of Sc, as well as the $2s$ and $2p$ electrons of N, are all included in the valence. As a result, the studied primitive unit cell exhibits 32 valence electrons per cell. We also use the Ceperley-Alder exchange

PHYSICAL REVIEW B 66, 220103(R) (2002)

Properties of vacancy-rich ordered $(A,[\ ])Nb_2O_6$ perovskites

H. Crogman and L. Bellaiche
Physics Department, University of Arkansas, Fayetteville, Arkansas 72701
(Received 29 October 2002; published 31 December 2002)

Using first-principles calculations, we have investigated properties of the $(A,[\ ])Nb_2O_6$ perovskite systems exhibiting a rocksalt ordering between divalent A atoms—A=Ca, Sr, Pb, or Ba—and neutral vacancies [ ]. Their properties can be understood by simple rules and by analogy with the corresponding $ATiO_3$ simple perovskites. Contrary to common belief, all the studied vacancy-rich systems exhibit ferroelectric instability. Furthermore, their ground state can be ferroelectric, antiferrodistortive, and may be sensitive to pressure or quantum effects, depending on the A atom.

DOI: 10.1103/PhysRevB.66.220103 PACS number(s): 61.72.Ji, 61.72.Bb, 77.84.Dy, 81.05.Zx

The search for perovskite materials with better and/or new properties is being extensively pursued. So far, four different strategies have been successful for that search. One strategy is related to *sample quality*, as highlighted by the large piezoelectric coefficients found when growing single crystals rather than ceramics of $Pb(Mg_{1/3}Nb_{2/3})O_3$-$PbTiO_3$ and $Pb(Zn_{1/3}Nb_{2/3})O_3$-$PbTiO_3$ compounds.[1] *Varying the composition in solid solutions* is another possibility yielding spectacular results, as pointed out by the discovery of a monoclinic phase in a narrow compositional range in $Pb(Zr_{1-x}Ti_x)O_3$.[2,3] *Applying an external electric field* to ferroelectric materials can also lead to a drastic enhancement of the electromechanical properties and to the discovery of new structural phases.[4–6] Finally, recent theoretical works[7–11] predict that *playing with the atomic ordering in solid solutions* is very promising to generate perovskites with improved and even new properties.

The main aim of this paper is to explore another way in the quest for different perovskite materials with interesting properties. Specifically, our goals are to design and understand single crystals exhibiting "alloying" between real atoms and vacancies. More precisely, we choose to investigate properties of the $(A,[\ ])Nb_2O_6$ system that adopts a rocksalt ordering between *divalent* A atoms, i.e., A=Ca, Sr, Pb, or Ba, and [ ] (neutral) vacancies. Such a system has not been synthesized yet (to our knowledge), contains nine atoms per primitive cell and is electrically neutral (as a whole). It exhibits 50% of vacancy at the A site of the perovskite structure and consists of one pure plane of divalent A atoms alternating with one vacancy plane along the [111] direction. Our choice of supercell was motivated by two reasons. First of all, rocksalt ordering in $(A,[\ ])Nb_2O_6$ leads to the minimization of the electrostatic interactions between the +2 charges associated with the A atoms and the zero charges of vacancies.[12] Second, the size of the system is relatively small, thus allowing the use of accurate first-principles techniques to compute its properties. Technically, we perform ultrasoft-pseudopotential[13] local-density approximation (LDA) (Ref. 14) calculations on these materials, as well as, on the isovalent and simple $KNbO_3$ system for comparison. The semicore shells of all the metals are included in the valence as in Ref. 15. The plane-wave cutoff is chosen to be 25 Ry and (4,4,4) and (6,6,6,) Monkhorst-Pack meshes[16] are used in $(A,[\ ])Nb_2O_6$ and $KNbO_3$, respectively. We also use the Ceperley-Alder exchange and correlation.[17,18]

Properties of the paraelectric phase. We first focus on paraelectric cubic $(A,[\ ])Nb_2O_6$ systems, for which all the atoms are kept at the ideal perovskite positions. Such geometry automatically guarantees the forces to be null on each atom. The primitive lattice vectors are $\mathbf{R}_1=a_0[0,1,1]$, $\mathbf{R}_2=a_0[1,0,1]$, and $\mathbf{R}_3=a_0[1,1,0]$, where the lattice parameter a_0 is optimized by minimizing the total LDA energy. a_0 and the lattice constant a_{SP} resulting from the tabulated Shannon-Prewitt radii for A and O ions[19] are displayed in Table I. One can see that there is a linear relationship between a_0 and a_{SP}, which implies that the increase of a_0 occurring when going from $(Ca,[\ ])Nb_2O_6$ to $(Ba,[\ ])Nb_2O_6$, via $(Sr,[\ ])Nb_2O_6$ and $(Pb,[\ ])Nb_2O_6$, can be understood by simple ionic radii consideration. The strong relationship between LDA lattice constants and tabulated ionic radii is further confirmed by the fact that $(Ba,[\ ])Nb_2O_6$ and $KNbO_3$ have the same a_{SP} while possessing similar a_0.

Table I further reports the Born effective charges Z^*_{33}—as computed within the Berry-phase approach[20]—for each atom in all the studied systems. Practically, we use roughly 2000 and 1000 Bloch states in the cubic $(A,[\ ])Nb_2O_6$ and $KNbO_3$ systems, respectively, to assure a good convergence of the effective charges. Note that the oxygen atoms are grouped into two kinds: those denoted $O_\parallel$, located between two Nb atoms along the z direction; and those denoted $O_\perp$, located between two B atoms in the perpendicular directions.[21,22] The effective charges of Nb and $O_\parallel$ atoms in $(A,[\ ])Nb_2O_6$ are predicted to be (i) anomalously large in magnitude with respect to their nominal ionic value of +5 and −2, respectively, (ii) nearly independent of the A atom, and (iii) very close to their respective values in cubic $KNbO_3$. Feature (i) is due to a subtle hybridization between the O $2p$ orbitals and the $4d$ orbitals of Nb,[21,23] while items (ii) and (iii) reflect a very strong correlation between $Z^*_{33}(Nb)$ and $Z^*_{33}(O_\parallel)$, as also observed in simple perovskites.[21] $Z^*_{33}(A)$ and $Z^*_{33}(O_\perp)$ are also correlated in the sense that systems exhibiting effective charges of A atoms close to their nominal ionic value have very similar $Z^*_{33}(O_\perp)$ around −1.7—see $(Ca,[\ ])Nb_2O_6$, $(Sr,[\ ])Nb_2O_6$, and $KNbO_3$—while a significant enhancement of $Z^*_{33}(A)$ with

Ferroelectrics, 2002, Vol. 266, pp. 41–56
Reprints available directly from the publisher
Photocopying permitted by license only

Low-Temperature Properties of $Pb(Zr_{1-x}Ti_x)O_3$ Solid Solutions Near the Morphotropic Phase Boundary

L. BELLAICHE,[1] ALBERTO GARCÍA,[2] and DAVID VANDERBILT[3]

[1]*Physics Department, University of Arkansas, Fayetteville, Arkansas 72701, USA*
[2]*Departamento de Fisica Aplicada II, Universidad del Pais Vasco, Apartado 644, 48080 Bilbao, Spain*
[3]*Center for Materials Theory, Department of Physics and Astronomy, Rutgers University, Piscataway, New Jersey 08855-0849, USA*

(Received October 30, 2000)

A first-principles-derived approach is used to study structural, piezoelectric and dielectric properties of $Pb(Zr_{1-x}Ti_x)O_3$ (PZT) solid solutions near the morphotropic phase boundary at low temperature. Three ferroelectric phases are found to exist: a tetragonal phase for larger x compositions, a rhombohedral phase for smaller x compositions, and the recently discovered monoclinic phase in between. In this monoclinic phase, the polarization associated with the Zr atoms behaves differently from the polarization associated with the Ti atoms. As the composition x decreases, the former rotates more quickly towards the pseudo-cubic [111] direction and grows in magnitude, while the latter lags in its rotation and its magnitude shrinks. The local microscopic structure is found to deviate significantly from the average structure in these PZT alloy phases as a result of fluctuations in the directions and magnitudes of the local polarizations. The monoclinic phase is characterized by a very large piezoelectric and dielectric response.

Keywords: Macroscopic phases; local structure; piezoelectricity; dielectric response

PACS: 77.84.Dy; 77.65.Bn; 77.22.Ch

I. INTRODUCTION

Since the beginning of the 70's, $Pb(Zr_{1-x}Ti_x)O_3$ (PZT) alloys have been known to exhibit a morphotropic phase boundary (MPB) separating a ferroelectric region with a tetragonal ground state ($x > 0.52$) from a ferroelectric region with rhombohedral symmetry ($x < 0.45$) [1]. Very recently, synchrotron x-ray powder diffraction studies have revealed that there is in fact a third phase in the vicinity of the MPB at low temperature [2]. This phase is ferroelectric, adopts a monoclinic symmetry and occurs within a narrow

Piezoelectric Coefficients of Complex Semiconductor Alloys from First-Principles: The Case of $Ga_{1-x}In_xN$

A. Al-Yacoub,[1] L. Bellaiche,[1] and S.-H Wei[2]

[1]*Physics Department, University of Arkansas, Fayetteville, Arkansas72701*

[2]*National Renewable Energy Laboratory, Golden, Colorado 80401*

(Received 8 January 2002; published 15 July 2002)

A first-principles-derived scheme is developed to compute the piezoelectric coefficients e_{ij} of semiconductor alloys. This method is applied to study the effect of atomic arrangement and composition on e_{33} in wurtzite $Ga_{1-x}In_xN$. Results obtained by this method for ordered structures are in good agreement with direct first-principles calculations. We predict that atomic ordering can have a large effect on piezoelectricity and that e_{33} of *disordered* materials is nearly linear with composition. Microscopic origins for these features are revealed.

DOI: 10.1103/PhysRevLett.89.057601 PACS numbers: 77.84.Bw, 61.66.Dk, 77.65.Bn

The compositional dependence of many properties in disordered semiconductor $A_{1-x}B_xC$ alloys is well established and is usually well described by a second-order polynomial of the composition x [1,2]. Examples of such properties are the band gap and the mixing enthalpy. Interestingly, the compositional behavior of the piezoelectric coefficients in disordered semiconductor alloys is mainly unknown, despite the fact that many unusual physical features of wurtzite solid solutions, such as $Ga_{1-x}In_xN$, are related to these coefficients [3–9]. Traditionally, one assumes for simplification that the piezoelectric coefficients can be determined by a compositionally linear interpolation between the corresponding coefficients of their parent compounds [6,8]. Recently, a first-principles study [10] suggests that this linear assumption holds closely only if the nonlinear strain dependence of the piezoelectricity in the parent compounds is accounted for. However, this pioneering *ab initio* study [10] was done only for strained alloys at a unique composition and by using small cells. In principle, a more accurate description of the compositional behavior of piezoelectricity in random solid solutions requires the use of large cells, in order to better mimic the different possible local chemical environments of a real disordered alloy in the whole compositional range.

Another aspect that is poorly understood is the microscopic effect(s) responsible for the deviation of piezoelectricity from a linear compositional behavior occurring in some *atomically ordered* cation-mixed nitride alloys and not in others [10–12].

Obviously, accurate simulations on large supercells are needed to understand the properties of piezoelectric semiconductor alloys in general, and of $Ga_{1-x}In_xN$, in particular. First-principles methods do offer a high accuracy but are (currently) restricted to the study of small cells.

The aims of this Letter are threefold. First, we want to demonstrate that it is possible to develop an *ab initio* computational scheme with the capability of predicting the piezoelectric coefficients of large supercells with the accuracy of first principles. Second, we wish to apply this scheme to study the effect of composition and atomic ordering on the piezoelectric coefficient of $Ga_{1-x}In_xN$ alloys. Finally, our last goal is to reveal the microscopic features associated with piezoelectricity in $Ga_{1-x}In_xN$ solid solutions.

Decomposition of e_{33}—We now illustrate in detail this proposed scheme for calculating the e_{33} piezoelectric coefficient, which is the derivative of the polarization P_3 induced along the z axis with respect to the macroscopic strain η_3 (in Voigt notation) along this z axis. As indicated in Refs. [12–16], e_{33} can be decomposed into "clamped-ion" and "internal-strain" contributions:

$$e_{33} = e_{33,c} + \frac{ec}{\Omega}\sum_k Z^*_{33}(k)\,\frac{du_3(k)}{d\eta_3}, \qquad (1)$$

where k runs over all the atoms in the unit cell, e is the magnitude of the electron charge, and c and Ω are the equilibrium lattice constant along the z direction and the volume of the unit cell, respectively. The clamped-ion coefficient $e_{33,c}$ measures the contributions to e_{33} coming from *vanishing internal strain,* that is associated with internal atomic coordinates frozen at their equilibrium positions. $Z^*_{33}(k)$ is the Born effective charge of atom k, and $du_3(k)/d\eta_3$ characterizes the response of the kth atom's internal coordinate along the z axis to a macroscopic strain η_3. Equation (1) indicates that the full knowledge of e_{33} in any piezoelectric material requires the determination of three different quantities, namely, (i) $e_{33,c}$, (ii) $Z^*_{33}(k)$ for all the atoms, and (iii) $du_3(k)/d\eta_3$ for any k. Our proposed method "simply" consists in finding ways to determine these three quantities in complex systems. In the following, we explain in detail how such determination is accomplished in $Ga_{1-x}In_xN$ alloys.

Determining $e_{33,c}$—We first select four simple $Ga_{1-x}In_xN$ structures, all exhibiting atomic ordering along the c axis. The first structure will be denoted 1×1 and consists of a single Ga plane alternating with a single In plane. This structure has been studied in Refs. [10–12] and has an overall indium composition $x = 0.5$. The

 0031-9007/02/89(5)/057601(4)$20.00

INSTITUTE OF PHYSICS PUBLISHING SEMICONDUCTOR SCIENCE AND TECHNOLOGY
Semicond. Sci. Technol. 17 (2002) 851–859 PII: S0268-1242(02)37912-4

Pseudopotential theory of dilute III–V nitrides

P R C Kent[1], L Bellaiche[2] and Alex Zunger[1]

[1] National Renewable Energy Laboratory, Golden, CO 80401, USA
[2] Physics Department, University of Arkansas, Fayetteville, AR 72701, USA

Received 8 February 2002
Published 12 July 2002
Online at stacks.iop.org/SST/17/851

Abstract
We review the empirical pseudopotential method and its recent applications to the III–V nitride alloys GaAsN, GaPN, GaInAsN and GaAsPN. We discuss how studies using this method have provided an explanation for many experimentally observed anomalous nitride phenomena, including sharp photoluminescence lines in dilute alloys, high effective masses, Stoke's shift between emission and absorption in higher concentration alloys for GaAsN and GaPN ternaries. We also discuss predictions of unusual effects that remain to be experimentally discovered in GaInAsN quaternaries and complex GaAsPN solid solutions.

1. The unusual phenomenology of III–V nitrides

Although the primary interest in anion-mixed III–V nitrides has been due to the large reduction in bandgap observed on addition of nitrogen, many other properties are now known to be different from conventional, non-nitride II–V alloys (InGaAs, GaAsP, etc).

In the ultra-dilute regime (nitrogen concentration $x < 0.01\%$) one observes:

(i) *Localized, single-impurity levels appear near the bandgap* [1–5]. In conventional isovalent alloys such as GaAs:P or GaAs:In the ensuing perturbation potential $V_{As} - V_P$ or $V_{Ga} - V_{In}$ is too weak to create a bound state in the gap. In contrast, absorption and photoluminescence excitation (PLE) of GaP:N and GaAs:N show the 'N_γ centre' due to anion-substitutional isolated nitrogen. In GaP:N this level appears as in impurity-bound exciton at $E_{CBM} - 33$ meV *below* the conduction band minimum (CBM) [1–4], whereas in GaAs:N it appears as a *sharp resonance* at $E_{CBM} + 180$ meV [5–8] above the CBM.

(ii) *Anomalously small pressure dependence of single impurity states is observed.* Shallow, effective-mass like impurity levels (GaAs:Zn or GaAs:Si) are constructed from the wavefunction of the single nearest host crystal state. Consequently, when pressure is applied, such impurity levels change their energy at the same rate as the energetically nearest host crystal state [9]. In contrast, the impurity levels in dilute GaP:N and GaAs:N have anomalously small pressure coefficients: in GaP:N the energy of the impurity-bound exciton is almost pressure independent [10, 11], whereas the X_{1c} CBM of the GaP host crystal descends at a rate of -14 meV GPa^{-1}. In GaAs:N, the nitrogen level moves with pressure to higher energies at a much slower rate (~40 meV GPa^{-1} [7, 8]) than the Γ_{1c} CBM of GaAs [12] (+110 meV GPa^{-1}). Such small pressure coefficients are usually indicative of localization, whereby the wavefunction is constructed from many bands of the host crystal, rather than from the nearest host crystal state [13].

In the intermediate concentration regime (up to ~1% nitrogen), one observes:

(iii) *Sharp photoluminescence (PL) lines appear due to impurity clusters.* Even random substitution of impurities onto the atomic sites of a host crystal creates, by chance, impurity pairs and higher-order clusters. In conventional isovalent III–V alloys, such pairs give rise to broad resonances, *within* the valence and conduction continua [14–18], but no gap levels. In contrast, in GaPN and GaAsN, the N–N pairs form discrete levels inside the bandgap extending in GaP down to $E_{CBM} - 160$ meV [4, 19–21] and in GaAs down to $E_{CBM} - 10$ [8, 7, 22] or $E_{CBM} - 80$ meV [23–25]. Such clusters do not appear to create deep levels in ordinary, non-nitride, alloys.

(iv) *Redshift between absorption/PLE and emission is observed.* In high structural quality random, direct-gap III–V alloys, absorption and emission occur at the same energy. In contrast, already at a concentration of 0.05–0.1% nitrogen in GaAs, the emission lines are redshifted with respect to absorption [26]. At higher concentrations the shift increases in energy [27, 23].

ELSEVIER

Current Opinion in Solid State and Materials Science 6 (2002) 19–25

Current Opinion in **Solid State & Materials Science**

Piezoelectricity of ferroelectric perovskites from first principles

L. Bellaiche

Physics Department, University of Arkansas, Fayetteville, AR 72701, USA

Abstract

The very recent use of first-principles-derived approaches to investigate piezoelectricity in simple and complex ferroelectric perovskites has not only provided a deep microscopic understanding but also has led to the design of materials with striking electromechanical responses.

1. Introduction

Piezoelectricity is a fundamental process linking electrical and mechanical properties [1,2]. This process has been put in use to convert mechanical energy to electricity (and vice-versa) in various applications ranging from ultrasonic to sonar listening devices, via phonograph needles and telephone speakers [3]. In general, the larger the so-called piezoelectric coefficients, the more efficient is the application.

Of the 32 crystallographic point groups, 12 possess symmetry elements preventing the existence of piezoelectricity [1,2]. Consequently, only some materials are piezoelectric. An important class of such materials are the ferroelectric perovskite compounds, which are currently used in piezoelectric transducers and actuators [4]. Intriguing piezoelectric effects have been reported in these perovskite compounds. For instance, the $Pb(Zr_{1-x}Ti_x)O_3$ (PZT) solid solutions have been known for more than 30 years to exhibit a very high piezoelectric response, but only for a very narrow range of composition x [5]. Similarly, the class of $Pb(Mg_{1/3}Nb_{2/3})O_3$–$PbTiO_3$ (PMN–PT) and $Pb(Zn_{1/3}Nb_{2/3})O_3$–$PbTiO_3$ (PZN–PT) materials were found to exhibit remarkably large piezoelectric constants, when synthesized in single-crystal form [6]. These latter materials thus promise dramatic improvements in the resolution and range of piezoelectric devices [3]. The desire to understand these intriguing effects, as well as the quest for new materials with even better electromechanical responses, has motivated the recent use and development of first-principles techniques in perovskite compounds.

The purposes of the present review are threefold: (1) to provide a description of the different numerical procedures allowing the determination of piezoelectric coefficients from first-principles techniques; (2) to summarize the understanding of piezoelectric effects in perovskites that has been gained in the past 5 years using these techniques; and (3) to describe the findings of first-principles-based works, published in the last 2 years and predicting striking piezoelectric response in perovskite compounds that remain to be grown.

2. Piezoelectric coefficients from first principles

In fact, piezoelectricity is a phenomenon incorporating *different* electromechanical effects [1,2]. For instance, applying a mechanical stress to piezoelectric crystals (under fixed macroscopic electric field) leads to an induced electric polarization P_{ind} whose magnitude is proportional to the applied stress σ. When using the Voigt (or matrix) notation and the Einstein summation convention, this so-called *direct* piezoelectric effect can be mathematically described by [1]:

$$P_{\text{ind},i} = d_{ij}\sigma_j \tag{1}$$

where $\{d_{ij}\}$ is a third-rank piezoelectric tensor. The component i is an integer equal to 1, 2 or 3, while the suffix j can adopt integer values ranging from 1 to 6.

Piezoelectric materials also change shape when subject to an external macroscopic electric-field E, which is known as the *converse* piezoelectric effect and which can be written (for a fixed stress σ) as [1]:

$$\eta_j = d_{ij}E_i \tag{2}$$

where $\{\eta\}$ is the strain tensor and where the piezoelectric coefficients d_{ij} are exactly the same as those of Eq. (1).

E-mail address: laurent@uark.edu (L. Bellaiche).

1359-0286/02/$ – see front matter
PII: S1359-0286(02)00017-7

Planar Defects and Incommensurate Phases in Highly Ordered Perovskite Solid Solutions

Igor A. Kornev* and L. Bellaiche

Physics Department, University of Arkansas, Fayetteville, Arkansas 72701

(Received 18 June 2002; published 22 August 2002)

A first-principles-derived approach is used to study the effects of planar defects on structural properties of a rocksalt-ordered $Pb(Sc_{0.5}Nb_{0.5})O_3$ alloy. These defects lead to unusual features, including a less symmetrical ground state with respect to the perfectly ordered material. We also propose that a simple and original mechanism, involving these defects, may be responsible for the existence and anomalous characteristics of the incommensurate phases observed in insulating perovskites.

DOI: 10.1103/PhysRevLett.89.115502 PACS numbers: 61.72.Nn, 61.44.Fw, 61.72.Bb, 77.84.Dy

Complex insulating perovskite solid solutions with the general formula $(A', A'', A''' \ldots)(B', B'', B''' \ldots)O_3$ are currently receiving a lot of attention, mainly because they (i) can exhibit huge electromechanical responses [1–4], (ii) adopt ground states of unexpected symmetry [3–6], and (iii) lead to new phenomena [3,4,7–10]. One important class of perovskite solid solutions is formed from the so-called *heterovalent* alloys, i.e., from systems possessing a mixing between atoms belonging to different columns of the periodic table. These heterovalent alloys have a tendency to adopt an atomic ordering between the mixed atoms [11]. Examples include the rocksalt ordering exhibited by $Pb(B'_{1/2}B''_{1/2})O_3$ perovskites for which the A atom is Pb and B' and B'' belong to columns III and V (or II and VI) of the periodic table, respectively. Single crystals and ceramics of these "Pb-(III-V)" and "Pb-(II-VI)" materials have been extensively studied both experimentally and theoretically, and a better understanding resulted from these studies (see Refs. [12–15], and references therein). On the other hand, very little is known on the microscopic and macroscopic effects of *planar defects* on their properties, despite the fact that antiphase boundaries (APBs) and stacking faults (SFs) have been observed in highly ordered alloys [16–18].

Another intriguing feature of the rocksalt-ordered Pb-(III-V) and Pb-(II-VI) solid solutions is that they are the only insulating perovskites reported to have incommensurate (IC) phases. As a matter of fact, up to now, IC phases have been found only in $Pb(Co_{1/2}W_{1/2})O_3$ [14,19], $Pb(Sc_{1/2}Ta_{1/2})O_3$ [15], $Pb(Cd_{1/2}W_{1/2})O_3$ [20], $Pb(Mg_{1/2}Nb_{1/2})O_3$ [21,22], and, possibly, $Pb(Yb_{1/2}Ta_{1/2})O_3$ [23]. The reason behind this general feature, as well as the unusual fact that no lock-in transition between incommensurate and commensurate phases has been seen in some of these solid solutions [22], remains poorly understood, despite the pioneering works of Caracas and Gonze [24].

The aim of this Letter is twofold: first, to demonstrate that — and explain why — planar defects strongly affect structural properties of highly ordered perovskite solid solutions, and second, to suggest — and provide evidence supporting the hypothesis — that a simple mechanism, involving these defects, may be responsible for the existence and anomalous features of the IC phases.

Here, we choose the heterovalent $Pb(Sc^{3+}_{0.5}Nb^{5+}_{0.5})O_3$ (PSN) solid solution as a prototype of a Pb-(III-V) alloy. We first generate two *kinds* of atomic configurations, both mimicked by $12 \times 12 \times 12$ supercells. The first one is the perfectly rocksalt-ordered PSN supercell (to be denoted by RS-PSN); i.e., the structure in which the atomic ordering between the different B atoms is characterized by one pure plane of Sc atoms alternating with one pure niobium plane along the [111] direction. The second one exhibits a specific density of defects. More precisely, we have introduced stacking faults [see Fig. 1(a)] and antiphase boundaries [see Fig. 1(b)] along the direction of cation ordering [25]. These structures will be denoted by SF-PSN and APB-PSN, respectively. Note that (1) the average concentration of these structures preserves the charge neutrality of PSN; i.e., there are 50% of Sc and 50% of Nb atoms, and (2) the characteristic period of the defect supercells correspond to 12 B planes. As pointed out in previous studies [3,4,8,26], the difference of ionic valence between Sc and Nb atoms leads to the occurrence of an

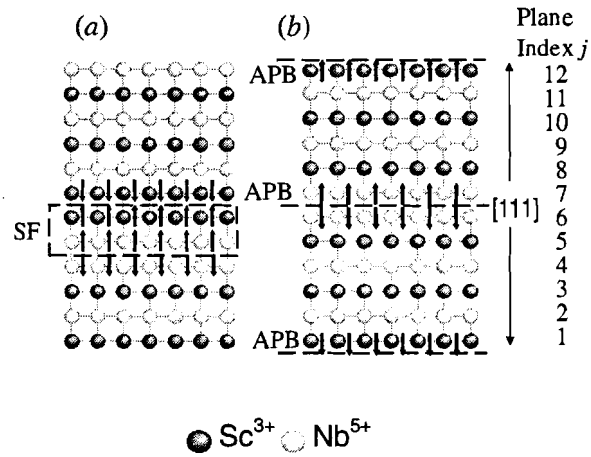

FIG. 1. Schematic illustration of the presently studied PSN supercell exhibiting (a) stacking faults and (b) antiphase boundaries defects. Arrows indicate the internal electric fields.

 0031-9007/02/89(11)/115502(4)$20.00

2000 International Conference on High-Density Interconnect and Systems Packaging

Two-Layer, Planar, Superconducting Multichip Module Technology

W. A. Luo, H. J. Yao, G. Zhang, F. T. Chan, S. S. Ang, W. D. Brown, G. J. Salamo, and J. W. Cooksey
High Density Electronics Center (HiDEC)
The University of Arkansas
Fayetteville, AR 72701, U.S.A.
Phone: 501-575-6045
Fax: 501-575-7967
wdb@engr.uark.edu

ABSTRACT

Given that the speed of integrated circuits (ICs) is projected to continue to increase at its present rate, the packaging of ICs may become a formidable task not too distant into the future. In fact, as circuit integration and IC switching speeds continue to increase, chip-to-chip interconnection becomes the limiting factor in realizing the system performance benefits of using faster ICs. Multichip modules (MCMs) offer a high performance alternative to conventional printed wiring boards (PWBs), and one of the more promising applications for high temperature superconductors (HTSCs) is as signal interconnects between bare ICs in MCMs. We report on the successful development and fabrication of a superconducting MCM packaging technology using a novel yttrium-barium-copper-oxide (YBCO)/yttrium-stabilized zirconia (YSZ)/silicon dioxide (SiO_2)/yttrium-stabilized zirconia (YSZ)/yttrium-barium-copper-oxide (YBCO) multilayer substrate using either a chemical-mechanical planarization technique or a conventional lift-off process on a single-crystal YSZ substrate. To reduce the complexity of the processing required, the two-layer Interconnected Mesh Power System (IMPS) MCM topology was used. For demonstration purposes, a 100 MHZ ring oscillator multichip module using gallium arsenide technology was successfully fabricated.

Key Words: multichip module, high-temperature superconductor

Introduction

One of the fundamental challenges to reducing the linewidth of interconnects in both integrated circuits (ICs) and multichip modules (MCMs) is the resulting increase in parasitic resistance. The increased parasitic resistance increases the propagation delay of signals traveling along the interconnect. High-temperature superconductors offer an attractive solution to this parasitic resistance problem since they exhibit a negligible resistance when operated in their superconducting state. Consequently, the propagation delay of signals is reduced significantly. Furthermore, high interconnect bandwidths (up to 100 GHz) are possible without sacrificing packaging density. Other advantages of superconducting interconnects are that faster device switching and lower voltage operation for CMOS and GaAs are possible when operating at the liquid nitrogen temperature of 77K. The liquid nitrogen operating environment also reduces heat dissipation problems and increases MCM reliability. In this paper, we report on two approaches to the successful fabrication of a superconducting MCM using a novel yttrium-barium-copper-oxide (YBCO)/yttrium-stabilized zirconia (YSZ)/silicon dioxide (SiO_2)/yttrium-stabilized zirconia (YSZ)/yttrium-barium-copper-oxide (YBCO) multilayer substrate. A chemical-mechanical planarization technique, as well as a conventional lift-off process, were used to fabricate superconducting MCMs on a single-crystal YSZ substrate.

Device Design and Fabrication

Typically, conventional MCM-D technologies require at least a four-layer metallization system to provide power, ground, and signal distribution for the ICs they contain [1]. However, it is very difficult to fabricate more than two layers of superconducting interconnects on a substrate due to the necessity for maintaining critical structural alignment of the superconducting thin film in a multilayer structure. The surface onto which the superconductor is deposited must be planar since any

ARTICLES

Virtual crystal approximation revisited: Application to dielectric and piezoelectric properties of perovskites

L. Bellaiche
Physics Department, University of Arkansas, Fayetteville, Arkansas 72701

David Vanderbilt
Center for Materials Theory, Department of Physics and Astronomy, Rutgers University, Piscataway, New Jersey 08855-0849

(Received 25 August 1999)

We present an approach to the implementation of the virtual crystal approximation (VCA) for the study of properties of solid solutions in the context of density-functional methods. Our approach can easily be applied to any type of pseudopotential, and also has the advantage that it can be used to obtain estimates of the atomic forces that would arise if the real atoms were present, thus giving insight into the expected displacements in the real alloy. We have applied this VCA technique within the Vanderbilt ultrasoft-pseudopotential scheme to predict dielectric and piezoelectric properties of the $Pb(Zr_{0.5}Ti_{0.5})O_3$ solid solution in its paraelectric and ferroelectric phases, respectively. Comparison with calculations performed on ordered alloy supercells and with data on parents compounds demonstrates the adequacy of using the VCA for this perovskite solid solution. In particular, the VCA approach reproduces the anomalous Born effective charges and the large value of the piezoelectric coefficients.

I. INTRODUCTION

The application of first-principles electronic band-structure methods to the study of disordered alloys and solid solutions requires some approximation for the treatment of the alloy disorder. A "direct" approach is to make use of the supercell approximation, i.e., to study one or more disordered configurations in a supercell with artificially imposed periodic boundary conditions. Such calculations generally require the use of very large supercells in order to mimic the distribution of local chemical environments, and tend to be computationally very demanding. A much simpler and computationally less expensive approach is to employ the virtual crystal approximation (VCA),[1] in which one studies a crystal with the primitive periodicity, but composed of fictitious "virtual" atoms that interpolate between the behavior of the atoms in the parent compounds. This technique has seen wide use in band-structure calculations.[2–11] Another possible approach would be to make use of the coherent potential approximation (CPA),[12] but unfortunately the CPA is generally not well suited for use in first-principles total-energy methods. A different way to go beyond the VCA is to carry out a systematic perturbation expansion in the difference between the true and VCA potentials, an approach that is sometimes referred to as "computational alchemy."[2–4] However, this method is much more complicated than the usual VCA, requiring the use of density-functional linear-response techniques.

Clearly the VCA has the advantages of simplicity and computational efficiency, if two possible concerns can be addressed. First and foremost is the question of the accuracy of the VCA approximation. Previous work has demonstrated good accuracy for the VCA in some semiconductor and ferromagnetic materials,[2–7] but it was found to be inadequate for an accurate treatment of the electronic structure of some unusual semiconductor systems.[8–10] Until the recent pioneering work of Ramer and Rappe,[11] nothing was known about the ability of the VCA to describe the properties of an important class of materials, the ferroelectric perovskite solid solutions. Their work strongly suggests that these alloys are good candidates for modeling with the VCA, since it reproduces the strain-induced transitions of ordered supercells of $Pb(Zr_{0.5}Ti_{0.5})O_3$. However, it is not known whether the VCA is good enough to predict the anomalous dielectric and piezoelectric properties of perovskite solid solutions.

A second concern is more technical. By its nature, the VCA is closely tied to the pseudopotential approximation. Indeed, unless pseudopotentials are used, it is hopeless to apply the VCA to the usual case of isoelectronic substitution (i.e., atoms belonging to the same column but different rows of the Periodic Table). However, as pseudopotential methods have matured, it has become less obvious what is the correct or optimal way to implement the VCA. For the case of local pseudopotentials, the implementation is straightforward:[8] the potential of the virtual system made from the $(A_{1-x}B_x)C$ alloy is generated simply by compositionally averaging the potentials of the parent AC and BC compounds,

$$V_{\mathrm{VCA}}(\mathbf{r})=(1-x)V_{\mathrm{AC}}(\mathbf{r})+xV_{\mathrm{BC}}(\mathbf{r}). \tag{1}$$

In practice this is usually done in Fourier space by averaging $V_{\mathrm{AC}}(\mathbf{G})$ and $V_{\mathrm{BC}}(\mathbf{G})$. In the case of semilocal (e.g, Hamann-Schlüter-Chiang[13]) pseudopotentials, a similar averaging of the radial potentials $V_{\mathrm{A},l}(r)$ and $V_{\mathrm{B},l}(r)$ can be done

Microscopic View of a Two-Dimensional Lattice-Gas Ising System within the Grand Canonical Ensemble

V. P. LaBella, D. W. Bullock, M. Anser, Z. Ding, C. Emery, L. Bellaiche, and P. M. Thibado
Department of Physics, The University of Arkansas, Fayetteville, Arkansas 72701
(Received 4 October 1999)

A reversible 2D critical transition is observed on the GaAs(001) surface and modeled as a lattice-gas Ising system. Without depositing any material, 2D GaAs islands spontaneously form. The order parameter, *four* critical exponents, and coupling energies are measured from scanning tunneling microscope images of the microscopic domain structure and correlation functions as a function of temperature and pressure. Unprecedented insight into the domain structure of a 2D Ising system through the critical point and a complete Hamiltonian for modeling the GaAs(001) surface are presented.

PACS numbers: 68.35.Bs, 05.50.+q, 68.35.Rh

The epitaxial techniques used in manufacturing compound semiconductor device structures have demanded insight into the physical process undergone when atoms are deposited on top of a single crystal surface. This insight is of both fundamental and technological importance and modeling these surfaces is challenging due to their two-component nature. Much success has been achieved using various techniques, such as first-principles theory [1], kinetic Monte Carlo simulations [2], rate equations [3], and thermodynamics [4].

On single component surfaces, one of the oldest and simplest approaches to modeling is the celebrated two-dimensional (2D) lattice-gas Ising model [5]. Clever researchers have been able to artificially create 2D systems with a fixed, submonolayer amount of one material deposited on a host surface made of a different material, and successfully applied the 2D lattice-gas Ising model [6–10]. These studies advance our understanding of phase transitions while illuminating the nature of interactions between atoms on surfaces, since the 2D Ising model has been theoretically studied in rigorous detail [11,12]. The above types of experiments are within the canonical ensemble (i.e., fixed number of particles) and therefore, they can fit their data to Onsager's exact solution similar to some 2D Ising-like magnetic phase transitions (i.e., fixed number of spins) that have been observed by neutron scattering [13–15]. The lattice-gas Ising model was originally framed within the more general context of the grand canonical ensemble, where the number of particles is free to fluctuate as it exchanges with a reservoir. This is unlike the ferromagnetic case where the number of spins is fixed. To the best of our knowledge no experimental test of the general solution to the 2D lattice-gas Ising model within the grand canonical ensemble exists.

In this Letter, we discovered a single crystal surface where the surface atoms can exchange with the substrate in a reversible manner consistent with the general solution 2D lattice-gas Ising model within the grand canonical ensemble. Surprisingly, the system is the technologically important two-component GaAs(001) compound semiconductor surface. This experiment is performed by imaging individual domains on a scale comparable to its constituents (i.e., the atoms) with scanning tunneling microscopy (STM), giving unprecedented insight into the microscopic domain structure of a 2D Ising system through the critical point. Equally exciting, this study provides a complete 2D Ising Hamiltonian for modeling the equilibrium and nonequilibrium properties of the GaAs(001) surface.

Experiments were carried out in an ultrahigh vacuum (UHV) multichamber facility [$(5-8)\times10^{-11}$ Torr throughout] which contains a molecular beam epitaxy (MBE) chamber (Riber 32P) that includes a substrate temperature determination system accurate to ±2 °C [16] and a surface analysis chamber with a custom integrated STM (Omicron) [17]. Commercially available, "epi-ready," $n+$ (Si doped $10^{18}/\text{cm}^3$) GaAs(001) $\pm0.1°$ substrates were loaded into the MBE system without any chemical cleaning. The surface oxide layer was removed and a 1.5-μm-thick GaAs buffer layer was grown at 580 °C using an As_4 to Ga beam equivalent pressure ratio of 15 and a growth rate of 1.0 μm/h as determined by reflection high-energy electron diffraction oscillations.

The spontaneous formation of islands on this surface occurred after each sample was annealed for a fixed time (between 0.25–33 h), a fixed temperature (between 500–700 °C), and a fixed As_4 flux (between 0.01–10.0 μTorr), resulting in an exhaustive study of the accessible parameter space. To ensure the samples were in equilibrium, the anneal times were successively increased until the surface morphology remained unchanged, which resulted in 33 h anneals for the lowest temperatures. The samples are cooled to room temperature using a procedure that freezes in the surface morphology present at higher temperatures and has been described elsewhere [18]. The samples were transferred to the STM without breaking UHV and imaged at room temperature. For each sample, 5–10 1 μm $\times$ 1 μm filled-state STM images were acquired using tips made from single crystal ⟨111⟩-oriented tungsten wire, a sample bias of -3.0 V, and a demanded tunneling current of 0.05–0.1 nA.

 0031-9007/00/84(18)/4152(4)$15.00

Microscopic View of a Two-Dimensional Lattice-Gas Ising System within the Grand Canonical Ensemble

V. P. LaBella, D. W. Bullock, M. Anser, Z. Ding, C. Emery, L. Bellaiche, and P. M. Thibado
Department of Physics, The University of Arkansas, Fayetteville, Arkansas 72701
(Received 4 October 1999)

A reversible 2D critical transition is observed on the GaAs(001) surface and modeled as a lattice-gas Ising system. Without depositing any material, 2D GaAs islands spontaneously form. The order parameter, *four* critical exponents, and coupling energies are measured from scanning tunneling microscope images of the microscopic domain structure and correlation functions as a function of temperature and pressure. Unprecedented insight into the domain structure of a 2D Ising system through the critical point and a complete Hamiltonian for modeling the GaAs(001) surface are presented.

PACS numbers: 68.35.Bs, 05.50.+q, 68.35.Rh

The epitaxial techniques used in manufacturing compound semiconductor device structures have demanded insight into the physical process undergone when atoms are deposited on top of a single crystal surface. This insight is of both fundamental and technological importance and modeling these surfaces is challenging due to their two-component nature. Much success has been achieved using various techniques, such as first-principles theory [1], kinetic Monte Carlo simulations [2], rate equations [3], and thermodynamics [4].

On single component surfaces, one of the oldest and simplest approaches to modeling is the celebrated two-dimensional (2D) lattice-gas Ising model [5]. Clever researchers have been able to artificially create 2D systems with a fixed, submonolayer amount of one material deposited on a host surface made of a different material, and successfully applied the 2D lattice-gas Ising model [6–10]. These studies advance our understanding of phase transitions while illuminating the nature of interactions between atoms on surfaces, since the 2D Ising model has been theoretically studied in rigorous detail [11,12]. The above types of experiments are within the canonical ensemble (i.e., fixed number of particles) and therefore, they can fit their data to Onsager's exact solution similar to some 2D Ising-like magnetic phase transitions (i.e., fixed number of spins) that have been observed by neutron scattering [13–15]. The lattice-gas Ising model was originally framed within the more general context of the grand canonical ensemble, where the number of particles is free to fluctuate as it exchanges with a reservoir. This is unlike the ferromagnetic case where the number of spins is fixed. To the best of our knowledge no experimental test of the general solution to the 2D lattice-gas Ising model within the grand canonical ensemble exists.

In this Letter, we discovered a single crystal surface where the surface atoms can exchange with the substrate in a reversible manner consistent with the general solution 2D lattice-gas Ising model within the grand canonical ensemble. Surprisingly, the system is the technologically important two-component GaAs(001) compound semiconductor surface. This experiment is performed by imaging individual domains on a scale comparable to its constituents (i.e., the atoms) with scanning tunneling microscopy (STM), giving unprecedented insight into the microscopic domain structure of a 2D Ising system through the critical point. Equally exciting, this study provides a complete 2D Ising Hamiltonian for modeling the equilibrium and nonequilibrium properties of the GaAs(001) surface.

Experiments were carried out in an ultrahigh vacuum (UHV) multichamber facility [$(5-8)\times10^{-11}$ Torr throughout] which contains a molecular beam epitaxy (MBE) chamber (Riber 32P) that includes a substrate temperature determination system accurate to $\pm2\,^{\circ}$C [16] and a surface analysis chamber with a custom integrated STM (Omicron) [17]. Commercially available, "epi-ready," $n+$ (Si doped $10^{18}/\mathrm{cm}^3$) GaAs(001) $\pm0.1^{\circ}$ substrates were loaded into the MBE system without any chemical cleaning. The surface oxide layer was removed and a 1.5-μm-thick GaAs buffer layer was grown at 580 °C using an As_4 to Ga beam equivalent pressure ratio of 15 and a growth rate of 1.0 μm/h as determined by reflection high-energy electron diffraction oscillations.

The spontaneous formation of islands on this surface occurred after each sample was annealed for a fixed time (between 0.25–33 h), a fixed temperature (between 500–700 °C), and a fixed As_4 flux (between 0.01–10.0 μTorr), resulting in an exhaustive study of the accessible parameter space. To ensure the samples were in equilibrium, the anneal times were successively increased until the surface morphology remained unchanged, which resulted in 33 h anneals for the lowest temperatures. The samples are cooled to room temperature using a procedure that freezes in the surface morphology present at higher temperatures and has been described elsewhere [18]. The samples were transferred to the STM without breaking UHV and imaged at room temperature. For each sample, 5–10 1 μm $\times$ 1 μm filled-state STM images were acquired using tips made from single crystal ⟨111⟩-oriented tungsten wire, a sample bias of -3.0 V, and a demanded tunneling current of 0.05–0.1 nA.

 0031-9007/00/84(18)/4152(4)$15.00

Finite-Temperature Properties of $Pb(Zr_{1-x}Ti_x)O_3$ Alloys from First Principles

L. Bellaiche,[1] Alberto García,[2] and David Vanderbilt[3]

[1]*Physics Department, University of Arkansas, Fayetteville, Arkansas 72701*

[2]*Departamento de Fisica Aplicada II, Universidad del Pais Vasco, Apartado 644, 48080 Bilbao, Spain*

[3]*Center for Materials Theory, Department of Physics and Astronomy, Rutgers University, Piscataway, New Jersey 08855-0849*

(Received 4 January 2000)

A first-principles-derived approach is developed to study finite-temperature properties of $Pb(Zr_{1-x}Ti_x)O_3$ (PZT) solid solutions near the morphotropic phase boundary (MPB). Structural and piezoelectric predictions are in excellent agreement with experimental data and direct first-principles results. A low-temperature monoclinic phase is confirmed to exist, and is demonstrated to act as a bridge between the well-known tetragonal and rhombohedral phases delimiting the MPB. A successful explanation for the large piezoelectricity found in PZT ceramics is also provided.

PACS numbers: 77.84.Dy, 77.65.Bn, 81.30.Bx

Ferroelectric perovskite $A(B'B'')O_3$ alloys are of growing importance for a variety of device applications [1,2], and are also of great current fundamental interest since little is known about the effects responsible for their anomalous properties. A good example of an $A(B'B'')O_3$ solid solution that is of both fundamental and technological importance is the $Pb(Zr_{1-x}Ti_x)O_3$ system. Usually denoted as PZT, this mixed-cation alloy is currently in widespread use in piezoelectric transducers and actuators [1]. Its phase diagram exhibits a morphotropic phase boundary (MPB) separating a region with a tetragonal ground state ($x > 0.52$) from a region with rhombohedral symmetry ($x < 0.45$) [3].

High piezoelectric response is experimentally found in *ceramics* of PZT around the MPB. The origin of this large piezoelectric response is unclear. On the one hand, semiempirical simulations predict that the large experimental value of the d_{33} piezoelectric coefficient results mainly from the large value of d_{33} that a *single-crystal* PZT would exhibit [4]. On the other hand, recent first-principles calculations [5,6] have found that the d_{33} coefficient of a tetragonal single crystal of $Pb(Zr_{0.5}Ti_{0.5})O_3$ is estimated to be *3 times smaller* than the experimental value obtained for ceramics at low temperature.

Furthermore, recent synchrotron x-ray powder diffraction studies have revealed the existence of an unexpected low-temperature monoclinic phase of PZT at $x = 0.48$ [7], which implies that the phase diagram of PZT is more complex than previously thought. This monoclinic phase may act as a second-order transitional bridge between the tetragonal phase, for which the electrical polarization **P** lies along the pseudocubic [001] direction, and the rhombohedral phase, for which **P** is along the pseudocubic [111] direction. If this is indeed the case, the polarization of the monoclinic phase continuously rotates as the composition x decreases in the MPB region [7]. Such a continuous rotation has yet to be observed.

Obviously, accurate simulations are needed to understand the properties of perovskite alloys in general, and of PZT, in particular. Since the beginning of the present decade, first-principles methods have emerged as a powerful tool for investigating properties of ferroelectric systems theoretically (see [5,6,8,9], and references therein). However, these methods are essentially restricted to the study of the zero-temperature properties of small cells, while accurate and interesting predictions of alloy properties would require calculations on much larger cells at finite temperature. Ideally one desires a computational scheme with the capability of predicting the properties of "real" perovskite alloy systems at finite temperature, with the accuracy of the first-principles methods.

The purpose of this Letter is to demonstrate that it is possible to develop such a scheme, and to apply it to study the finite-temperature behavior of PZT in the vicinity of the MPB. Remarkably, we find that the existence of an intermediate monoclinic phase emerges naturally from this approach. Moreover, the theory provides a novel and successful explanation for the large piezoelectric response of PZT near the MPB, thereby explaining and resolving the previous theoretical difficulties in obtaining agreement with the known experimental values of the piezoelectric coefficients.

Our scheme is based on the construction of an effective Hamiltonian from first-principles calculations. A *ferroelectric* effective Hamiltonian [10] must include the ferroelectric local soft mode and the strain variables, since ferroelectric transitions are accompanied by a softening of a polar phonon mode and by the appearance of a strain. An *alloy* effective Hamiltonian must also include the compositional degrees of freedom. We propose to incorporate all such degrees of freedom by writing the total energy E as a sum of two energies,

$$E(\{\mathbf{u}_i\},\{\mathbf{v}_i\},\eta_H,\{\sigma_j\}) = E_{\rm ave}(\{\mathbf{u}_i\},\{\mathbf{v}_i\},\eta_H) + E_{\rm loc}(\{\mathbf{u}_i\},\{\mathbf{v}_i\},\{\sigma_j\}), \quad (1)$$

where $\mathbf{u}_i$ is the local soft mode in unit cell i, $\{\mathbf{v}_i\}$ are the dimensionless local displacements which are related to the inhomogeneous strain variables inside each cell [10], η_H

Intrinsic Piezoelectric Response in Perovskite Alloys: PMN-PT versus PZT

L. Bellaiche[1] and David Vanderbilt[2]
[1]*Physics Department, University of Arkansas, Fayetteville, Arkansas 72701*
[2]*Department of Physics and Astronomy, Rutgers University, Piscataway, New Jersey 08855-0849*
(Received 16 March 1999)

First-principles supercell calculations and the modern theory of polarization are used to compute the e_{33} piezoelectric coefficients of $Pb(Zr_{0.5}Ti_{0.5}O_3)$ (PZT) and $0.60\ Pb(Mg_{1/3}Nb_{2/3})O_3 + 0.40\ PbTiO_3$ (PMN-PT) alloys. A drastic enhancement by a factor of 2.7 is found for e_{33} when going from PZT to PMN-PT. The huge value of e_{33} in PMN-PT comes from the large response of the internal coordinates of Pb, Ti, Nb, and O atoms to a macroscopic strain. On the other hand, the Mg atoms contribute little to the piezoelectricity for dielectric and elastic reasons.

PACS numbers: 61.66.Dk, 77.65.Bn, 77.84.Dy

Complex insulating perovskite $A(B'B'')O_3$ and $A(B'B''B''')O_3$ alloys are of great current interest for actual or potential uses based on their exceptional piezoelectric properties [1]. Examples include the $Pb(Zr_{1-x}Ti_x)O_3$ (PZT) alloys that are currently used in piezoelectric transducers and actuators [2–4], and most recently, the class of $Pb(Mg_{1/3}Nb_{2/3})O_3$-$PbTiO_3$ (PMN-PT) and $Pb(Zn_{1/3}Nb_{2/3})O_3$-$PbTiO_3$ (PZN-PT) materials which, when synthesized in single-crystal form, exhibit remarkably large piezoelectric constants and maximum strain levels [5]. These latter materials thus promise dramatic improvements in the resolution and range of ultrasonic and sonar listening devices [6].

A recent *ab initio* study has concluded that the large piezoelectric response observed experimentally in PZT is not consistent with the calculated "intrinsic" response of a supercell realization of the alloy at zero temperature [7], and should instead be ascribed to an "extrinsic" source. Of course, care must be taken in making comparisons between a piezoelectric constant computed under such ideal conditions and one measured experimentally for a real material. Obviously, the piezoelectric response is generally temperature dependent, and may tend to diverge when approaching the Curie temperature [5]. Moreover, the piezoelectricity can depend sensitively on alloy concentration when close to the morphotropic phase boundary [8,9], so that comparisons should only be made at the same composition. Still, the intrinsic response of a supercell realization of a single-crystal material at given x and T may not be the whole story. The most obvious extrinsic contribution to the piezoelectric response is the motion of ferroelectric domain walls. However, several other factors, that could be regarded as extrinsic, may also play a role. The coexistence of tetragonal and rhombohedral phases in the vicinity of the morphotropic phase boundary is believed to enhance the piezoelectric response of PZT (see Ref. [10], and references therein). The partial compositional order is rather complicated in compounds such as PMN-PT: one finds some degree of short-range disorder, partial rock-salt-like order at intermediate length scales (~50 Å), and an absence of true long-range order [11]. The compositional fluctuations are likely to be coupled in some way to the "nanopolar domains" that are thought to be important for the strain response of PMN-PT-like compounds [12,13]. In the case where experiments are done on ceramic samples, the measured piezoelectric response is really some type of complicated orientational average of the microscopic single-crystal response. And finally, stoichiometric nonuniformities and defects of all types (point defects, dislocations, grain boundaries) may affect the piezoelectric response if present in the material.

The thrust of this paper is to investigate the contribution of *intrinsic* effects on the enhancement of the piezoelectric response when going from PZT to PMN-PT. We want both to quantify such effects and to identify their microscopic origins. Motivated to clarify these issues, we decided to calculate the e_{33} piezoelectric coefficient of *ordered* supercells of $Pb(Zr_{0.5}Ti_{0.5}O_3)$ and $0.60\ Pb(Mg_{1/3}Nb_{2/3})O_3 + 0.40\ PbTiO_3$ alloys at zero temperature. Such a calculation obviously leaves out any effects of finite temperature or compositional disorder (e.g., compositional fluctuations on the scale of the "nanopolar regions"). We also performed simulations on the common parent end member $PbTiO_3$ (PT) to assess the intrinsic role of alloying on piezoelectricity. The Ti compositions of the alloys are chosen to be slightly *larger* than those at the morphotropic phase boundary—47% in PZT vs 35%-38% in PMN-PT [10,14]—in order that the ferroelectric ground states of the presently studied systems have experimentally the same tetragonal point group ($P4mm$) as their common parent compound $PbTiO_3$.

For PT, we adopt the ferroelectric tetragonal cell denoted "Theory II" in Ref. [15]. To facilitate comparison between the PZT and PMN-PT alloys, we choose supercells that are similar in the sense that they both exhibit atomic ordering along the [100] direction. For PZT, there are two different (100) B planes ($n = 2$) corresponding to an alternance of pure Zr planes with pure Ti planes, with a total of 10 atoms per cell. For PMN-PT, we use the minimal number of planes ($n = 5$) consistent with a Ti composition of 40%, yielding a 25-atom cell. We

